# TWDB Report

# A model-based Investigation of Streamflow Trends in Upper Brazos River Basin

By Yu Zhang, Ph. D
University of Texas at Arlington

Sarah Fakhreddine, Ph.D
James Hayes
Carnegie Mellon University



DRAFT Final Report: A model-based Investigation of Streamflow Trends in Upper Brazos River Basin

TWDB Contract Number 2200012624

This page is intentionally blank.

# Table of Contents

# List of Tables



# List of Figures

# List of Acronyms

| | |
|---|---|
| AORC | Analysis of Record for Calibration |
| ET | Evapotranspiration |
| HL-RDHM | Hydrology Lab- Research Distributed Hydrologic Model |
| MPE | Multisensor Precipitation Estimates |
| MRLC | Multi-resolution land characteristics |
| NCAR | National Center for Atmospheric Research |
| NCEP | National Centers for Environmental Predictions |
| NEXRAD | Next Generation Radar |
| NHD-Plus | National Hydrographic Database-Plus |
| NLCD | National Land Cover Database |
| NLDAS-2 | North American Land Data Assimilation System-Phase 2 |
| NOAA | National Oceanic and Atmospheric Administration |
| NWM | National Water Model |
| NWS | National Weather Service |
| OWP | Office of Water Prediction (NWS) |
| PRISM | Precipitation-elevation Regressions on Independent Slopes Model |
| RFC | River Forecast Center |
| RMSE | Root-mean squared error |
| SAC-SMA | Sacramento Soil Moisture Accounting |
| SAC-HTET | SAC Heat transfer/ET |
| TAMU | Texas A&M University |
| TCEQ | Texas Commission for Environmental Quality |
| TWDB | Texas Water Development Board |
| WAM | Water Availability Model |
| WRAP | Water Right Analysis Package |
| WRF-Hydro | Weather Research and Forecasting - Hydro |
| USACE | US Army Corps of Engineers |
| USGS | US Geological Survey |

# Executive Summary

Previous investigations conducted by the USGS and Freese & Nichols have found declining trends in streamflow and runoff yield in a number of watersheds in the upper portion of Brazos River Basin. These trends have raised concerns among stakeholders about the future water supply in the region, and there is broad interest from the water suppliers, state and federal partners in identifying the causes underlying the declines. The earlier study by Freese & Nichols touched upon changes in precipitation and temperature from the 1960s, but did not go far to mechanistically relate these changes to the trends in streamflow.

The current investigation aims to illuminate the roles of potential drivers of the declining trends in runoff over six watersheds where such trends are evident. These drivers include temperature, precipitation, and land cover. In contrast to prior studies which focused on empirical analysis of trends, the present project employs a combination of hydrologic and land surface model reanalysis, sensitivity experiments and empirical analysis of land cover to determine the probable contributions of the foregoing drivers.

The project comprises the following four elements, namely

1. Implementing a hydrologic model [National Weather Service (NWS) Hydrologic Laboratory Research Distributed Hydrologic Model (HL-RDHM; Koren et al., 2004)] for simulating streamflow for all control points in the Brazos Water Availability Model (WAM), and develop a forcing data set for driving the model.

2. Using controlled simulations to determine the potential roles of temperature and precipitation changes on the trends in the streamflow.

3. Corroborating the simulation results from HL-RDHM using alternative land surface model reanalysis, namely the North American Land Data Assimilation System-2 (NLDAS-2; Xia et al., 2012) and the National Water Model version 2.1 (NWM 2.1).

4. Examining land cover changes and correlate the changes with changes in streamflow patterns.

A key aspect of the project is to assess the effects of rising temperature on runoff yields: near surface temperature over the region has seen steady increase over the past forty years, and this may have elevated evapotranspiration and reduced soil moisture, leading to a reduction in soil water available for runoff generation. To this end, the project team established a distributed hydrologic model (HL-RDHM) with a hybrid, physics-based water balance scheme (SAC-HTET). The team also created a new precipitation data set by bias-correcting the National Weather Service Analysis of Record for Calibration (AORC) gridded product. With this model as the platform, a set of sensitivity experiments are performed wherein the trend in temperature is artificially removed over the period of 1980–2020 to discern the impacts of warming.

The key findings from the investigation are summarized as follows.

1. The sensitivity experiments point to small, but discernible impacts of warming on runoff yields in a majority of the watersheds being examined. Nonetheless, these impacts are unlikely to fully explain the trends in runoff, as the model is unable to reproduce the downward trend with the baseline configuration (with warming).
2. Other contemporary hydrologic and land surface models, such as the National Water Model, and the North America Land Data Assimilation System have similar difficulties in reproducing the downward trends in runoff. In fact, trends in simulated streamflow by these models diverge from the observations at sites with downward trends.
3. Analysis of land cover change from the early 2000s reveals an expansion in agricultural land that is consistently seen across the watersheds. Owing to the limited duration of the land cover data, it remains unclear if this expansion contributed to the downward shift in runoff.

On the basis of the findings, the project team makes the following recommendations for diagnosing and interpreting the declining trends in runoff.

I. Gather historical data on additional variables that may have contributed to the trends in runoff, such as expansion of agricultural impoundments, change in irrigation practice, and depletion in groundwater. In particular, as declining groundwater level has been reported in the upper basin, it is key to investigate the impacts of this decline on the discharge to surface water to illuminate its potential contribution to the declining runoff yield.
II. Assess, and potentially improve the precipitation product for the period prior to 1998 when the AORC was based on primarily gauge reports. The switch to radar-gauge merged products during the late 1990s may have caused a shift in precipitation bias that artificially suppresses the ability of the models to resolve the downward trend.
III. Perform additional analysis of streamflow dynamics at the two sites, namely DMAS09 and SFAS06, for selected events in the past two decades, and incorporate remotely sensed soil moisture products to diagnose the physics of SAC-HTET. This will help provide clues on whether exogenous mechanisms are in play that led to more rapid depletion of soil moisture than what models are able to resolve.
IV. Improve monitoring of the watersheds to better discern impacts of impoundments, soil moisture during dry and wet conditions.

# 1. Background

With its headwaters in New Mexico, the Brazos River spans the Panhandle, the Hill Country, Prairies Lakes, and the Gulf Coast of Texas; and drains to the Gulf of Mexico near Freeport, TX (Figure 1-1). The river serves as an important water supply across much of its drainage (Wurbs, 2019, 2020).


**Figure 1-1 The geographic extent of Brazos River Basin. (Source: Brazos River Authority).**

In the past century, the Brazos River Basin has undergone major changes in land cover, climate and hydrology (Zhang and Wurbs, 2018; Harwell et al., 2020; Wolaver et al., 2024). A report published by USGS in 2022 found that the annual streamflow in the upper watershed has overall declined between 1900-2017 (Harwell et al., 2020). The downward trend is especially pronounced in the northern parts of the drainage upstream of Seymour, TX. Over the same region, similar downward trends are observed in the annual peak discharge and annual runoff yield (ratio of streamflow volume to precipitation volume). These changes prompt concerns from stakeholders about future water availability over the upper basin.

In a recently concluded project sponsored by the Texas Water Development Board (TWDB), investigators from Freese and Nichols (FNI) assessed the changes in naturalized flow across the Brazos Basin, and reviewed the changes in temperature and net evaporation within climate divisions that overlap with the Brazos River Basin.

The FNI study, henceforth referred to as FNI2021, relies primarily on the Kendall-Tau statistic for assessing trends of time series as did Harwell at al., 2020 (henceforth referred to as USGS2020). Nonetheless, there are a few notable differences between the two studies. For example, while the earlier USGS2020 employed flow records at USGS stations, the latter study used naturalized flow that serves as input to Water Availability Model (WAM) at each WAM control point. Some of the WAM control points are collocated with USGS stations, but many are not. For the former, the naturalized flow was produced from collocated USGS observations by removing human alterations such as withdrawal and return flow, whereas for the latter, the water area ratio method as described in Emerson et al. (2005) was applied to relate flow at an adjacent USGS station to that at the control point before the human alternations are removed. In addition, in the FNI2021, the flow data prior to the late 1950s was identified as outliers and excluded from the trend analysis. Even with shorter records, the results point to similar downward trends at a majority of control points in the upper basin.

FNI2021 also performed analyses that illustrate broad, rising trends in temperature and evaporation in climate divisions overlapping the Brazos River Basin, an increasing trend in groundwater level, and changes in precipitation patterns. Specifically, there appears to be a monotonic trend in the average temperature from the 1960s in some of the climate divisions, e.g., north central Texas. The trends in precipitation are mixed across the climate divisions. In climate divisions overlapping with the upper basin, precipitation tends to increase over time, and most of the increase occurs outside of the summer season.

While the two earlier studies served to uncover and depict the trends, much remains unknown about mechanisms that give rise to the trends. The aforementioned trends in meteorological forcings such as precipitation and temperature may have played roles, but they are likely not the only drivers. Many parts of the Brazos River Basin have undergone major changes in land cover, population, and water management practice, and these may have contributed to changes in streamflow.

# 2. Project Overview

The present study sets out to examine the potential roles of three drivers, namely, precipitation, temperature, and land cover, played in the appearance of the downward trends in streamflow over the upper portion of Brazos River Basin. Prior to undertaking the investigation, we acquired streamflow records at USGS stations collocated with each WAM control point. We further performed the Kendall-Tau test on the annual flow between 1979 and 2022 to confirm the results from FNI2021. As shown in Table 2-1, only at a small minority (five) of the stations was the trend statistically significant over this time window. The remaining stations either feature excessive amounts of missing data (> 20%), or statistically insignificant trends.

**Table 2-1 Summary of available streamflow record at USGS stations in the Brazos River Basin and temporal trends**

| WAM ID | USGS ID | Tau | P-value | Record Length [years]] | % Missing |
|---|---|---|---|---|---|
| AQAQ34 | 08093500 | 0.385 | 0.019 | 20 | 5 |
| BGFR65 | 08110430 | 0.141 | 0.182 | 44 | 2 |
| BGNE71 | 08115000 | -0.015 | 0.895 | 44 | 2 |
| BOWA40 | 08095600 | - | - | 4 | 20 |
| BRAQ33 | 08093100 | -0.085 | 0.424 | 44 | 2 |
| BRBR59 | 08109000 | - | - | 15 | 31 |
| BRDE29 | 08090800 | -0.122 | 0.260 | 44 | 7 |
| BRGR30 | 08091000 | -0.135 | 0.199 | 44 | 2 |
| BRHB42 | 08098290 | -0.036 | 0.739 | 44 | 2 |
| BRHE68 | 08111500 | - | - | 44 | 27 |
| BRPP27 | 08089000 | -0.114 | 0.279 | 44 | 2 |
| BRRI70 | 08114000 | -0.015 | 0.895 | 44 | 2 |
| BRRO72 | 08116650 | -0.032 | 0.779 | 44 | 9 |
| BRSB23 | 08088000 | -0.11 | 0.317 | 44 | 9 |
| BRSE11 | 08082500 | -0.254 | 0.016 | 44 | 2 |
| BRWA41 | 08096500 | -0.049 | 0.649 | 44 | 2 |
| BSB$R^2$0 | 08086290 | -0.017 | 0.879 | 44 | 2 |
| BSLU07 | 08079550 | - | - | 0 | 0 |
| CAST17 | 08084800 | 0.008 | 0.944 | 44 | 2 |
| CCIV25 | 08088450 | 0.091 | 0.755 | 11 | 8 |
| CFEL22 | 08087300 | - | - | 4 | 20 |
| CFFG18 | 08085500 | -0.07 | 0.511 | 44 | 2 |
| CFHA14 | 08083240 | - | - | 44 | 60 |
| CFNU16 | 08084000 | -0.163 | 0.122 | 44 | 2 |
| CFRO13 | 08083100 | -0.268 | 0.011 | 44 | 2 |
| COPI48 | 08101000 | 0.038 | 0.723 | 44 | 2 |
| CRJA05 | 08081200 | - | - | 8 | 11 |
| DCLY63 | 08110100 | -0.008 | 0.944 | 44 | 2 |
| DMAS09 | 08080500 | -0.246 | 0.022 | 42 | 2 |
| DMJU08 | 08079600 | -0.014 | 0.903 | 44 | 2 |
| DUGI03 | 08080950 | 0.273 | 0.276 | 11 | 8 |
| EYDB61 | 08109800 | -0.047 | 0.664 | 44 | 2 |
| GAGE56 | 08105000 | - | - | 4 | 20 |
| GALA57 | 08105700 | -0.015 | 0.895 | 44 | 2 |
| GHGH24 | 08088400 | - | - | 0 | 100 |
| HCAL19 | 08086212 | -0.033 | 0.762 | 44 | 2 |
| HCB$R^2$1 | 08086500 | - | - | 44 | 64 |
| HGCR39 | 08095400 | - | - | 44 | 49 |
| LABE52 | 08104100 | - | - | 44 | 22 |
| LAKE50 | 08103800 | 0.022 | 0.840 | 44 | 2 |
| LAYO51 | 08104000 | - | - | 2 | 33 |

| | | | | | |
|---|---|---|---|---|---|
| LEBE49 | 08102500 | 0.040 | 0.708 | 44 | 2 |
| LEDL43 | 08099100 | - | - | 44 | 24 |
| LEGT47 | 08100500 | 0.068 | 0.524 | 44 | 2 |
| LEHM46 | 08100000 | - | - | 44 | 24 |
| LEHS45 | 08099500 | - | - | 44 | 36 |
| LRCA58 | 08106500 | 0.013 | 0.911 | 44 | 2 |
| LRLR53 | 08104500 | 0.006 | 0.960 | 44 | 2 |
| MBMG38 | 08095300 | - | - | 44 | 44 |
| MCBL69 | 08111700 | - | - | 44 | 16 |
| MSMN12 | 08082700 | 0.068 | 0.524 | 44 | 2 |
| MUHA15 | 08083245 | 0.330 | 0.184 | 11 | 8 |
| MYDB60 | 08109700 | 0.047 | 0.664 | 44 | 2 |
| NABR67 | 08111000 | - | - | 19 | 10 |
| NAEA66 | 08110500 | 0.044 | 0.678 | 44 | 2 |
| NAGR64 | 08110325 | 0.066 | 0.537 | 44 | 2 |
| NBCL36 | 08095000 | 0.047 | 0.664 | 44 | 2 |
| NBHI35 | 08094800 | - | - | 44 | 36 |
| NBVM37 | 08095200 | 0.063 | 0.558 | 44 | 4 |
| NCKN10 | 08082180 | - | - | 8 | 11 |
| NGGE54 | 08104700 | -0.167 | 0.112 | 44 | 2 |
| NRBL32 | 08092000 | - | - | 44 | 44 |
| PAGR31 | 08091500 | 0.003 | 0.983 | 42 | 2 |
| PPSA28 | 08090500 | - | - | 0 | 100 |
| RWPL01 | 08080700 | 0.067 | 0.695 | 21 | 5 |
| SADL44 | 08099300 | -0.098 | 0.375 | 44 | 9 |
| SFAS06 | 08082000 | -0.296 | 0.005 | 44 | 2 |
| SFPE04 | 08081000 | - | - | 8 | 11 |
| SGGE55 | 08104900 | -0.057 | 0.592 | 44 | 2 |
| SHG$R^2$6 | 08088600 | - | - | 7 | 12 |
| WRSP02 | 08080910 | - | - | 0 | 100 |
| YCSO62 | 08110000 | - | - | 44 | 38 |

Shaded in grey are stations with statistically significant trends in precipitation.

We performed similar trend analysis to the USGS records between 1940-2022 and found statistically significant trends at only seven stations. Therefore, the discrepancies between our results and FNI2021 are most likely a result of the latter's use of WAM records rather than USGS data directly in performing the trend analysis. For periods when records are missing at a given USGS station, the WAM flow records are constructed from data at an adjacent USGS gauge using the watershed area ratio method.

In this study, we mainly focus on the five WAM control points where USGS records exhibit statistically significant trends (Figure 2-1; Tables 2-1, 2-2). In some of the analyses, we include two additional points, namely DMJU08 (Double Mountain Fork, Brazos River at Justiceburg) and RWRP01 (Running Water Draw at Plainview), which are situated upstream of points with significant downward trend in streamflow, to confirm the geographic consistency of the trends.

DMJU08 is immediately upstream of DMSA09 (Double Mountain Fork Brazos River near Aspermont), and RWRP01 is upstream of SFAS06 (Salt Fork Brazos River near Aspermont).

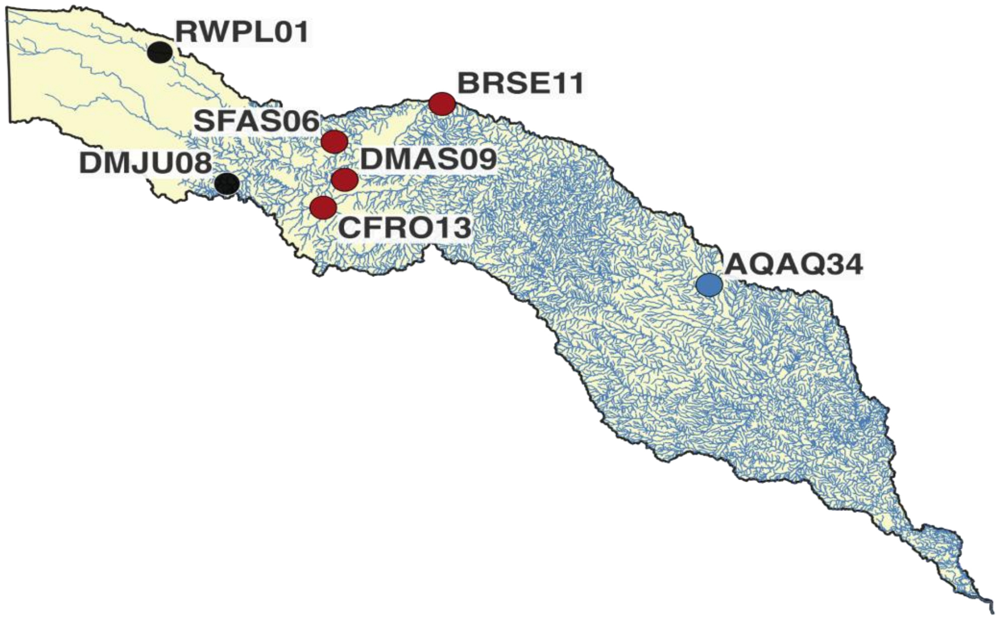


**Figure 2-1 Map of WAM control points (also USGS stations) used in this study. Those with statistically significant trends are highlighted in red (declining) and blue (increasing).**

**Table 2-2 Seven selected control points in Brazos River Basin for HL-RDHM simulation.**

| Control Point | USGS Gauge Number | Location | Drainage Area[1] ($km^2$) | Mean Naturalized Flow[2], 1982-2017 (AF/day) |
|---|---|---|---|---|
| AQAQ34 | 08093500/ 08093360 | Aquilla Creek near Aquilla | 795.1 | 255.4 |
| BRSE11 | 08082500 | Brazos River at Seymour | 4,147 | 511.0 |
| CFRO13 | 08083100 | Clear Fork Brazos River near Roby | 688.9 | 10.82 * |
| DMAS09 | 08080500 | Double Mountain Fork Brazos River near Aspermont | 4,211 | 214.0 |
| DMJU08 | 08079600 | Double Mountain Fork Brazos River at Justiceburg | 686.3 | 58.20 |
| RWPL01 | 08080700 | Running Water Draw at Plainview | 764.0 | 3.034 |
| SFAS06 | 08082000 | Salt Fork Brazos River near Aspermont | 5,721 | 121.3 |

[1]Drainage area is the incremental area that drains to the segment of stream between the station and its immediate upstream counterpart

[2]Daily WAM naturalized flows are used for naturalized flows for all points except CFRO13 which was not included as a primary control point in the daily WAM. Therefore, USGS streamflow observations are used to approximate naturalized flow at this point.

We also performed trend analysis on average daily temperature at each Global Historical Climate Network (GHCN) station in the state of Texas (computed by averaging the daily maximum and minimum temperatures). We identified 23 stations with statistically significant trends (Figure 2-2). The majority (18) of these show rising trends and only five stations exhibit negative trends. Most of the former are situated in the Panhandle Plains. These results are largely consistent with the outcomes from FNI2021 cited earlier.

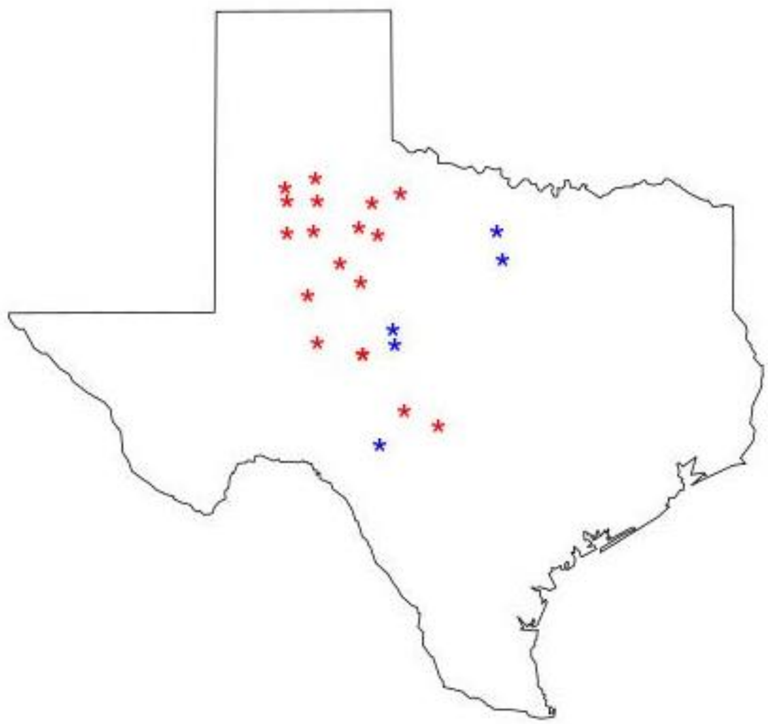

**Figure 2-2 Stations from the Global Historical Climate Network that exhibit significant trends in temperature in the state of Texas. Stations with positive and negative trends are marked in red and blue, respectively.**

The specific questions the study seeks to address include:

- Did the rising temperatures over the region outweigh changes in precipitation to cause declines in runoff?
- Did the upper basin experience large changes in land cover that may have altered the rainfall-runoff process?

There has been extensive research on impacts of rising temperature on droughts (Vicente-Serrano et al., 2014; Ahmadalipour et al., 2017; Samaniego et al., 2018). In recent years, some authors opined that these impacts are greater than previously thought. Notably, Brunner et al. (2021) suggested that rising temperature plays an increasingly important role in causing or amplifying streamflow droughts in the US. Over the upper basin, it is plausible that rising temperature enhances evaporative demand, reduces soil water, and thereby suppresses runoff. Yet, as precipitation exhibits upward trends in the region, there is a possibility that any impacts from rising temperatures on streamflow are negated by those in increasing precipitation.

To determine the relative importance of precipitation and temperature trends, we will employ a model-based approach which involves control experiments wherein the effects from the rising temperature are isolated. The experiments will be carried out using a distributed hydrologic model (HL-RDHM; Koren et al., 2004; Zhang et al., 2011; Smith et al., 2013), equipped with a physics-based evapotranspiration scheme (SAC-HTET; Koren et al., 2010). To discern the potential dependence of simulated trends on model structure, we include reanalysis of two land surface/hydrologic models, namely the National Water Model (Cosgrove et al., 2016), and the North America Land Data Assimilation System-2 (NLDAS-2; Xia et al., 2012). The analysis tacitly assumes that precipitation plays a predominant role in modulating streamflow volume whereas contribution of baseflow owing to deep groundwater discharge is minor.

In addition to the model-based assessments on roles of forcings, we also incorporate a set of qualitative analyses on land cover changes over the region which help gauge the potential of changing land surface controls on water balance.

# 3. Impacts of Rising Temperature on Runoff Yield

## 3.1. Preparation of Forcing Data Set

SAC-HTET requires gridded input data of daily minimum and maximum temperature (°F), hourly air temperature (°F) at the top of each hour, and hourly accumulated precipitation (mm) ending at the top of each hour.

Precipitation

For precipitation, a single historical forcing dataset was prepared (Section 4.1.1) and held constant for all model runs to isolate and study the potential impact of temperature. For temperature, both a historical forcing dataset (Section 4.1.2) and detrended forcing dataset (Section 4.1.3) are prepared to allow for comparative simulations of temperature impacts. Precipitation and temperature forcing data are prepared by modifying 4-km gridded Analysis of Record for Calibration (AORC) data, an NWS Office of Water Prediction (OWP) product (NOAA NWS OWP, 2021) available for each River Forecast Center (RFC). The OWP constructs AORC data using over a dozen individual time series and climatological datasets. The AORC data contain hourly accumulated surface precipitation ending at the “top” of each hour, in liquid water-equivalent units (kg/m2 to the nearest .01 kg/m2 or mm). The AORC temperature data consists of instantaneous, 2-m above-ground-level temperature at the top of each hour (°K, to the nearest .01 °K). Data are publicly available for CONUS from February 1979 to near present and reported in Universal Time Coordinated (UTC). All hourly data are temporally shifted from UTC to Central Standard Time (CST) to ensure direct comparison with WAM daily flows, although the 6-hr time difference from UTC to CST is expected to have minimal impact. The primary objective of the time zone adjustment was to align simulated runoff data (hourly simulations aggregated to daily values) with WAM daily naturalized flows used for calibration. No adjustments were made for shift in daylight time as this was not expected to appreciable impact simulated runoff.

Historical hourly accumulated precipitation forcing grids are developed by resampling the AORC 4-km gridded data to the model 4-km grid in the Hydrology Rainfall Analysis Project grid using a bilinear method (i.e., a 2-dimensional linear interpolation) as used in prior HL-RDHM modeling studies (e.g., Siddique et al., 2020). HRAP is a coordinate system used by NOAA NWS for gridded rainfall data and a default grid setting in HL-RDHM.

Additionally, the re-gridded precipitation data are bias corrected to improve its accuracy prior to its use in simulating streamflow. From 1979 to early 2000s, the AORC precipitation product was produced by disaggregating the 24-h totals from North American Land Data Assimilation System - version two (NLDAS-2) precipitation product, whereas in the later period it was essentially identical to the archived multisensor precipitation products produced by the NWS River Forecast Centers (RFCs). Past studies have reported biases in NLDAS-2 precipitation products for heavy rain events (Zhang et al., 2020), which may arise from manifold causes (Xia et al., 2006; 2007). The RFC multisensor product is also subject to bias. Zhang et al. (2011) devised a strategy to bias-correct this product using Precipitation-Elevation Regressions on Independent Slopes (PRISM; Daly et al., 1996), and demonstrated that applying this bias-correction scheme reduces the bias and its temporal consistency. Our preliminary analysis of PRISM and AORC products reveal large differences in many locations (see an example in Figure 3-1). As a result, this study adopts the bias-correction approach by Zhang et al. (2011) to create an adjusted AORC product using the PRISM daily product as reference.

Daily, 4-k gridded PRISM data are available for CONUS from 1981 to the near present. Therefore, the bias-correction is done to AORC data from 1981 onwards. The raw AORC precipitation data is used as forcings from February 1979 – 1980 owing to the lack of daily PRISM data during this period. This period is used as a ‘spin up’ for the model and output for these dates is not used for analysis. Therefore, the lack of bias correction in the initial < two years of simulation time is not expected to impact results of this study.

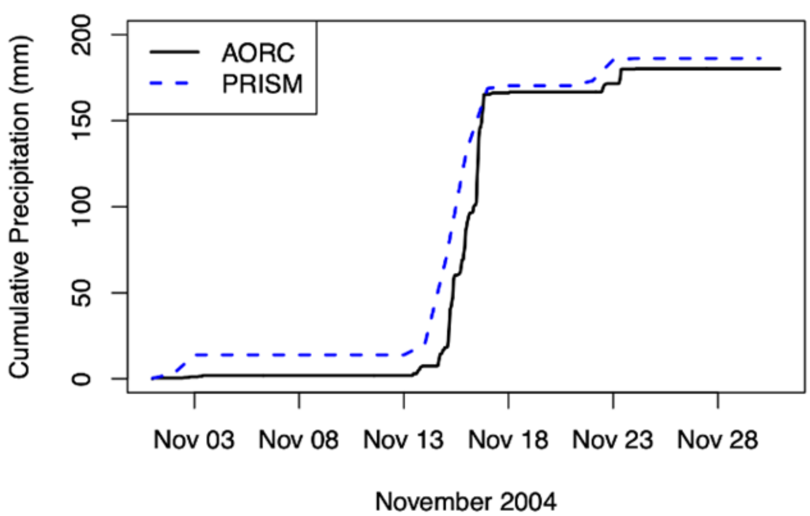


**Figure 3-1 Example of cumulative precipitation (mm) from hourly AORC and daily PRISM over a wet event occurring from Nov three – Nov 28, 2004 at point DMJU08.**

PRISM-corrected AORC data are produced by scaling the sum of hourly AORC data to match daily PRISM data. First, bilinear resampling of daily PRISM gridded data was conducted to match model grid as described above and bias correction was performed on a cell-by-cell basis. Hourly AORC data is summed for each day and scaled by the ratio of accumulated daily precipitation from PRISM and AORC such that the daily sums matched PRISM data. If the daily sum of AORC precipitation is zero, then the daily PRISM precipitation is divided uniformly across 24 hours.

The merit of the bias-correction strategy is demonstrated through a control experiment. In this experiment, the uncalibrated HL-RDHM is driven by raw and bias-corrected AORC products to produce two sets of streamflow simulations. These simulations are then evaluated against daily naturalized flow data from the daily Brazos WAM input files. The 2019 daily Brazos WAM (Wurbs, 2019) was used as it was the most recent version available at the time the project began. The WAM modeling system includes TCEQ's Water Rights Analysis Package (WRAP) to simulate water resources development, operations of 680 reservoirs, and water rights allocations for > 1,200 water rights permits as described in Wurbs (2019). Briefly, the daily Brazos is a disaggregated version of the coarser-resolution, monthly Brazos WAM. The expanded capabilities of the daily version allow for more temporally refined simulation of unappropriated water availability throughout the basin. Input files to the daily WAM contain valuable data on daily naturalized flows for the period of record of the 2019 daily WAM, 1940 - 2017, that were used in this study as described below.

Naturalized flows from the daily WAM were selected for use as calibration data because HL-RDHM simulated naturalized flows. Therefore, these WAM data are the most relevant compared to regulated flow. Daily WAM naturalized flows were used rather than monthly to provide finer temporal resolution calibration data. The daily WAM has flow records for 58 control points in the Basin which are all evaluated for improvements in model performance due to bias correction of precipitation forcing. Focusing on the model period of 1981-1992, PRISM-correction of AORC data decreased the mean daily percent bias in simulated streamflow compared to the raw AORC forcing. Bias decreased in 49 of the 58 WAM control point locations with an average decrease was ~10.1% mean daily bias (Figure 3-2). Therefore, the PRISM-corrected AORC product was used as the precipitation forcing for all simulations in this study.

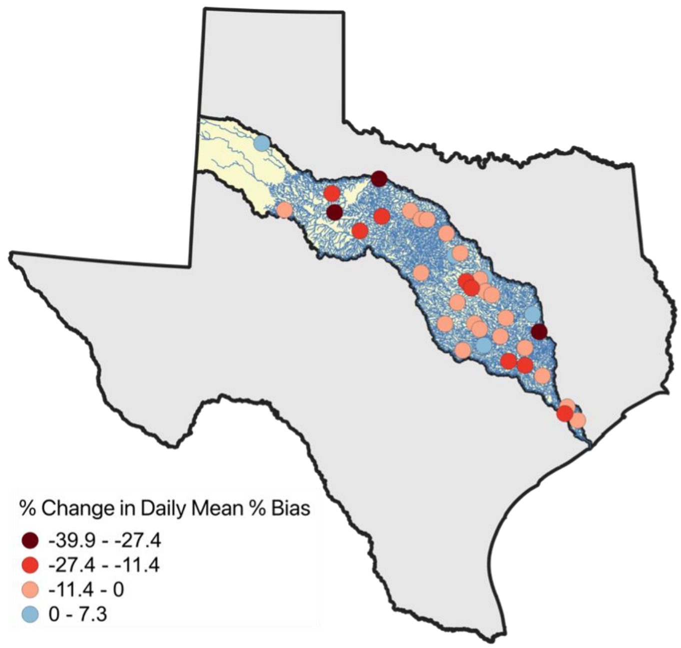


**Figure 3-2 Percent change in daily mean streamflow percent bias for 58 control points from the daily Brazos WAM when forcing HL-RDHM with PRISM-corrected AORC precipitation data versus raw AORC data.**

<u>Temperature</u>

The AORC hourly temperature products were created by interpolating daily maximum and minimum temperature observations from weather stations. To assess the accuracy of these products over the region, they were compared against daily observations from stations in the Global Historical Climate Network (GHCN). The outcome of the comparison of daily maximum, minimum and average temperatures is shown in Table 1. The two products are closely correlated at a majority of the stations (38 out of 49). At the remaining 11 stations, however, the daily maximum temperatures exhibit negative correlation though the daily averages are positively correlated. The causes of these discrepancies are beyond the scope of the present investigation, but we suspect that the use of reanalysis data in the NLDAS-2 product, which constitutes a major source of the AORC data, may have contributed to this.

**Table 3-1 Correlation between AORC temperature and GHCN observations**

| GHCN ID | Correlation-Tmax | Correlation-Tmin | Correlation-Tave |
|---|---|---|---|
| USC00410012 | 0.70 | 0.78 | 0.85 |
| USC00410120 | 0.68 | 0.84 | 0.88 |
| USC00410268 | 0.62 | 0.85 | 0.86 |
| USC00410394 | 0.63 | 0.85 | 0.86 |
| USC00410493 | 0.38 | 0.84 | 0.78 |
| USC00410832 | -0.48 | 0.83 | 0.38 |
| USC00411017 | 0.64 | 0.83 | 0.87 |

| | | | |
|---|---|---|---|
| USC00411042 | -0.37 | 0.83 | 0.44 |
| USC00411138 | -0.46 | 0.85 | 0.37 |
| USC00411250 | 0.04 | 0.83 | 0.65 |
| USC00411875 | -0.30 | 0.85 | 0.45 |
| USC00411974 | 0.66 | 0.83 | 0.87 |
| USC00412121 | -0.37 | 0.85 | 0.42 |
| USC00412741 | 0.48 | 0.76 | 0.80 |
| USC00413214 | 0.74 | 0.85 | 0.89 |
| USC00413257 | 0.59 | 0.78 | 0.84 |
| USC00413329 | 0.05 | 0.82 | 0.66 |
| USC00413411 | 0.63 | 0.84 | 0.86 |
| USC00413614 | 0.56 | 0.84 | 0.85 |
| USC00413828 | 0.56 | 0.84 | 0.84 |
| USC00413954 | 0.79 | 0.72 | 0.86 |
| USC00413992 | -0.31 | 0.84 | 0.45 |
| USC00414517 | -0.15 | 0.82 | 0.54 |
| USC00414570 | 0.67 | 0.84 | 0.87 |
| USC00414670 | -0.06 | 0.81 | 0.62 |
| USC00415272 | -0.44 | 0.84 | 0.44 |
| USC00415650 | 0.67 | 0.83 | 0.87 |
| USC00416747 | 0.83 | 0.85 | 0.92 |
| USC00417206 | 0.38 | 0.85 | 0.78 |
| USC00417327 | 0.68 | 0.83 | 0.88 |
| USC00417706 | 0.45 | 0.81 | 0.81 |
| USC00417743 | 0.62 | 0.84 | 0.86 |
| USC00417944 | 0.77 | 0.74 | 0.86 |
| USC00418221 | 0.77 | 0.90 | 0.92 |
| USC00418433 | 0.58 | 0.84 | 0.85 |
| USC00418566 | 0.60 | 0.83 | 0.85 |
| USC00418583 | 0.80 | 0.83 | 0.90 |
| USC00418630 | 0.61 | 0.86 | 0.87 |
| USC00418818 | 0.43 | 0.86 | 0.80 |
| USC00419163 | 0.66 | 0.85 | 0.87 |
| USC00419499 | 0.54 | 0.85 | 0.84 |
| USW00003969 | -0.30 | 0.84 | 0.48 |
| USW00013962 | 0.86 | 0.84 | 0.93 |
| USW00013966 | 0.86 | 0.85 | 0.93 |
| USW00013973 | 0.82 | 0.78 | 0.89 |
| USW00023034 | -0.10 | 0.84 | 0.59 |
| USW00023041 | 0.56 | 0.84 | 0.84 |
| USW00023042 | 0.85 | 0.86 | 0.93 |
| USW00093985 | 0.78 | 0.83 | 0.91 |

Re-gridding of hourly temperature data was completed using a bilinear method as described previously for precipitation data (Section 4.1.1). Temperature values are converted from °K to °F to meet HL-RDHM input requirements. Then, re-gridded, hourly temperature data are used to produce daily minimum and maximum temperature grids by calculating minimums and maximums on a cell-by-cell basis, respectively. These processed historic temperature data are used as 'control' forcing for the comparative modeling experiments. We use the term historic and control temperature interchangeably throughout the report.

Various approaches exist for detrending temperature time series data for hydrological modeling experiments (California Delta Council, 2023). A commonly employed approach from previous studies focuses on removing a linear trend from historic time series. This approach calculates historical climatological monthly averages over a period of interest to 'anchor' the climatological data. Subsequently, a linear trend is computed for each month using the monthly averages for each year of the study period. A month-specific trend can then be subtracted from the historical daily temperature data to produce a detrended time series such that the detrended data have a trendline of slope zero and an average value equal to the average temperature over the study period (California Water Commission, 2016; California Department of Water Resources, 2019).

This study applied a linear regression detrending approach on a cell-by-cell basis over the entire spatial extent of the model. Gridded historic temperature data (Section 4.1.2) was used to calculate a monthly average for each year (i.e., 12 monthly averages per year) from 1980 – 2020, resulting in 41 years with average monthly temperature for year (i.e., 41 data points for each monthly regression.  The year of 1980 was selected as a start year since it was the first year of fully available AORC data as the data are available February 1979 onwards. The end year of 2020 was selected as it was the last full year of data available at the time of data download when this study began in 2021. For each month, a linear regression of temperature on year was performed for the annual monthly averages. For each study point and month, values of coefficient of determination $R^2$, y intercept, and slope are calculated and reported in Appendix A for grid cells corresponding to the study points. Notably, the grid cells had poor linear fits ($R^2 \leq 0.22$) though all slopes are positive indicating increasing temperature over time except for one slightly negative slope of -0.01 °F/year for SFAS06 for July months). Slope and intercepts values are used to remove the linear increase in temperature across all hourly data from 1981-2020 while data are unchanged for 1980 as the first year of the linear regression data. As an example of the detrending procedure, data of monthly averages and linear trend lines for both historical and detrended data are included for each month and grid cells corresponding to each study point (Appendix A).

Additionally, Mann-Kendall trend tests are conducted for each point to evaluate potential trends in monthly average temperatures. Mann-Kendall tau and p-values are reported in Appendix B-Notably, a limited number of points had statistically significant (Mann-Kendall p-value $\leq 0.05$) temperature trends for January, March, April, June, and December. All other remaining months had no statistically significant trends for any of the study points.

## 3.2. HL-RDHM Implementation and Calibration

The Hydrologic Laboratory Research Distributed Hydrologic Model (HL-RDHM; Koren et al., 2004) is a spatially distributed, computationally efficient model that implements the Sacramento Soil Moisture Accounting (SAC-SMA) runoff model and its extension, the Sacramento– Heat

Transfer Evapotranspiration (SAC-HTET; Kim et al., 2013). The model divides the soil strata into an upper and a lower zone, with water storage within each zone divided into tension and free water storages. The SAC-HTET augments SAC-SMA by incorporating surface temperature in calculating evapotranspiration and therefore offering the ability to examine impacts of temperature trends on the long-term water balance and naturalized (i.e., unregulated) streamflow. The grid-based model uses the NWS Hydrologic Rainfall Analysis Project (HRAP) grid coordinate system. HL-RDHM combines the gridded water balance module with a kinematic routing scheme to simulate naturalized streamflow. HL-RDHM SAC-HTET uses Noah soil moisture distribution and ET with ET demand calculated using the Penman equation. Other processes include bare soil evaporation, rootzone uptake, and redistribution of soil water using Richard's equation.

HL-RDHM has previously been applied in Texas over the Lavaca River Basin to study discharge to Matagorda Bay (Zhang et al., 2020). Implementation and calibration procedures for HL-RDHM are briefly summarized herein and described in detail in prior work (Zhang et al., 2020) and model documentation (Anderson et al., 2002; Koren et al., 2004). HL-RDHM is implemented for the entire Brazos River Basin and on a full HRAP grid mesh (~ 4-km resolution). The hydrologic connectivity is implemented based on topography data available a prior in HL-RDHM. Subbasin outlets are visually identified from NHD-Plus flow network data. Locations of the 58 daily Brazos WAM control points are identified using shapefiles for the monthly Brazos WAM, publicly available from TCEQ. The monthly Brazos WAM contains 77 control points (TCEQ; Wurbs, 2005). The daily WAM contains disaggregated monthly naturalized flows at a subset of 58 control points (Wurbs, 2019). These daily WAM records are used as 'observations' of naturalized flows for model calibration (Section 4.2.2) as they are reconstructed naturalized flow records.

The model is run at hourly time steps for a simulation period from February 1979 - 2017 as determined by the availability of forcing data (Section 4.3) and WAM records. The first 23 months of HL-RDHM simulated flows are used to 'spin up' the model to prevent numerical errors. Output for this period is not analyzed in this study. Rather, model output from 1982 – 2017 is used in the trend analysis.

The HL-RDHM is first implemented using SAC-SMA with manual calibration then extended to the SAC-HTET module to further refine calibration. The SAC-SMA model requires seventeen parameters summarized in Table 3-1. Eleven of the seventeen parameters can be estimated from a combination of soil texture and land cover data through an a priori estimation scheme available in HL-RDHM as described in Koren et al. (2004). Observations from USGS stream gauge stations, including cross-section area, discharge, and flow velocity, are used to estimate channel routing parameters throughout the Basin via the rating curve method. Gridded channel routing parameters across the model extent can then be estimated from the USGS stations via an HL-RDHM module.

HL-RDHM is calibrated using gridded, historic precipitation and temperature forcings (Section 4.1) and fit to WAM records of daily naturalized flows, which are nearly identical to USGS observations. Six of the seven control points used in this study had daily WAM records. CFRO13 does not have daily naturalized flows available in the direct input files for the daily

Brazos WAM . While the WAM can be run to obtain the daily naturalized flows for CFRO13, this study used the USGS streamflow data for the corresponding gage 8083100 to calibrate HL-RDHM at this location. A visual comparison of monthly USGS streamflow and monthly WAM records for CFRO13 showed minimal differences in monthly flows. Additionally, the 2019 daily WAM uses USGS gage daily streamflow for 1998-2017 to disaggregate monthly data. Therefore, it was assumed that daily USGS streamflow would serve as a valid proxy for naturalized flows from the WAM for CFRO13.

Points are calibrated in order of most upstream to downstream as upstream locations impact downstream flows. A calibration period of 1997–2017 is used and 1982–1996 is held as a validation period. The calibration is done first using automatic searching via the Sequential Line Search option provided by the model (Kuzmin et al. 2008), and then manual adjustments following the guidelines from NWS. Parameters that are altered include UZFWM, UZTWM, and UZK, LZTWM, LZFWM (see Table 3-2 for definitions).

**Table 3-2 Parameter Definitions in SAC-SMA.**

| Parameter | Parameter Name and Units |
|---|---|
| UZTWM | Upper Zone Tension Water Capacity (mm) |
| UZFWM | Upper Zone Free Water Capacity (mm) |
| UZK | lnterflow depletion rate ($day^{-1}$) |
| ZPERC | Ratio of maximum/minimum percolation rate |
| REXP | Shape parameter for percolation curve |
| LZTWM | Lower zone tension water capacity (mm) |
| LZFSM | Lower zone supplemental free water capacity (mm) |
| LSFPM | Lower zone primary free water capacity (mm) |
| LZSK | Depletion rate of lower zone supplemental water storage ($day^{-1}$) |
| LZPK | Depletion rate of lower zone primary water storage ($day^{-1}$) |
| PFREE | Percolation fraction to lower zone free water |
| PCTIM | Percentage connected impervious surface |
| ADIMP | Additional impervious surface |
| RIVA | Riparian vegetated area |
| SIDE | Deep recharge to channel baseflow |
| RSERV | Lower zone free water not transferable to tension water |
| EFC | Effective forest cover |

The fit of the calibrated HL-RDHM SAC-HTET model is assessed for the calibration (Tables 3-3 and 3-4) and validation (Table 3-5) periods using percent bias and coefficient of determination $R^2$ to represent goodness of fit in terms of streamflow magnitude and timing, respectively.

**Table 3-3 Bias in HL-RDHM simulations for the calibration period, 1997-2017**

| Control Point | WAM/USGS Average Naturalized Flow (AF/day) | RDHM Control Average Naturalized Flow (AF/day) | Percent Bias |
|---|---|---|---|
| AQAQ34 | 258.61 | 265.57 | 2.69 |
| BRSE11 | 379.86 | 355.07 | -6.53 |
| CFRO13* | 5.99 | 6.41 | 6.96 |
| DMAS09 | 191.86 | 173.46 | -9.59 |
| DMJU08 | 68.30 | 67.38 | -1.35 |
| RWPL01 | 1.48 | 6.08 | 311.12 |
| SFAS06 | 84.10 | 81.13 | -3.53 |

*Calibrated to USGS streamflow records rather than WAM

The calibration period percent bias is < 10% for all control points except RWPL01, which has an exceptionally high percent bias. This control point also has the lowest average naturalized flow of the seven locations, including prolonged periods of zero flow conditions. Therefore, the HL-RDHM control simulation significantly overpredicts streamflow for this control point given the difficulty in reproducing low and zero flow conditions. The model underestimates flow at four points (BRSE11, DMAS09, DMJU08, SFAS06) as indicated by negative percent bias, and overestimates at the remaining three points (AQAQ34, CFRO13, RWPL01).

The coefficient of determination ($R^2$) between the WAM naturalized flow records and the model output are determined for daily, monthly, and annual timescales (Table 3-3).

**Table 3-4 Coefficient of correlation between WAM and HL-RDHM control naturalized flow, calibration period, 1997-2017.**

| Control Point | Daily $R^2$ | Monthly $R^2$ | Annual $R^2$ |
|---|---|---|---|
| AQAQ34 | 0.28 | 0.87 | 0.92 |
| BRSE11 | 0.49 | 0.76 | 0.78 |
| CFRO13* | 0.26 | 0.25 | 0.05 |
| DMAS09 | 0.14 | 0.61 | 0.66 |
| DMJU08 | 0.59 | 0.78 | 0.87 |
| RWPL01 | 0.28 | 0.51 | 0.43 |
| SFAS06 | 0.37 | 0.70 | 0.62 |

*Calibrated to USGS streamflow records rather than WAM

For a given control point, the $R^2$ generally increases as the resolution of the data becomes less fine. Only two control points have a daily calibration $R^2$ at or above 0.50, but 6 have for monthly and five have for annual. The difference between daily and monthly $R^2$ is especially large for most control points. Three control points actually have a lower annual $R^2$ than monthly $R^2$: CFRO13, RWPL01, and SFAS06. The decrease is small for RWPL01 and SFAS06, but it is significant for CFRO13, from 0.25 to 0.05. Furthermore, CFRO13 does not see an increase in $R^2$

from daily to monthly. It also has the lowest calibration monthly and annual $R^2$ of the seven control points.

**Table 3-5 Percent bias and coefficient of correlation between WAM/USGS and HL-RDHM control naturalized flow, validation period, 1982-1996.**

| Control Point | Percent Bias | Daily $R^2$ | Monthly $R^2$ | Annual $R^2$ |
|---|---|---|---|---|
| AQAQ34 | -27.43 | 0.67 | 0.82 | 0.81 |
| BRSE11 | -59.95 | 0.33 | 0.56 | 0.81 |
| CFRO13* | -63.22 | 0.31 | 0.54 | 0.71 |
| DMAS09 | -47.35 | 0.26 | 0.48 | 0.87 |
| DMJU08 | 19.19 | 0.29 | 0.46 | 0.63 |
| RWPL01 | -24.39 | 0.13 | 0.31 | 0.17 |
| SFAS06 | -62.15 | 0.52 | 0.55 | 0.74 |

*Calibrated to USGS streamflow records rather than WAM

Similar $R^2$ are observed for the validation period (Table 3-4), except some of the values are lower, especially for RWPL01. Annual $R^2$ are the highest among the timescales for every control point except RWPL01. CFRO13 has significantly better $R^2$ in the validation period than the calibration period, particularly for annual timescale. The overall fit of the HL-RDHM control simulation naturalized flow results to the WAM records is suitable (Table 3-2, Table 3-3) for the calibration period. With the exception of RWPL01, all percent biases for the calibration period are low (< 10%) and the $R^2$ are acceptable, particularly at larger timescales.

However, the model has higher percent bias over the validation period (Table 3-4). The percent biases in the validation period are much higher than calibration, with three exceeding 50% (BRSE11, CFRO13, SFAS06). The negative percent biases of all the control points except DMJU08 also reflect the average HL-RDHM control streamflow results being higher than the WAM records during this period. The WAM records have a significant fraction of days with zero runoff, including four points with > 25% of daily flows as zero flow (AQAQ34, CFRO13, DMJU08, RWPL01), and one point with > 50% zero flows (RWPL01). The hydrologic model rarely simulates zero flow rate days, resulting in very high percent bias for low flow points. This is especially true for the control points with the most zero flow days, DMJU08 and RWPL01. Given that RWPL01 is the control point with the most zero flow days (and lowest average flow), this limitation may explain why the percent bias for this control point is so extreme (311% for calibration), and its $R^2$ is low relative to other control points, especially outside the calibration period. Potential biases for low flow points are taken into account when interpreting results of perturbation experiments.

## 3.3. Temperature Perturbation Experiments

The overarching methodology (Figure 3-3) involves preparation of precipitation and temperature forcing datasets, detrending of temperature data, implementation of a hydrologic model, simulation of naturalized flows for both control and detrended temperature conditions, and simulation of regulated flows for both conditions. Simulated naturalized flows and regulated flows are then evaluated statistically to elucidate potential impacts of increasing temperature on streamflow in the Upper Brazos River Basin.

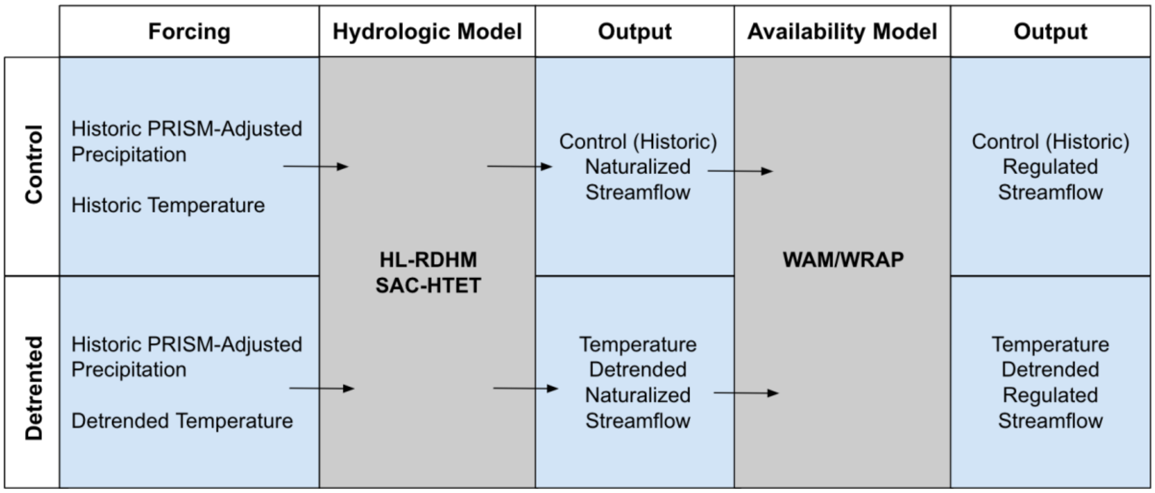


**Figure 3-3** **Overarching methodology of the temperature perturbation experiments.**

Summary statistics are calculated to quantitatively compare naturalized flows for the control and detrended simulations. First, the average flows are compared among the WAM, HL-RDHM control, and HL-RDHM detrended results for the study period. The percentage difference between the detrended and control average naturalized flows is calculated by:

$$Percent\ Difference\ (\%) = 100 * \left(\frac{Q_{RDHM\ Detrended} - Q_{RDHM\ Control}}{Q_{RDHM\ Control}}\right)$$

where QRDHM Detrended is the average naturalized flow for the HL-RDHM detrended simulation results from 1982 – 2017, and QRDHM Control is the average naturalized flow for the HL-RDHM control simulation results from 1982 – 2017. Percentiles of the naturalized flow records are used to compare the distributions of HL-RDHM-simulated and WAM streamflow at each specific control point. A particular focus is given to the percentiles 25th, 50th, and 75th, as well as high magnitude flows (HMFs). For the Texas region, HMFs are defined as at or above the 95th percentile of flows (Yang and Scanlon, 2019). Box and whisker plots are generated to visualize the distribution. The aim of this analysis is to better understand how temperature trends might be impacting low and high flows.

Trends in streamflow over time are evaluated using Mann-Kendall tests. Preceding studies USGS2020 and FNI2022, used Mann-Kendall to evaluate trends in USGS gauge data and WAM naturalized flows, respectively. Consistent with prior work, this study used Mann-Kendall with a p-value threshold $\leq 0.05$ for statistical significance using the R function “MannKendall” in the package “Kendall” (RDocumentation). Mann-Kendall analysis is well suited because it can handle outliers and a low number of data points. For this study, there are 36 data points in annual

streamflow (1982 – 2017) to consider which is above the minimum data requirement (~ 10 points) for Mann-Kendall (FNI2022). It should be noted that Mann-Kendall is not well suited for data with seasonal variation; therefore, it is generally not used on raw monthly or daily streamflow records. A separate test called Seasonal Mann-Kendall is applicable to these records. Data must be aggregated to annual to be analyzed with the original Mann-Kendall test.
The Mann-Kendall test is performed for various timescales and flow characteristics on the HL-RDHM-modeled naturalized flows, including (1) control simulations, (2) temperature detrended simulations, and (3) difference between magnitude and percentage difference in control and temperature detrended simulations. To allow for direct comparison with ‘observations’, the WAM naturalized flow records over the same study period of 1982 – 2017 are used. Specific analyses included trends in annual streamflow, annual peak streamflow, individual seasons, and individual months, similar to USGS2020. This study used the same three seasons considered in USGS2020 as summarized in Table 3-5. When calculating annual peak or annual minimum streamflow, the maximum or minimum daily streamflow is determined within each year and the Mann-Kendall test is performed on this record.

**Table 3-6 Seasons considered for Mann-Kendall trend analyses as used by Harwell et al., 2020**

| Season | Start Date | End Date |
|---|---|---|
| Winter | November 1st | February 28/29th |
| Spring | March 1st | June 30th |
| Summer | July 1st | October 31st |

Finally, the Mann-Kendall and percentile analyses are combined to determine trends in the annual streamflow volumes separated by the 25th, 50th, 75th, and 95th (HMF) percentiles. First, daily naturalized WAM flow data are used to calculate streamflow thresholds (AF/day) for percentiles of interest. These thresholds are then used to sum the streamflow volumes for each year corresponding to each percentile and each point (i.e., an annual total volume for each percentile). The WAM thresholds are used for all simulated data to control for potential variations in percentile distributions in the simulated streamflow. Then, Mann-Kendall is performed on annual total volumes for each percentile.

All the statistical tests used on the streamflow volume time series are summarized in Table 3-6.

**Table 3-7 Statistical tests used for comparison of temperature detrended and control naturalized and regulated flow.**

| Statistical Test | Flow Type | Timescale and Description |
|---|---|---|
| Percentage difference | Naturalized | Entire Period, 1982-2017 |
| | Regulated | Entire Period, 1982-2017 |
| Box and Whisker | Naturalized | Daily |
| Mann-Kendall | Naturalized | Annual |
| | | Annual Peak |

| | | |
|---|---|---|
| | | Annual Minimum |
| | | Annual Difference |
| | | Annual Percentage difference |
| | | Individual Seasons |
| | | Individual Months |
| | | Annual, within Percentile Ranges |
| | | Individual Seasons, within Percentile Ranges |
| | | Individual Months, within Percentile Ranges |
| | Regulated | Annual |
| | | Annual Difference |
| | | Annual Percentage difference |

Given the importance of streamflow trends on water rights, this study further examined the impact of temperature on regulated flows. The temperature detrended naturalized flow results from the HL-RDHM presented a unique opportunity to investigate the impact of temperature on regulated flow in the Brazos River Basin. To accomplish this, the HL-RDHM simulated naturalized flows, both control and temperature detrended, are used as input to the Water Rights Analysis Package (WRAP) Modeling System (TAMU, 2022).

Briefly, both the daily Brazos WAM and WRAP are published by the TCEQ. The WAM and WRAP are designed to work together. The WAM includes basin specific data on water rights (including permitted withdrawals and discharges), net evaporation-precipitation, monthly/daily naturalized flow, etc. The period of record of these files is 1940 – 2017 for the Brazos WAM (TCEQ; Wurbs, 2019). The version of the Brazos WAM used for this study is referred to as “fully authorized,” meaning it assumes that water rights holders use all the water they are authorized to in their permits.

These files are used as input to the WRAP software, which allows users to simulate how much water would be available at each control point after water rights appropriations have taken place, referred to as regulated flow. Reflecting how TCEQ handles water rights in reality, the model sorts water rights in order of priority, starting with senior rights holders. The WRAP can also be run on either daily or monthly resolution (SIM vs SIMD options, respectively).

These input files are used in the WRAP modeling system, which allows users to simulate unappropriated flow for conditions defined in the input files. Unappropriated flow reflect regulation through reservoirs and water supply diversions for water rights holders throughout the basin. The WRAP can also be run on either daily or monthly timestep (SIM vs SIMD options, respectively).

To simulate the impact of detrended temperature within the WRAP modeling system, input files were modified to include temperature-detrended naturalized flows and estimates of temperature-detrended evaporation. Evaporation was estimated using the Penman equation and the temperature detrended data as described in Appendix C. The naturalized flow results from the HL-RDHM simulations replaced the naturalized flow records in the WAM for the seven control points. The monthly naturalized flow records in the WAM are denoted as “IN” and daily are “DF.” With this modified input, the WRAP can be used to generate temperature detrended and control regulated flow records. Three WRAP simulations are run: one where all seven control points had their IN/DF records modified based on the HL-RDHM detrended results, and another based on the HL-RDHM control results. An additional simulation uses the default Brazos WAM files. The WRAP simulations are run over the period January 1st, 1981 to December 31st, 2017, as this is the overlap between the WAM records and HL-RDHM output. Monthly SIM option is run since daily regulated flow results are not needed to perform Mann-Kendall tests.

The simulated monthly regulated flows are used for quantitative comparisons between control and detrended temperature simulations, including trend analyses, consistent with the analyses conducted for HL-RDHM-simulated naturalized flows.

The temperature perturbation experiments demonstrate a modest yet statistically significant impact of increasing temperature on declining annual streamflow at all selected points in the upper and middle Brazos River Basin. All points evaluated in this study showed greater average naturalized streamflow under temperature detrended conditions compared to the historical control conditions over the period of 1982 – 2017 (Table 3-7 and Figure 3-4). The percentage difference ranged from 1.1% to 5.3% across locations studied in the basin. The difference between temperature detrended streamflow and control streamflow is statistically significant ($p < 0.001$) as determined by a t-test. Potential impacts of low flow may exist with points with lower average flows generally associated with a greater percent bias, with the exception of RWPL01 which has the lowest flow (~ three AF/day based on WAM) and a low difference between control and detrended simulations (~ 1.2%). Discrepancies in this trend for RWPL01 could also be attributed to the relatively poorer HL-RDHM calibration metrics (Section 3.2) for this point owing to the difficulty in calibration of low and/or zero flow conditions.

**Table 3-8 Comparison of HL-RDHM detrended and HL-RDHM control naturalized streamflow, 1982-2017.**

| Control Point | WAM/USGS Average Naturalized Flow (AF/day) | RDHM Control Average Naturalized Flow (AF/day) | RDHM Detrended Average Naturalized Flow (AF/day) | Percentage difference |
|---|---|---|---|---|
| AQAQ34 | 255.4 | 230.8 | 234.1 | 1.47 |
| BRSE11 | 511.0 | 323.1 | 328.9 | 1.80 |
| CFRO13 | 10.82 | 6.433 | 6.774 | 5.30 |
| DMAS09 | 214.0 | 154.9 | 156.7 | 1.13 |
| DMJU08 | 58.20 | 61.18 | 63.21 | 3.31 |
| RWPL01 | 3.034 | 5.187 | 5.250 | 1.22 |
| SFAS06 | 121.3 | 74.68 | 76.89 | 2.96 |

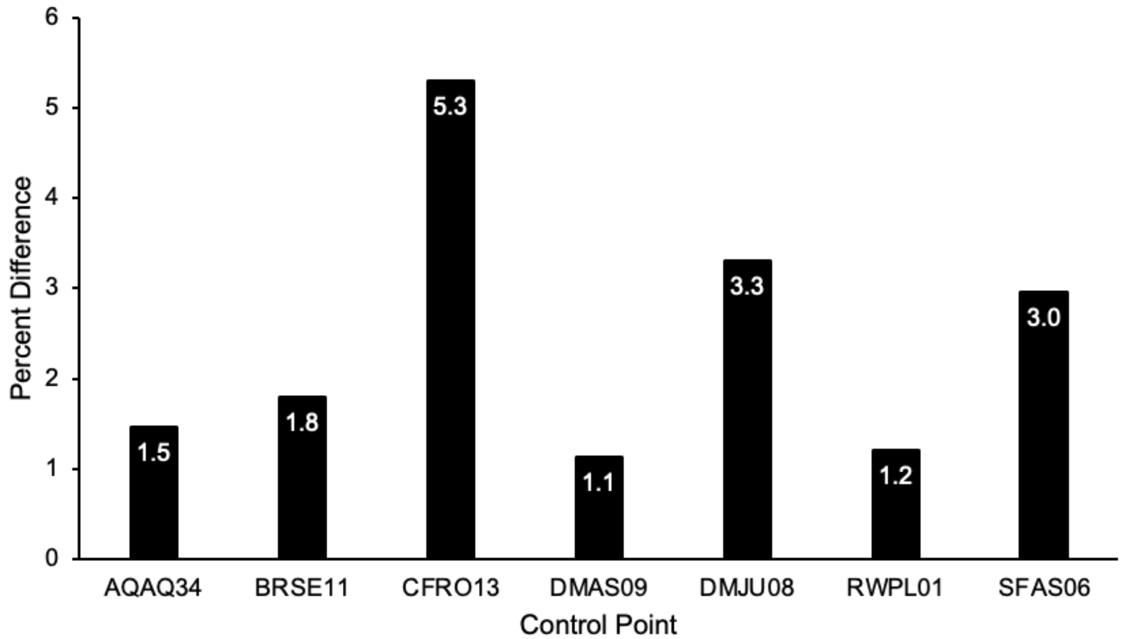


**Figure 3-4 Percentage difference between HL-RDHM detrended and HL-RDHM control average naturalized streamflow, 1982-2017.**

The time series for both the annual and daily difference in detrended and control streamflow showed that it is consistently positive (Figure 3-5 and Appendix Figure B-7). Several control points show a large negative difference during a short period in December 2015, but differences are generally positive, especially in the past two decades. The annual percentage differences also reflect larger differences in streamflow for the results in the second half of the simulation period (2000-2017).

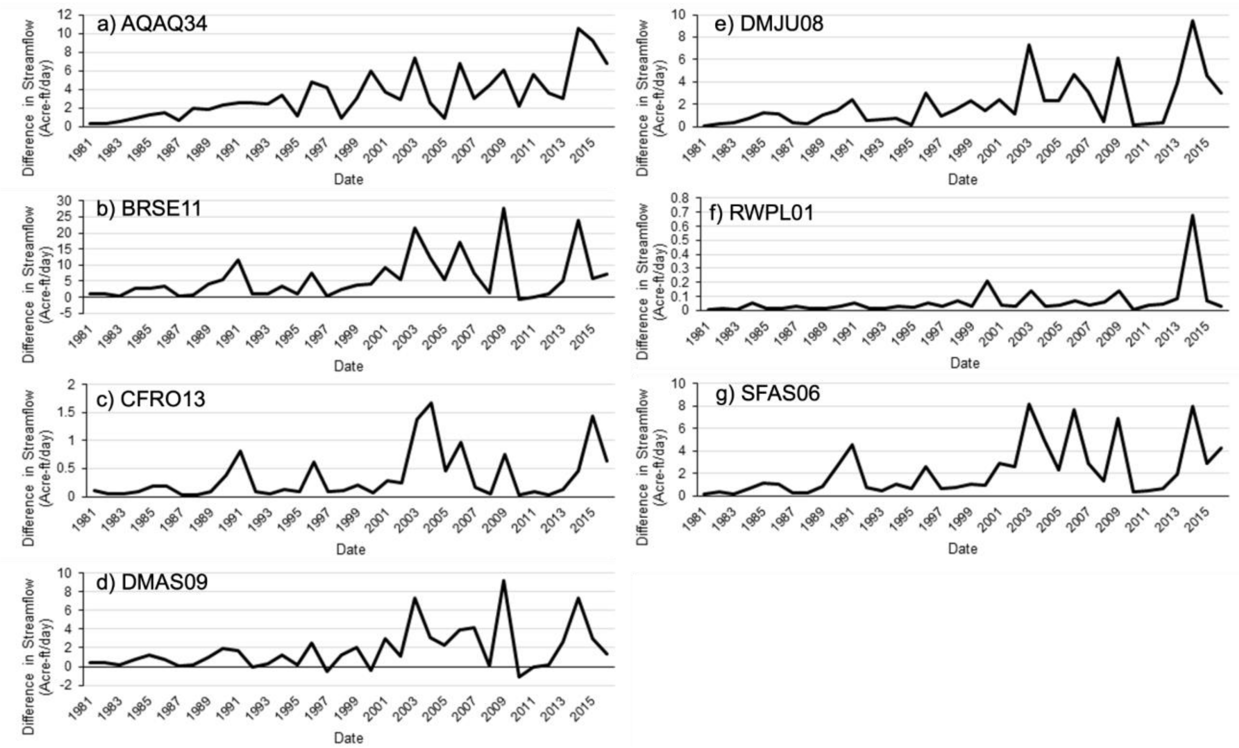


**Figure 3-5 Time series of difference in annual naturalized streamflow between HL-RDHM detrended and control (AF/day). 1982-2017.**

In addition to average annual streamflow, similar differences between detrended and control results are seen for seasonal flows (Appendix B, Table B-1). The average temperature detrended streamflow is consistently, modestly higher than the control results. The HL-RDHM simulation results show lower flow in the winter season and higher flow in the spring season. Interestingly, the WAM naturalized flow results reflect the same trend, but HL-RDHM results overpredict winter flows and underpredict spring flows.

The percentage difference between detrended and control streamflow varies from year to year (Appendix B, Table B-2) over the duration of the study period. Of the 36 annual averages per seven points (252 total annual streamflow percentage differences), only 6 are negative with five of the 6 negative values occurring at point DMAS09 which had the lowest overall, average percentage difference. The highest percentage differences exceeded 10% increases in streamflow with detrended temperature at point CFRO13, which had the highest overall, average percentage difference.

The daily naturalized flow distribution at each control point for the detrended and control simulations are compared using box-and-whisker plots (Figure 3-6). For all points, the detrended daily naturalized streamflow distribution is shifted modestly upwards relative to the control simulation results, with the exception of DMAS09 which is shifted downward for high percentiles. The difference is relatively more pronounced for lower percentiles (i.e., 25$^{th}$; Table 3-8) than higher percentiles (i.e., 75th) (with exceptions of CFRO13 and RWPL01) suggesting that temperature has a relatively greater impact on low flow events than high flows.

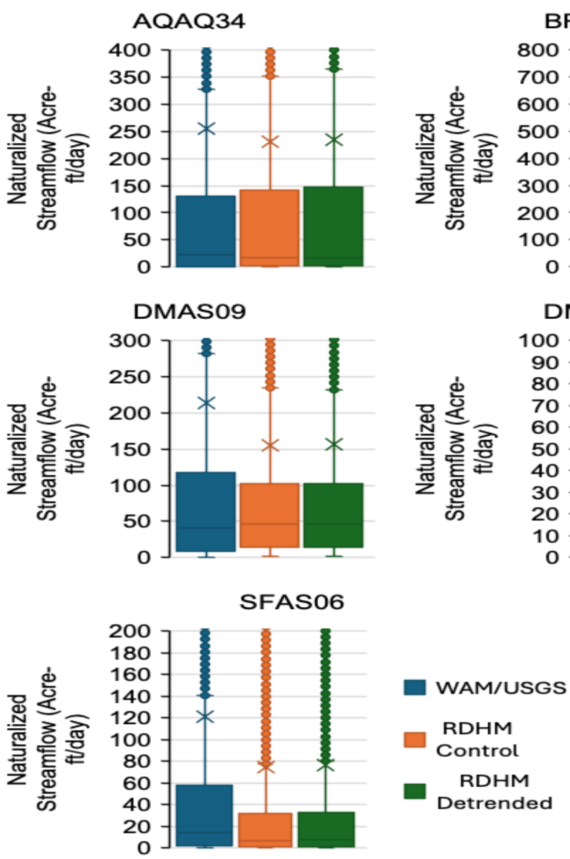


**Figure 3-6 Box and Whisker Plots of WAM, HL-RDHM control, and HL-RDHM detrended daily naturalized streamflow distribution, 1982-2017. Upper and lower whiskers are 90th and 10th percentile, respectively. "X" symbol is the mean flow. The upper side, median line, and bottom side of the colored boxes represent 75th, 50th, and 25th percentiles, respectively.**

**Table 3-9 WAM, HL-RDHM control, and HL-RDHM detrended daily naturalized flow quantiles, 1982-2017.**

| | 25th Percentile | 50th Percentile | 75th Percentile |
|---|---|---|---|

| Control Point | WAM | RDHM Control | RDHM Detrended | WAM | RDHM Control | RDHM Detrended | WAM | RDHM Control | RDHM Detrended |
|---|---|---|---|---|---|---|---|---|---|
| **AQAQ34** | 0.00 | 2.78 | 2.83 | 22.09 | 17.04 | 17.54 | 130.74 | 149.53 | 153.42 |
| **BRSE11** | 40.13 | 30.99 | 31.49 | 111.54 | 76.74 | 76.76 | 318.63 | 198.84 | 200.66 |
| **CFRO13** | 0.00 | 0.05 | 0.05 | 0.95 | 0.28 | 0.32 | 3.77 | 1.72 | 1.89 |
| **DMAS09** | 8.38 | 14.40 | 14.70 | 40.46 | 47.12 | 46.98 | 117.72 | 105.04 | 104.54 |
| **DMJU08** | 0.00 | 0.59 | 0.66 | 0.04 | 4.57 | 4.99 | 1.69 | 33.06 | 35.75 |
| **RWPL01** | 0.00 | 0.27 | 0.27 | 0.00 | 0.94 | 0.95 | 0.05 | 3.52 | 3.55 |
| **SFAS06** | 2.21 | 1.49 | 1.64 | 14.31 | 7.23 | 7.75 | 57.56 | 33.51 | 35.02 |

Despite this difference, the distribution of daily streamflow is skewed similarly for all HL-RDHM simulation results with the mean daily streamflow greater than the median streamflow. The daily streamflow means for each point lie between the 75th and 90th percentile. Many outliers occur corresponding to very high flow events.

This distribution is consistent with the WAM daily naturalized flow records. Unsurprisingly, points with higher calibration metrics exhibited distributions are much more similar to the HL-RDHM simulation results than others. For example, the WAM and HL-RDHM control streamflow distribution at AQAQ34 is relatively more similar than other points. AQAQ34 had a low percent bias and strong $R^2$. Conversely, RWPL01 and DMJU08 showed a very different distribution between the WAM and HL-RDHM streamflow.

The difference between the control and detrended average regulated flows are modest yet statistically significant (t-test p-value < 0.05) at all points. Temperature detrending resulted in an 0.7 to 5.4% increase in regulated flow (Table 3-9, Figure 3-7). As expected, the magnitudes of regulated flow (Table 3-9) are all less than the respective magnitude of naturalized flows (Table X). The percentage differences for detrended and control regulated streamflow are generally positive for individual years (Appendix B, Table B-3). The differences are similar to those observed for naturalized flow, with the exception of AQAQ34 in 2014 representing an outlier with a difference over 65%. The strong similarities between temperature impacts on naturalized flows and regulated flows indicate that regulation of flow does not appear to amplify the effects of temperature on streamflow.

**Table 3-10 Comparison of HL-RDHM detrended and HL-RDHM control regulated streamflow, 1982-2017.**

| Control Point | WAM Average Regulated Flow (Acre-ft/day) | RDHM Control Average Regulated Flow (Acre-ft/day) | RDHM Detrended Average Regulated Flow (Acre-ft/day) | Percent Difference |
|---|---|---|---|---|
| AQAQ34 | 221.5 | 189.2 | 193.0 | 2.0 |
| BRSE11 | 472.6 | 282.6 | 287.8 | 1.8 |
| CFRO13 | 10.7 | 6.28 | 6.62 | 5.4 |
| DMAS09 | 160.7 | 101.6 | 102.3 | 0.7 |
| DMJU08 | 57.28 | 60.31 | 62.33 | 3.4 |
| RWPL01 | 2.34 | 4.12 | 4.18 | 1.3 |
| SFAS06 | 112.1 | 66.19 | 68.37 | 3.3 |

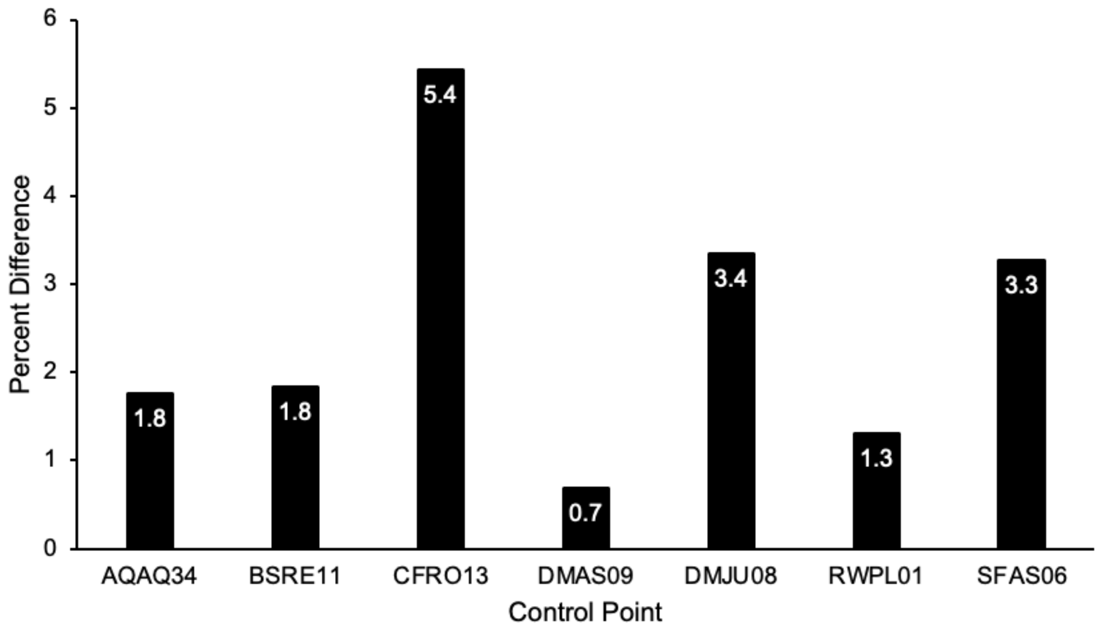


**Figure 3-7 Percent Difference between HL-RDHM Detrended and HL-RDHM Control Average Regulated Streamflow, 1982-2017.**

While temperature detrended evaporation is calculated using the Penman equation (Linacre, 1977) and adjusted in the WRAP software for consistency with detrended experiments, there is negligible impact on regulated flow in the output. Therefore, results are not shown here. This may reflect that only a few control points in the Basin model are adjusted using temperature detrended evaporation records and naturalized flows. Compounding effects of evaporation in reservoirs across the basin could potentially lead to greater declines in water availability if impacts are simulated across all interconnected points of the Basin.

Mann-Kendall trend tests are performed on annual naturalized and regulated streamflow (Figure 3-8 and Appendix B, Figure B-1). The WAM annual naturalized flow records have negative Kendall's tau for five out of the seven control points, four of which are statistically significant declining trends over the study period. This aligns with previous results of trend analysis of WAM records (FNI2021), which found significant declining trends for those same five control points. The HL-RDHM simulation results, both for the temperature detrended and control scenarios, show positive Kendall's tau for 6 of seven control points, but only RWPL01 is statistically significant.

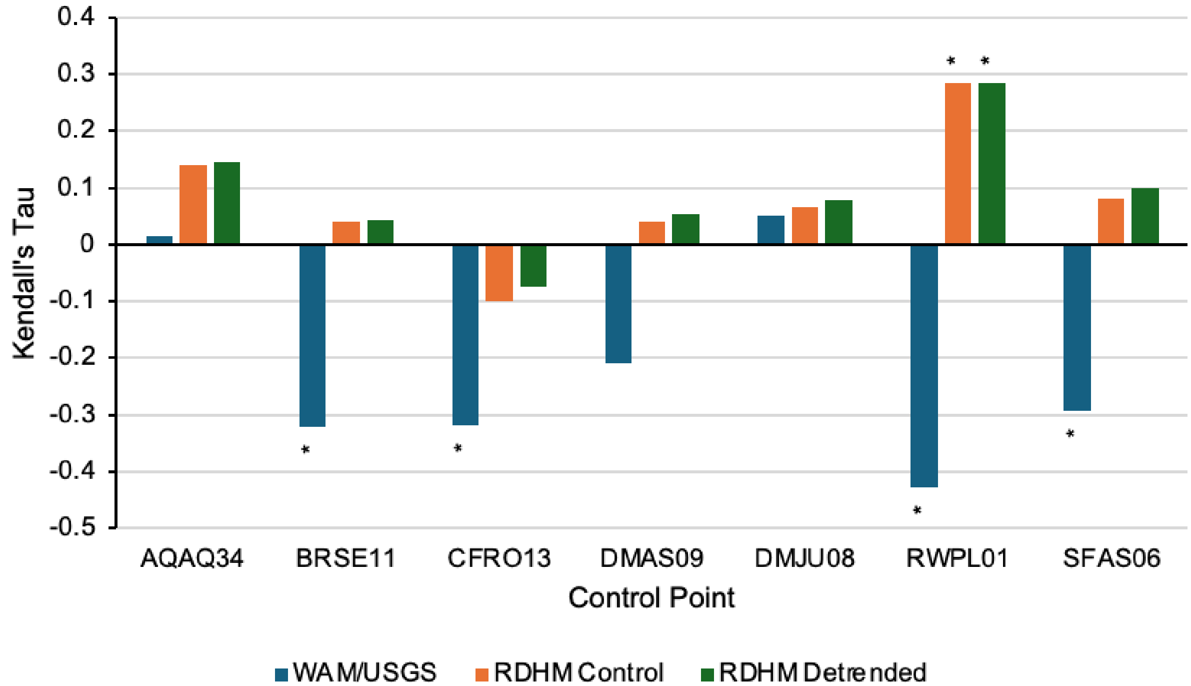


**Figure 3-8 Mann-Kendall test results for WAM, HL-RDHM control, and HL-RDHM detrended annual naturalized streamflow, 1982-2017. Statistically significant results (p<0.05) are reflected by "*" labels.**

There is a small difference in Kendall's tau between the HL-RDHM detrended and control annual naturalized streamflow results. Kendall's tau is greater for the detrended results for all seven control points, but this difference is only 0.01 on average, and most of the trends are not statistically significant. The annual regulated streamflow results (Appendix B, Figure B-1) show nearly identical trends to those seen for annual naturalized streamflow (Figure 3-8) for both WAM and HL-RDHM.

Notably, there is an appreciable and significant trend in the difference between HL-RDHM detrended and control streamflow (Figure 3-9) as calculated by subtracting the simulated detrended streamflow from the control streamflow and taking annual averages in order to perform Mann-Kendall test. This indicates that the impact of temperature on naturalized streamflow is becoming more pronounced over time for the duration of the study period and at all points evaluated. The tau values are positive for all points for both the difference in (1) detrended and control naturalized flows and (2) detrended and control regulated flows. AQAQ34 shows the strongest trend for both differences and corresponds to the only point in the mid-basin. All points show significant increasing trends for naturalized streamflow, and all but DMAS09 show a significant increasing trend for regulated streamflow.

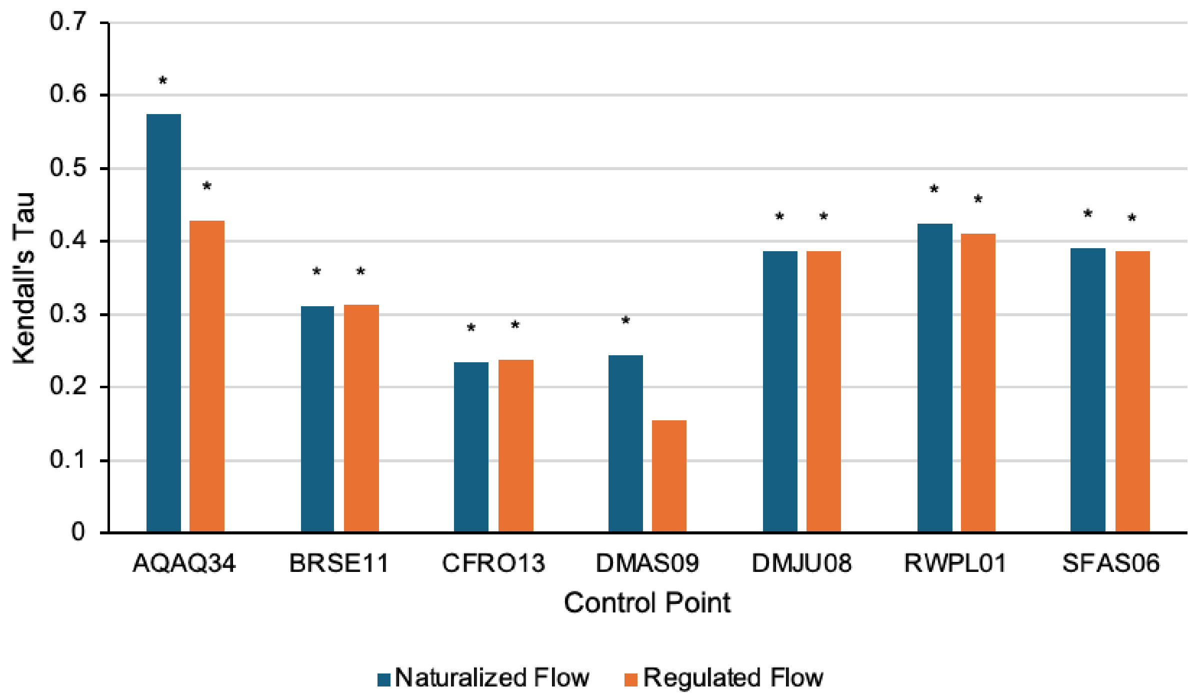


**Figure 3-9 Mann-Kendall test results for difference between HL-RDHM detrended and control annual streamflow, 1982-2017. Statistically significant results ($p<0.05$) are denoted by "*" labels.**

The increasing trend in temperature impact on difference in flow appears to be generally more pronounced for naturalized flows than regulated flows though tau values are comparable (Figure 3-9) but slightly higher for naturalized flows for five of seven points. The two control points which show a large difference are AQAQ34 and DMAS09 which exhibit a lower tau for regulated streamflow differences by 0.14 and 0.09, respectively. No other control points exceeded a difference of 0.02.

The trends in percent difference between HL-RDHM detrended and control streamflow (Appendix B, Figure B-2) show the same trends as those for the magnitude of difference in Figure 3-9 and are also statistically significant. The time series of annual and daily differences in naturalized streamflow (Figure 3-5 and Appendix B, Figure B-7) clearly reflect the positive trend seen in the Mann-Kendall analysis in Figure 3-9. The differences are noticeably higher in the second half of the analysis period (2000-2017). Larger peaks in the difference can be seen in the daily time series during this period.

The Mann-Kendall test is also performed for each individual season and month, aggregated to annual values (Appendix B, Figures B-3 and B-4). The winter season and months saw overall fewer significant trend results relative to annual, and the only significant trends seen are in the WAM naturalized flow records. The HL-RDHM detrended and control Kendall's tau are generally very close to 0 and range very little in either direction. For the spring season and months, the declines are more often significant for WAM records, but again the HL-RDHM results show little significance (only AQAQ34 in April has a significantly increasing trend). However, Kendall's tau values are generally positive for spring even if they are low and usually insignificant. The summer season shows the weakest trends for the WAM records. The only control point which shows significant declining trends is CFRO13. Interestingly, CFRO13 is the only control point that shows declining trends in the WAM for every time scale (annual, individual seasons, individual months). HL-RDHM control and detrended results have stronger positive trends in the summer, particularly for the month of July. For comparison, FNI2021 found similar trends for winter and spring similar, but stronger declines in summer WAM records relative to the results shown here.

Mann-Kendall trend analysis on annual minimum and annual peak streamflow are also performed (Figure 3-10 and Appendix B, Figure B-5), as is done in USGS2020. In general, the trends in annual peak streamflow (Appendix B, Figure B-5) are similar to what is seen for annual naturalized and annual regulated streamflow (Figure 3-8). The WAM record Kendall's Tau are mostly negative and three have statistically significant declining trends, while none of the HL-RDHM results have significant trends. HL-RDHM detrended Kendall's tau are only slightly higher than those for HL-RDHM control.

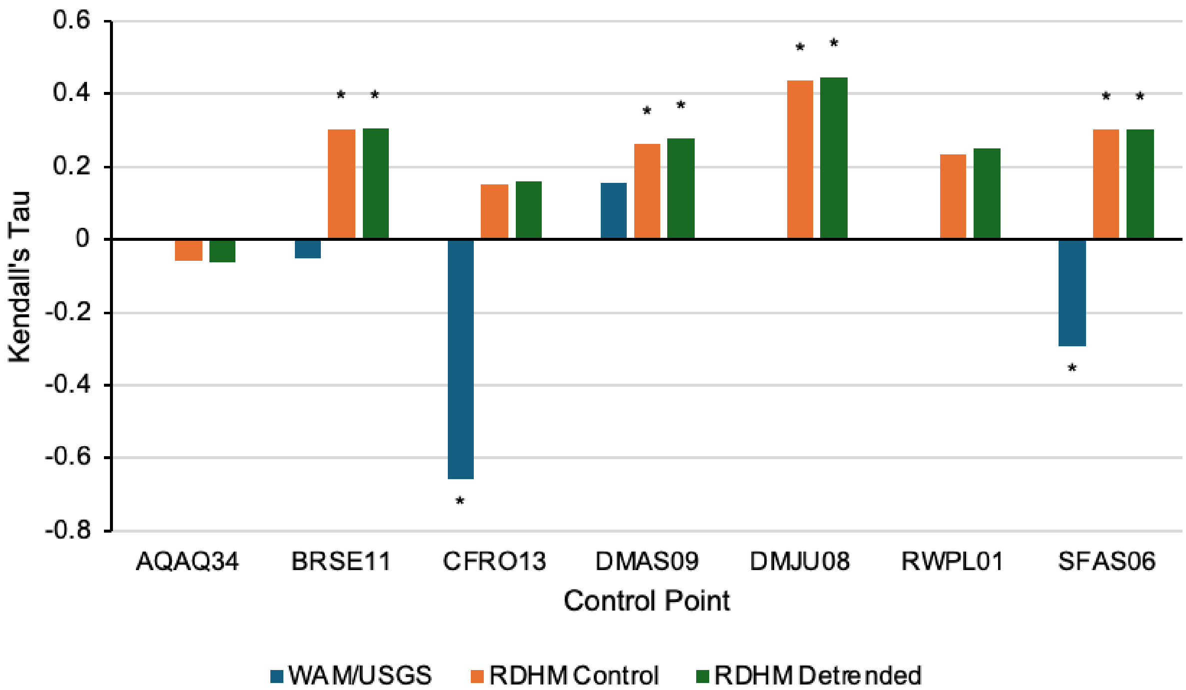


**Figure 3-10 Mann-Kendall test results for WAM, HL-RDHM control, and HL-RDHM detrended annual minimum naturalized streamflow, 1982-2017. Statistically significant results ($p<0.05$) are reflected by "*" labels.**

The trends in annual minimum streamflow (Figure 3-10) diverge strongly from those for annual naturalized streamflow (Figure 3-8). Many of the WAM naturalized flow records have no trend in annual minimum streamflow, even insignificant ones (in other words, $\tau$=0). Only two are statistically significant. The HL-RDHM simulation results show significant increasing trends in annual minimum streamflow for four out of seven control points. This is the only HL-RDHM record on which the Mann-Kendall test is performed that showed most of the control points having significant increasing trends in streamflow.

The Mann-Kendall test is also performed for total annual flows within percentile ranges, including the four quartiles and HMF events. Furthermore, the total flows within these percentile ranges are again divided by individual seasons and individual months to perform trend analysis. The results for HMF events are highlighted in Figure 3-11.

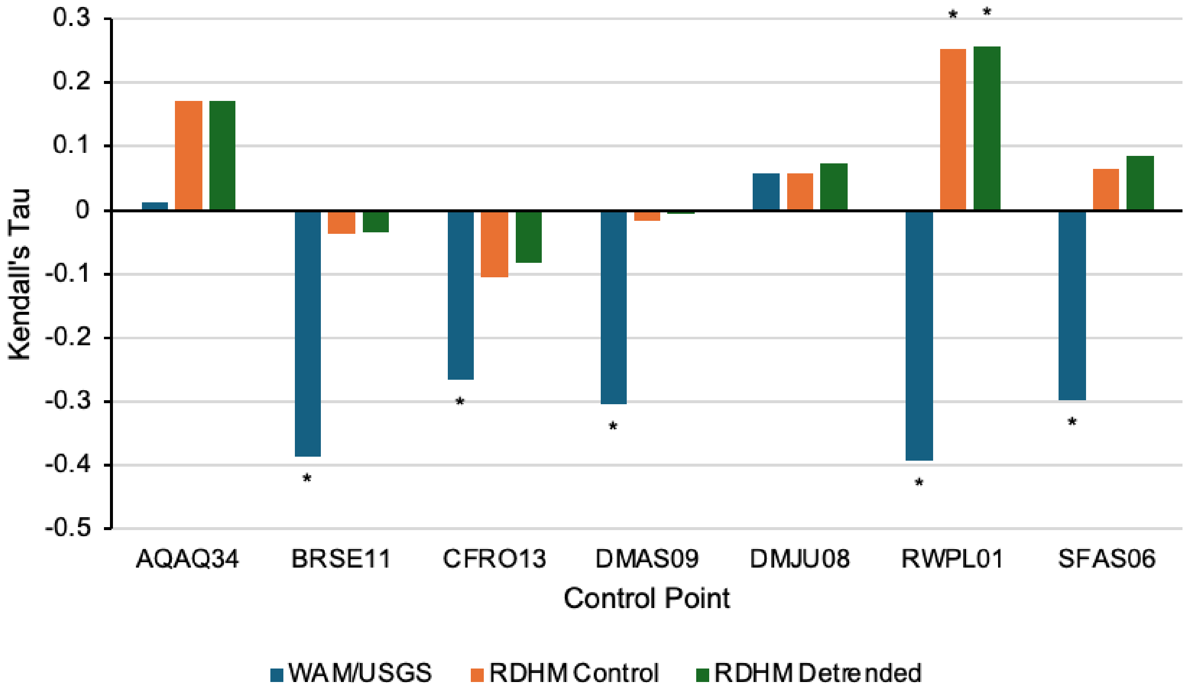


**Figure 3-11 Mann-Kendall test results for WAM, HL-RDHM control, and HL-RDHM detrended annual HMF total naturalized volume, 1982-2017. Statistically significant results ($p<0.05$) are reflected by "*" labels.**

The trends in HMF event total volume are extremely similar to those for annual naturalized streamflow (Figure 3-8). Most WAM records have a declining trend and only one HL-RDHM control point shows statistically increasing trends (RWPL01). Mann-Kendall tests are performed on HMF volume for each season. The results for the spring season are similar to Figure 3-11, but winter and summer seasons are not (Appendix B, Figure B-6). These two seasons instead show very few significant trends for WAM, HL-RDHM Control, and HL-RDHM Detrended HMF results.

Several additional trend analyses for each flow percentile are conducted over various timescales (e.g., individual months and seasons, various percentile ranges) but yielded very few significant trends. Therefore, percentile analyses are not discussed further but are provided in a supporting CSV file for reference.

The HL-RDHM control and temperature detrended results indicate that temperature itself has a modest, yet statistically significant, impact on naturalized and regulated streamflow at study points in the Upper and Middle Brazos River Basin. The temperature detrended results reflect a small increase in average naturalized flow (1.1%-5.3%) and regulated flow (0.7%-5.4%) (Figure 3-4 and Figure 3-7). These results are specific to the upper basin where most of the control points analyzed are located but might be generalizable for the rest of the basin as well. AQAQ34, which is in the middle basin, showed a similar difference in streamflow between the detrended and control simulations as the other 6 control points.

Notably, HL-RDHM temperature perturbation experiments resulted in a statistically significant trend in the difference between detrended and control streamflow magnitude (Figure 3-9). In other words, the impact of increasing temperature on declining streamflow is increasing over time, though the average magnitudes of these increases are modest. Accordingly, this suggests that future conditions characterized by continued increases in temperature may result in more pronounced streamflow declines.

While a series of additional Mann-Kendall trend tests are conducted on the simulated detrended and control streamflow for various timescales and flow characteristics, these seldom yielded significant trends. Specifically, the difference between Kendall’s tau for HL-RDHM detrended and HL-RDHM control is small (only 0.01 on average) , and the trends are not significant for either naturalized and regulated flow (Figure 3-8 and Appendix B, Figure B-1). Since the control simulation did not have a significant trend as observed in the WAM record, it is unlikely that detrended simulations would have exhibited a significant trend.

Results further suggest that, at least when considering a select number of points, temperature impacts naturalized and regulated flows similarly. The differences and trends in naturalized and regulated streamflow are comparable (Figure 3-8 and Appendix B, Figure B-1), which suggests that effects of increasing temperature are not amplified or muted by regulation of flows (e.g., diversions, reservoirs, etc.) represented in the WAM. In contrast, the trends in the difference in annual regulated streamflow between detrended and control simulations varied across points, and one is not statistically significant. The trends with regulated streamflow difference are often slightly less than those for naturalized flow difference and are much less only for AQAQ34 and DMAS09. This suggests a greater variance in the impact of temperature effects on regulated flows across points, particularly for these two control points. In this case, the trend in temperature’s impact is weaker for regulated flow. This may be attributed to AQAQ34 being immediately downstream of the Aquila Reservoir, where large volumes of water are unappropriated, but DMAS09 does not have an associated nearby upstream reservoir.

These results demonstrate that rising temperatures have had a significant impact on streamflow at select points in the Brazos River Basin. However, given the modest nature of the magnitude of this impact, temperature alone likely cannot explain the observed streamflow declines in the upper Brazos River Basin. There are several other complex factors which may contribute to declining streamflow, including land use change, impoundments, and changes to groundwater-surface water interaction which require further investigation.

# 4. Trends in Streamflow/Runoff by Alternative Operational Models

In Section 3, it was shown that the HL-RDHM with SAC-HTET is unable to reproduce the downward trend in streamflow at the four watersheds in the upper basin. In this section, we examine the streamflow simulations from two NWS reanalysis products, namely the NWM and the NLDAS, to determine if either is able to resolve the trends.

## 4.1. National Water Model Reanalysis

The National Water Model (NWM) is a gridded, distributed land surface/hydrologic modeling system that is based on the Weather Research Forecasting-Hydro (WRF-Hydro) system developed at National Centers for Atmospheric Research (NCAR). The first version of NWM became operational at NWS in 2016, and the current operational version is 3.0. A retrospective analysis (reanalysis) is produced each time a new version becomes online.

The structure and workflow of the WRF-Hydro/NWM are shown in Figure 4-1. The modeling system comprises column land surface models, terrain routing modules, and channel/reservoir routing modules. Since its operation, NWM has been using Noah-MP (Noah-MultiPhysics) as the land surface model, which computes a variety of land surface variables including evapotranspiration, runoff, soil moisture etc. In NWM, Noah-MP is coupled with the terrain routing module to compute surface and subsurface flow (interflow), and soil moisture on a 250m grid. The resulting surface/subsurface flow is aggregated onto a 1-km grid and feeds to the channel/reservoir routing module that yields streamflow and other variables.

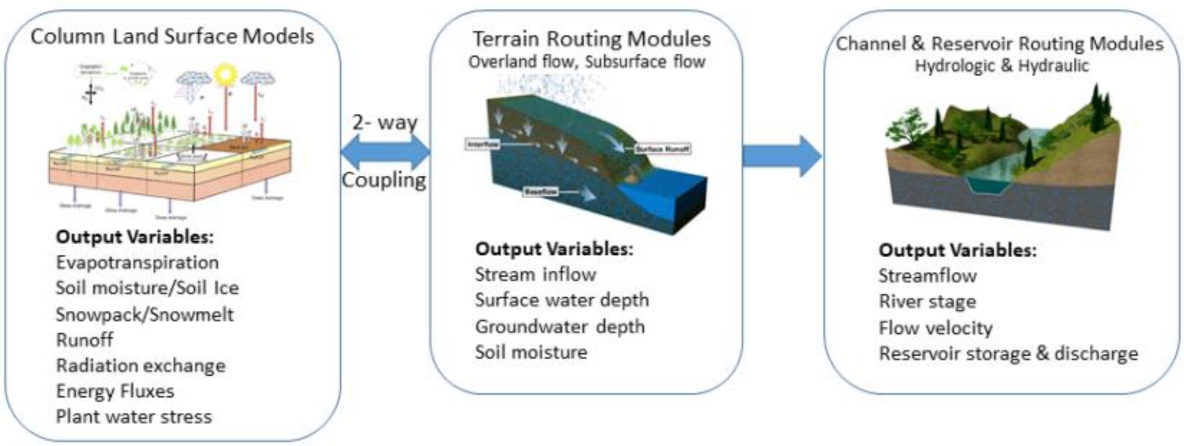


**Figure 4-1 The modules and workflow for WRF-Hydro/NWM. Source: NCAR (2023).**

In this study, we use the NWM 2.1 reanalysis as it was the latest version of reanalysis at the beginning of the project. For each of the WAM control point/USGS stations, we retrieve the streamflow time series from the NWM 2.1 reanalysis archive for the period of 1979-2020. We then compare the time series of annual streamflow from NWM simulations against USG observations and WAM naturalized flow.

Table 4-1 shows the Mann-Kendall statistics computed on annual flow based on NWM reanalysis at each of the seven points that are contrasted with those based on USGS flow observations. The first salient observation is that in none of the sites do the NWM simulated annual flows exhibit statistically significant trends. At most locations (six out of seven), NWM simulations exhibit an upward trend; only at CFRO13 (Clear Fork Brazos River near Roby) is Tau negative, but the trend is statistically insignificant (P-value > 0.05). Among the four sites with statistically significant downward trend, NWM simulations show opposite, rising trends.

**Table 4-1 Trends in USGS flow observations and NWM reanalysis.**

| WAM-ID | USGS_ID | Tau-USGS | P-USGS | Tau-NWM | P-NWM |
|---|---|---|---|---|---|
| AQAQ34 | 08093500 | **0.385** | 0.019 | 0.092 | 0.398 |
| BRSE11 | 08082500 | **-0.254** | 0.016 | 0.126 | 0.246 |
| CFRO13 | 08083100 | **-0.268** | 0.011 | -0.016 | 0.888 |
| DMAS09 | 08080500 | **-0.246** | 0.022 | 0.141 | 0.193 |
| DMJU08 | 08079600 | -0.014 | 0.903 | 0.206 | 0.056 |
| RWPL01 | 08080700 | 0.067 | 0.695 | 0.170 | 0.116 |
| SFAS06 | 08082000 | **-0.296** | 0.005 | 0.010 | 0.931 |

The series of annual mean flows from NWM reanalysis are contrasted against USGS observations and WAM records for each site (Figures 4-2 – 4-8). The annual precipitation series computed from the adjusted AORC product are also shown for context.

Figure 4-2 shows the time series plots for AQAQ34 (Aquilla Creek near Aquilla). This is the only study site where observed flows exhibit an upward trend. From the time series of streamflow, it is evident that the annual flows from NWM reanalysis are bounded in a much narrower range than the observed. The reanalyzed flows tend to be biased high/low for drier/wetter years. The year of 2015 is the wettest year during the period of analysis, featuring the highest annual precipitation. The observed annual flow is correspondingly higher, but NWM only produces a subdued spike.

Figure 4-3 shows the time series plots for BRSE11 (Brazos River at Seymour), situated in the upper basin. The downward trend in the observed annual flow series is appreciable, but NWM reanalysis exhibits a slight upward trend. It is worth noting that this upward trend is mostly due to the presence of a series of large peaks between 2004 and 2010, and in 2015. Additional observations of note include:

- In the 1980s and early 1990s, there are a series of large peaks in the observed streamflow series despite relatively unremarkable precipitation amounts.
- The year of 2004 features the highest precipitation amount, but the annual flow from NWM for that year is less than that for 2015. By contrast, the observed flow is clearly higher in 2004 than in 2015.

Figure 4-4 shows the time series plots for CFRO13 (Clear Fork Brazos River near Roby). This site is also located in the upper basin and the precipitation pattern largely resembles that of BRSE11, with distinctive peaks in 2004 and 2015. At this site, NWM reanalysis is negatively biased in the 1980s, but inflates the magnitude of peaks from 1990 on for a majority of the wet years. Similar to BRSE11, at CFRO13 NWM reanalysis exhibits a severe positive bias over the recent wet years (2015, 2015, 2019). But unlike the latter, the former’s bias over the wet spell of

2004-2010 is more subdued, and for some years (e.g., 2010), it accurately reproduces the annual flow.

Figure 4-5 shows the time series plots for DMAS09 (Double Mountain Fork Brazos River near Aspermont), another site located in the upper basin. The features largely mirror those for BRSE11. A persistent positive bias is seen in the NWM reanalysis, and this bias tends to be more pronounced in recent two decades, leading to a positive trend that diverges from the observation.

Figure 4-6 shows the time series plots for DMJU08 (Double Mountain Fork Brazos River near Justiceburg), a site along the same reach as, but situated upstream of DMAS09. Despite its proximity to the latter, the flow patterns at this site exhibit several distinct features that are summarized as follows.

- While NWM reanalysis exhibits severe positive biases at DMSA09, at DMJU08 it by and large reproduces the magnitude of observed flow for a major of years except 2004 and 2015, for which positive biases are evident.
- At DMJU08, observed streamflow exhibits an upward rather than a downward trend as seen at DMAS09. The observed flow peaks in the 1980s and early 1990s are mostly subdued relative to the later peaks after 2000, opposite of what is observed at DMAS09.

Figure 4-7 shows the time series plots for RWPL01 (Running Water Draw at Plainview), a site near the northern tip of the basin. Notable features include the following ones.

- Streamflow is persistently low at this site across years (~ three cfs), despite that the precipitation amount appears to be on par with other sites in the upper basin. For perspective, mean flow at DMJU08, which features a comparable upstream area, is around 58 cfs.
- NWM reanalysis features the most severe positive biases across years at this site. For 2004 and 2015, hardly any streamflow is seen from observations, whereas NWM produces prominent peaks.
- There is no conspicuous trend in the annual flow from NWM reanalysis, as streamflow is concentrated in a few wet episodes (mid-late 1980, 2004-2010, and 2015-2019).

Figure 4-8 shows the time series plots for SFAS06 (Salt Fork near Aspermont), a site in the upper basin with the largest drainage among the seven. The patterns largely mirror those at DMSA09 and BRSE11, with the NWM reanalysis exhibiting persistent, positive biases in the NWM reanalysis at this site. A subtle difference is that, while the biases are generally more elevated in recent years, this is more a result of declining streamflow response to precipitation. For example, in 2015, while the annual precipitation is higher than that in 2009, the observed flow was much less. By contrast, NWM reanalysis for 2015 is only slightly lower than in 2009.

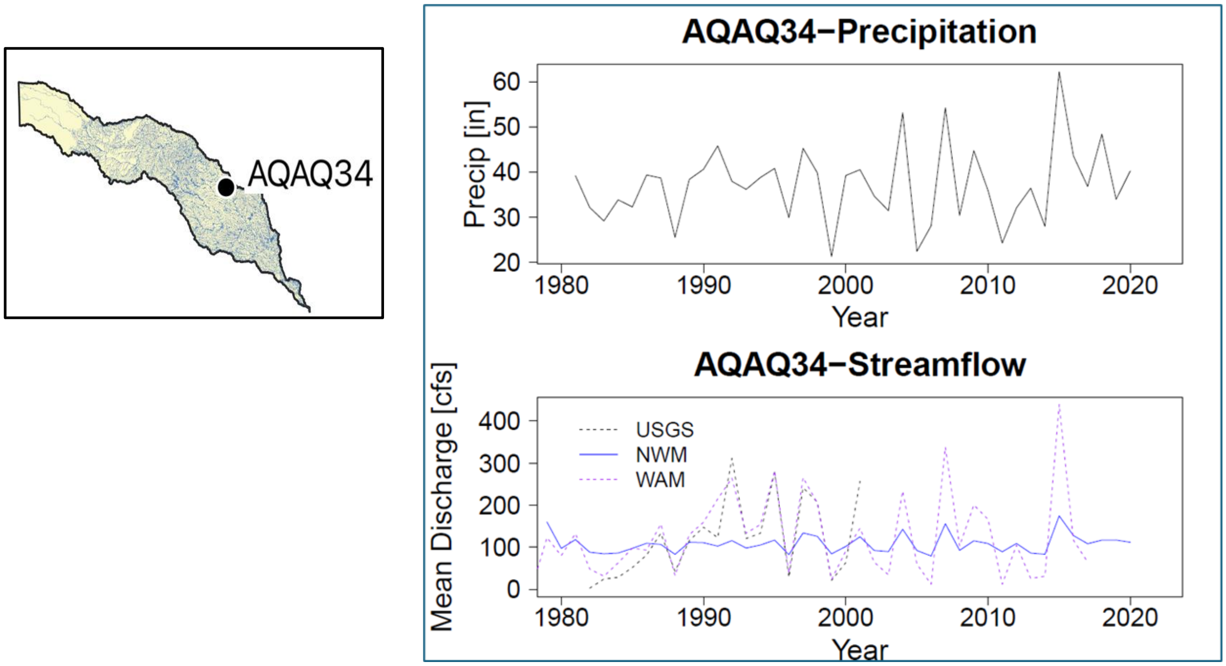


**Figure 4-2** **Time series of annual precipitation (top) and streamflow (bottom) at AQAQ34. The annual streamflow series include those derived from a) NWM 2.1 reanalysis, b) USGS observations, and c) WAM naturalized flow. The location of the WAM ID is illustrated in the map on the left.**

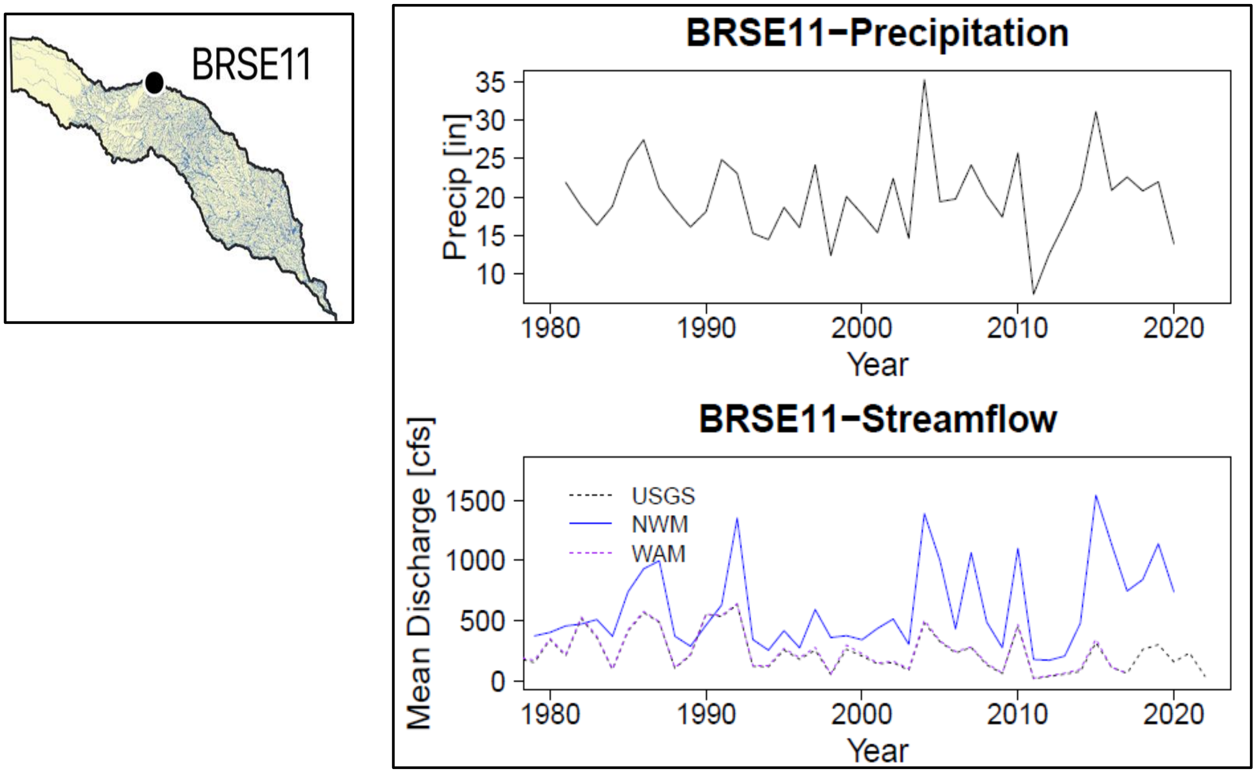


**Figure 4-3 Location of control point BRSE11 (left), and time series of annual precipitation and streamflow at BRSE11 (right). Shown in the bottom right panel are annual streamflow series derived from a) NWM 2.1 reanalysis, b) USGS observations, and c) WAM naturalized flow.**

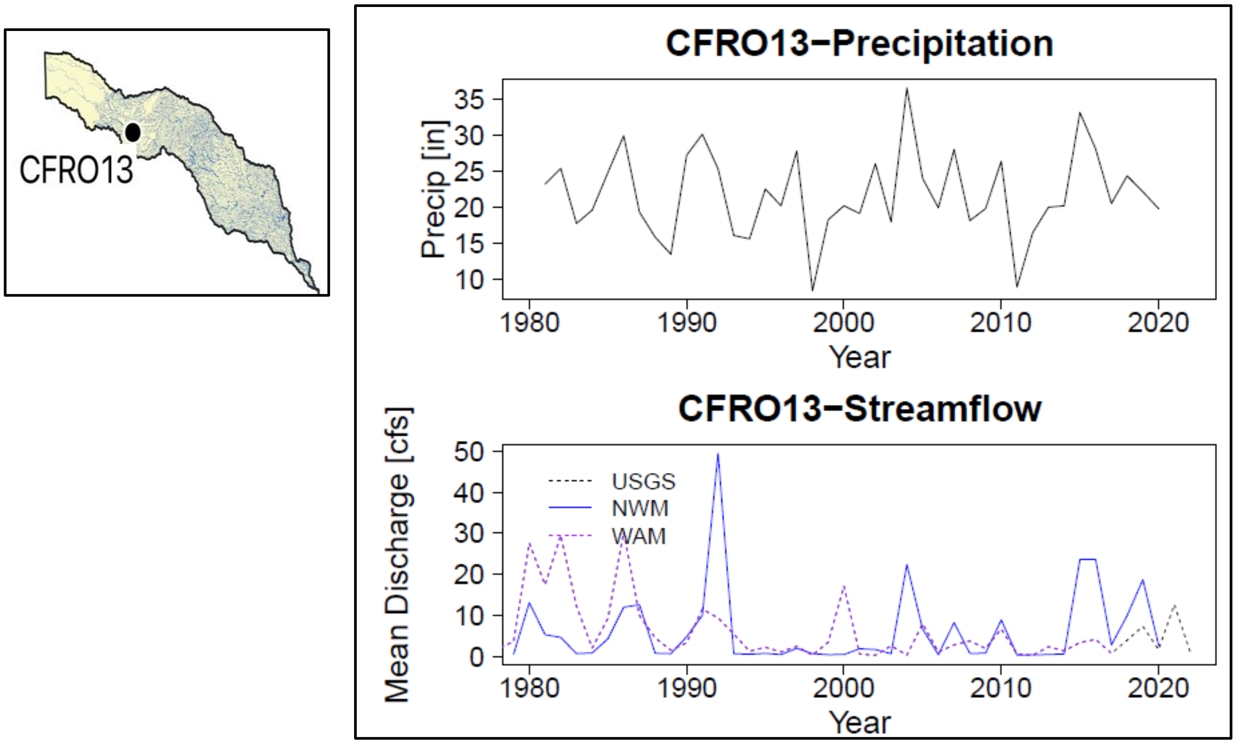


**Figure 4-4 Location of control point CFRO13 (left), and time series of annual precipitation and streamflow at CFRO13 (right). Shown in the bottom right panel are annual streamflow series derived from a) NWM 2.1 reanalysis, b) USGS observations, and c) WAM naturalized flow.**

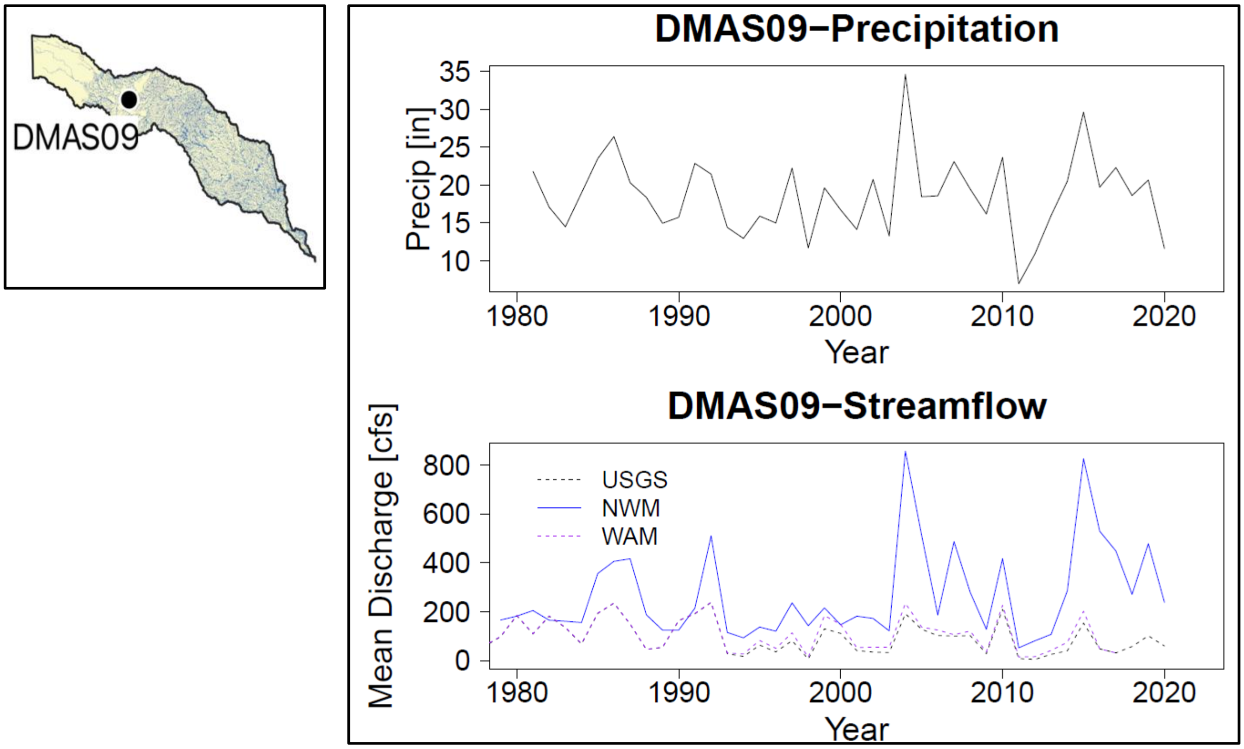


**Figure 4-5 Location of control point DMAS09 (left), and time series of annual precipitation and streamflow at DMAS09 (right). Shown in the bottom right panel are annual streamflow series derived from a) NWM 2.1 reanalysis, b) USGS observations, and c) WAM naturalized flow.**

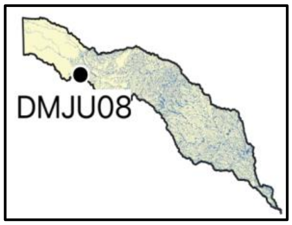


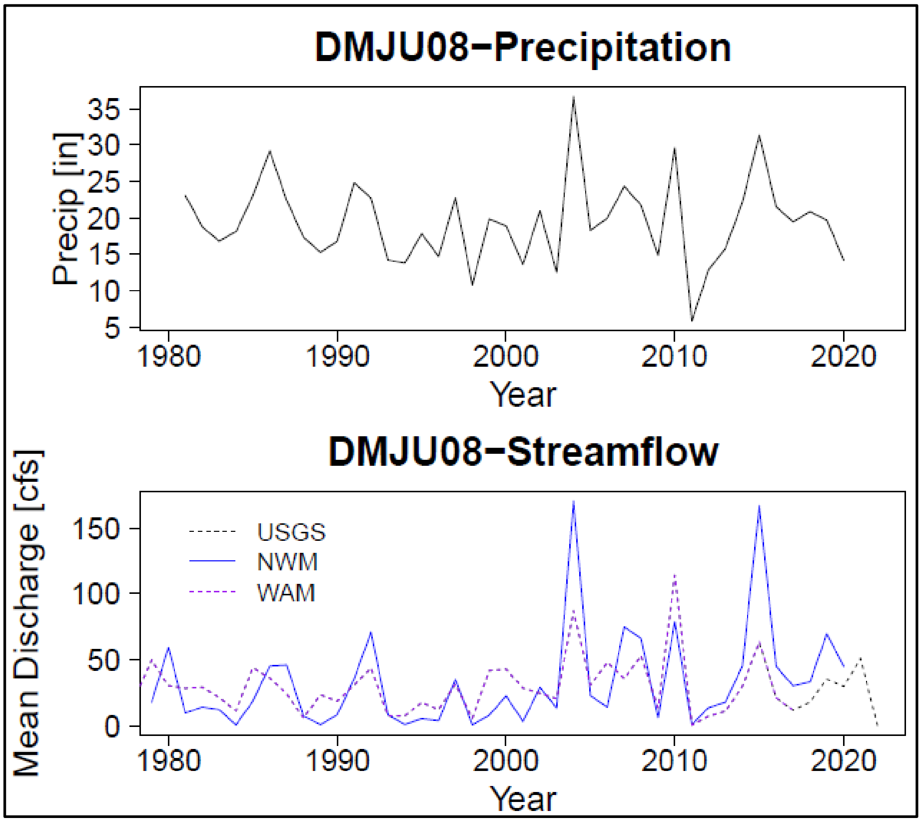


**Figure 4-6 Location of control point DMJU08 (left), and time series of annual precipitation and streamflow at DMJU08 (right). Shown in the bottom right panel are annual streamflow series derived from a) NWM 2.1 reanalysis, b) USGS observations, and c) WAM naturalized flow.**

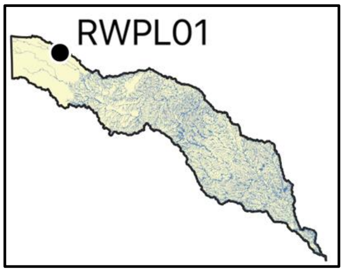


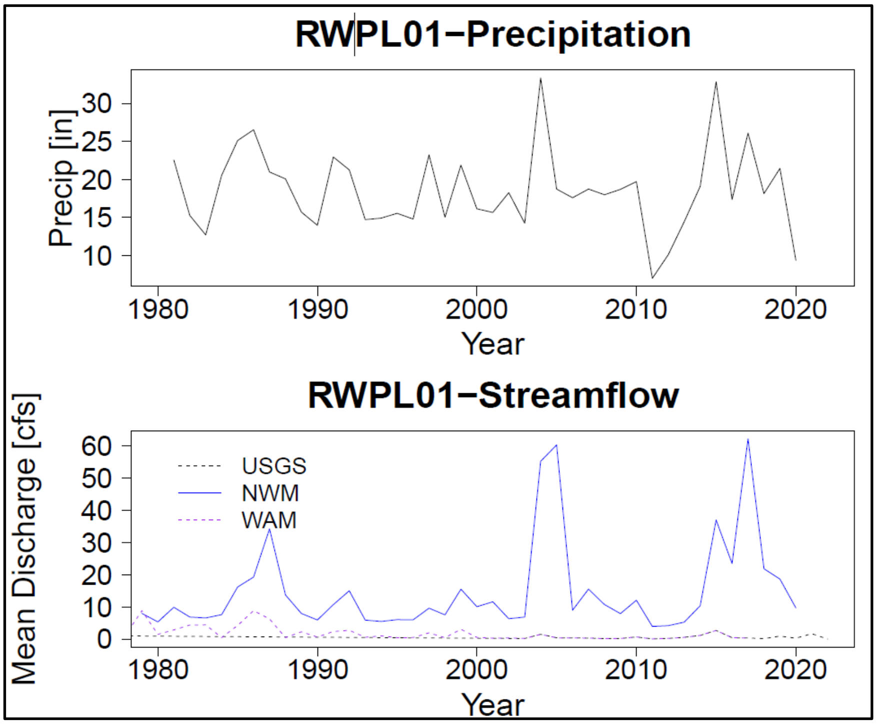


**Figure 4-7 Location of control point RWPL01 (left), and time series of annual precipitation and streamflow at RWPL01 (right). Shown in the bottom right panel are annual streamflow series derived from a) NWM 2.1 reanalysis, b) USGS observations, and c) WAM naturalized flow.**

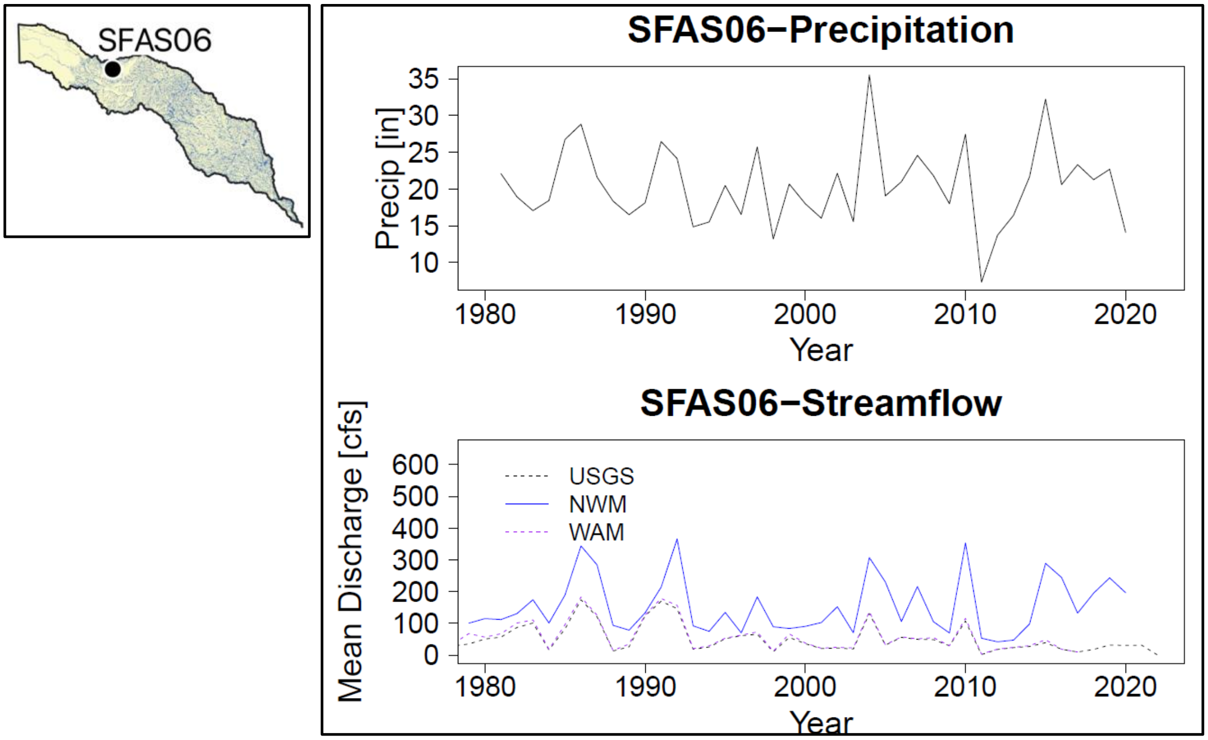


**Figure 4-8 Location of control point SFAS06 (left), and time series of annual precipitation and streamflow at SFAS06 (right). Shown in the bottom right panel are annual streamflow series derived from a) NWM 2.1 reanalysis, b) USGS observations, and c) WAM naturalized flow.**

## 4.2. North America Land Data Assimilation System-Phase 2

The North America Land Data Assimilation System - Phase two (NLDAS-2) is maintained at the NWS National Centers for Environmental Prediction (NCEP). The system comprises several land surface models (e.g., Noah; MOSAIC; VIC; and SAC), each producing analysis of land surface variables such as soil moisture, soil temperature, runoff and evapotranspiration (Xia et al., 2012). The precipitation forcing used in driving the models is derived by interpolating daily gauge reports onto a ⅛ degree grid, and disaggregating the result into hourly products using the hourly Stage-II mosaicked radar precipitation product (Lin and Mitchell, 2005). Note that the land surface models in NLDAS-2 produce runoff but not routed flow products. In this study, we retrieved the gridded runoff product by the Noah and computed the watershed averages. These results are compared against the USGS observations and WAM records in Table 4-2 and in Figures 4-9 – 4-16.

**Table 4-2 Trends in USGS flow observations and NLDAS-2 runoff product**

| WAM-ID | USGS_ID | Tau-USGS | P-USGS | Tau-NWM | P-NLDAS |
|---|---|---|---|---|---|
| AQAQ34 | 08093500 | 0.385 | 0.019 | 0.226 | 0.036 |
| BRSE11 | 08082500 | -0.254 | 0.016 | 0.124 | 0.251 |
| CFRO13 | 08083100 | -0.268 | 0.011 | 0.138 | 0.201 |
| DMAS09 | 08080500 | -0.246 | 0.022 | 0.11 | 0.308 |
| DMJU08 | 08079600 | -0.014 | 0.903 | 0.171 | 0.114 |
| RWPL01 | 08080700 | 0.067 | 0.695 | 0.164 | 0.129 |
| SFAS06 | 08082000 | -0.296 | 0.005 | 0.094 | 0.386 |

From Table 4-2, it is clear that, with the exception of AQAQ34, the NLDAS-2 is unable to reproduce the trends in flow. For AQAQ34, NLDAS-2 annual runoff shows a similar, upward trend that is statistically significant. For the remaining sites, NLDAS-2 runoff fails to exhibit statistically significant trends, and its Tau values are positive at the five sites where observed flows decline, suggesting divergence between the trends from the model simulations and observations.

The time series for each of the sites are shown in Figures 4-9 – 4-16. While NLDAS-2 runoff closely mimics the streamflow at AQAQ34 (Figure 4-9), at all other sites it tends to be much higher than the observed streamflow, pointing to much more severe biases in the water balance calculations at these sites.

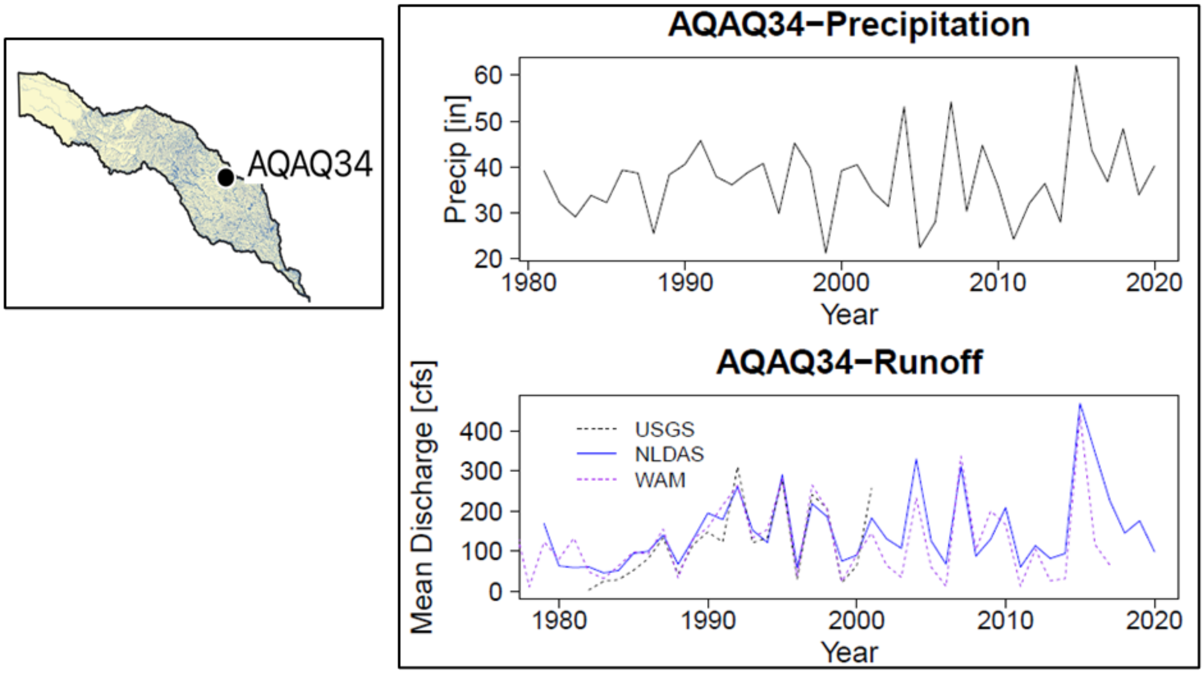


**Figure 4-9 Time series of annual precipitation (top) and streamflow (bottom) at AQAQ34. The annual runoff series include those derived from a) NLDAS-2 analysis, b) USGS observations, and c) WAM naturalized flow. The location of the WAM ID is illustrated in the map on the left.**

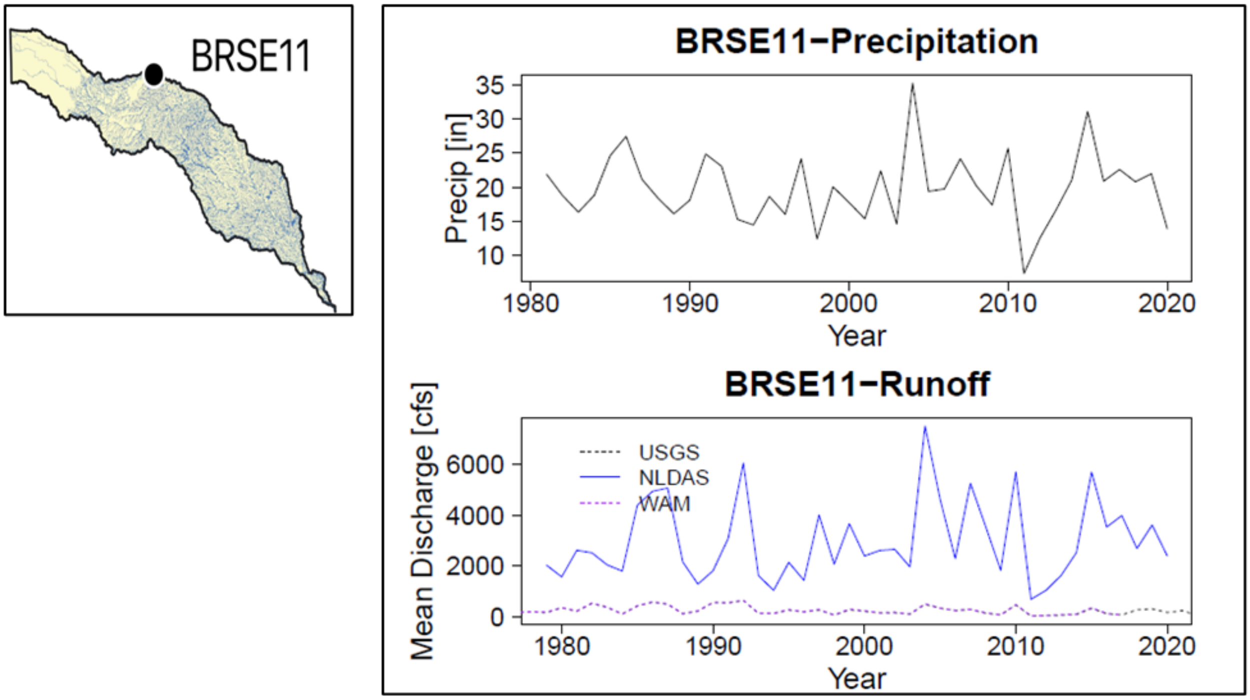


**Figure 4-10** **Location of control point BRSE11 (left), and time series of annual precipitation and streamflow at BRSE11 (right). Shown in the bottom right panel are annual streamflow series derived from a) NLDAS-2 analysis, b) USGS observations, and c) WAM naturalized flow.**

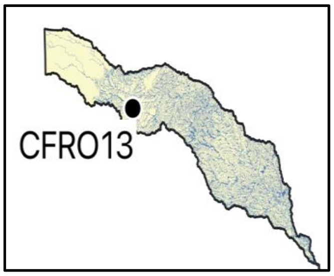


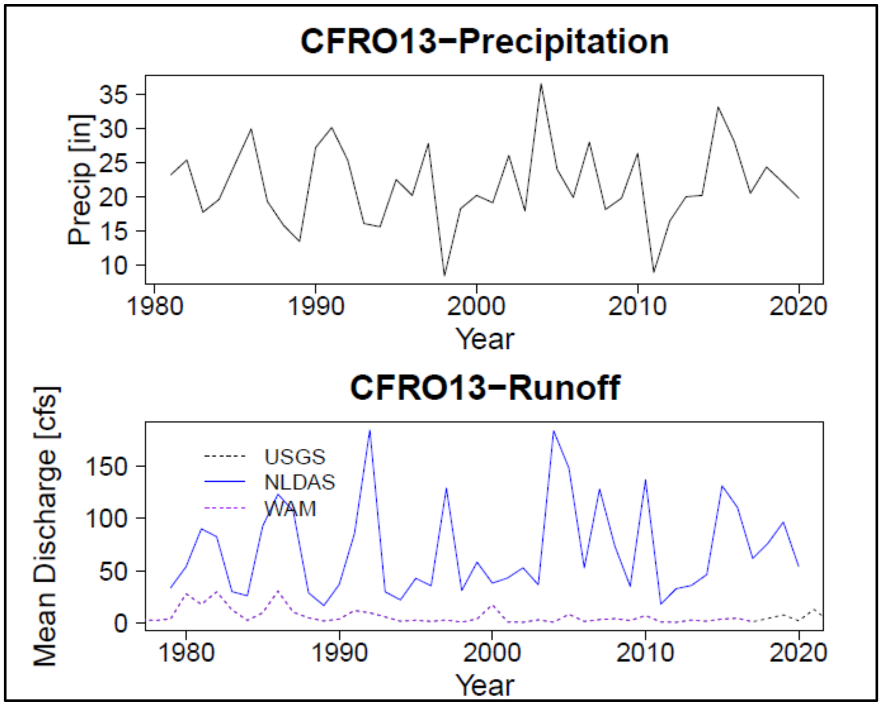


**Figure 4-11** **Location of control point CFRO13 (left), and time series of annual precipitation and streamflow at CFRO13 (right). Shown in the bottom right panel are annual streamflow series derived from a) NLDAS-2 analysis, b) USGS observations, and c) WAM naturalized flow.**

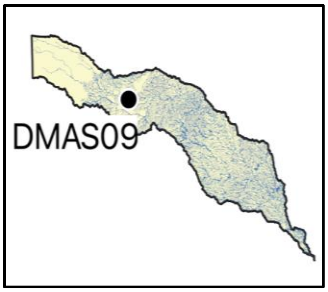


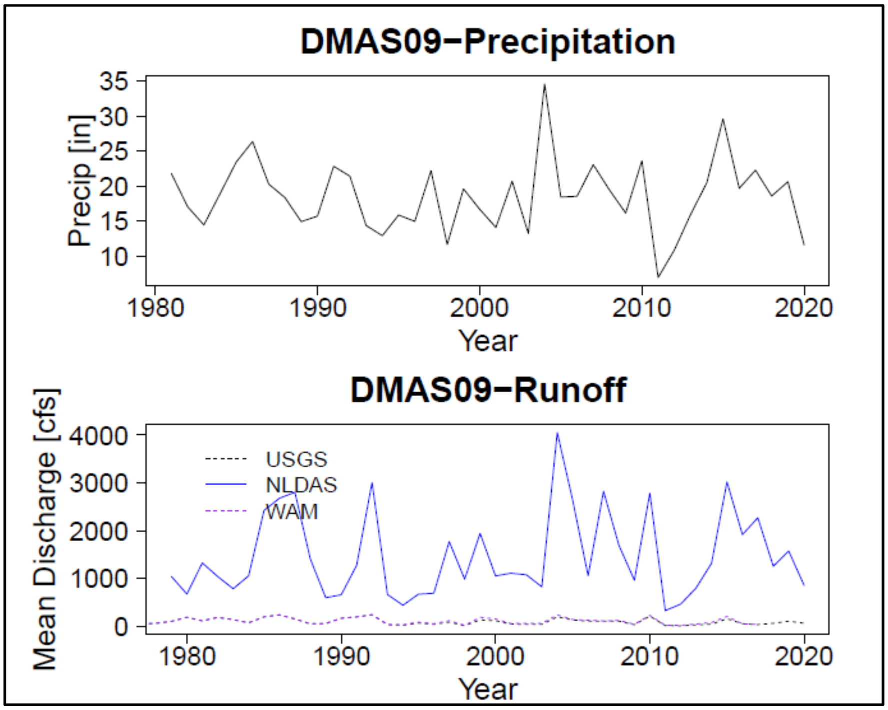


**Figure 4-12 Location of control point DMAS09 (left), and time series of annual precipitation and streamflow at DMAS09 (right). Shown in the bottom right panel are annual runoff series derived from a) NLDAS-2 analysis, b) USGS observations, and c) WAM naturalized flow.**

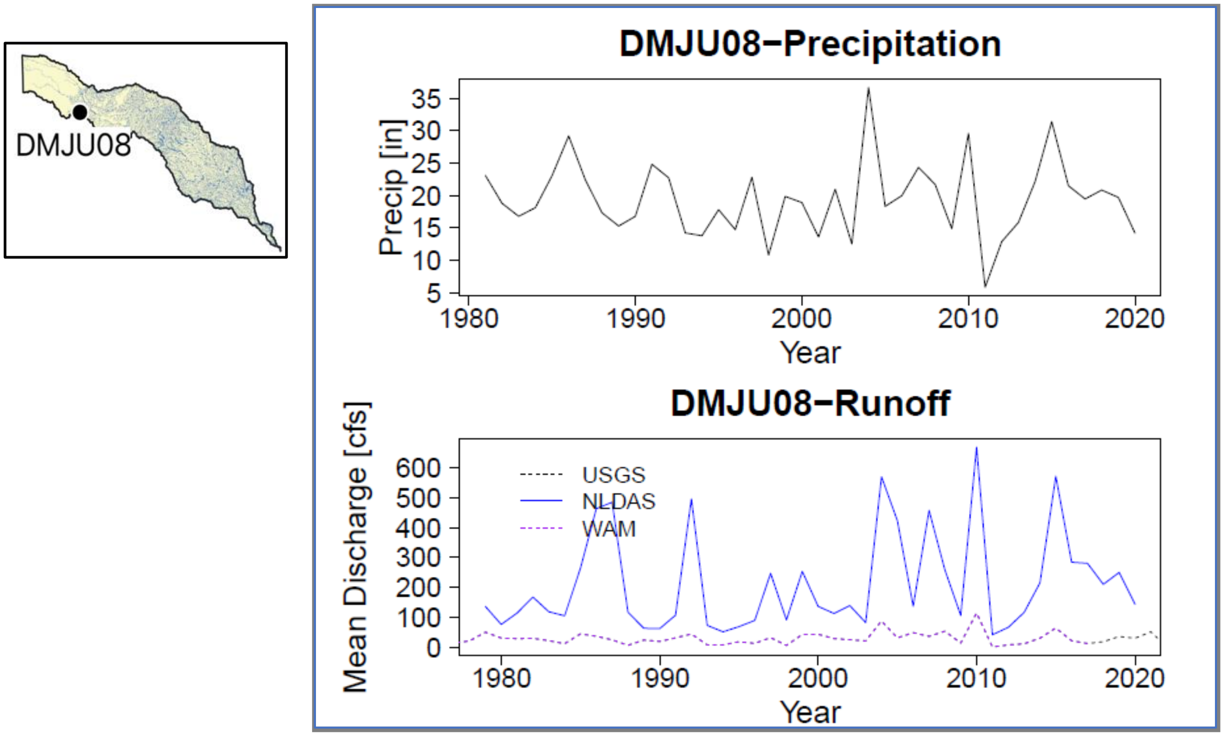


**Figure 4-13** **Location of control point DMJU08 (left), and time series of annual precipitation and streamflow at DMJU08 (right). Shown in the bottom right panel are annual runoff series derived from a) NLDAS-2 analysis, b) USGS observations, and c) WAM naturalized flow.**

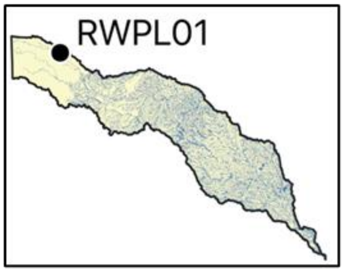


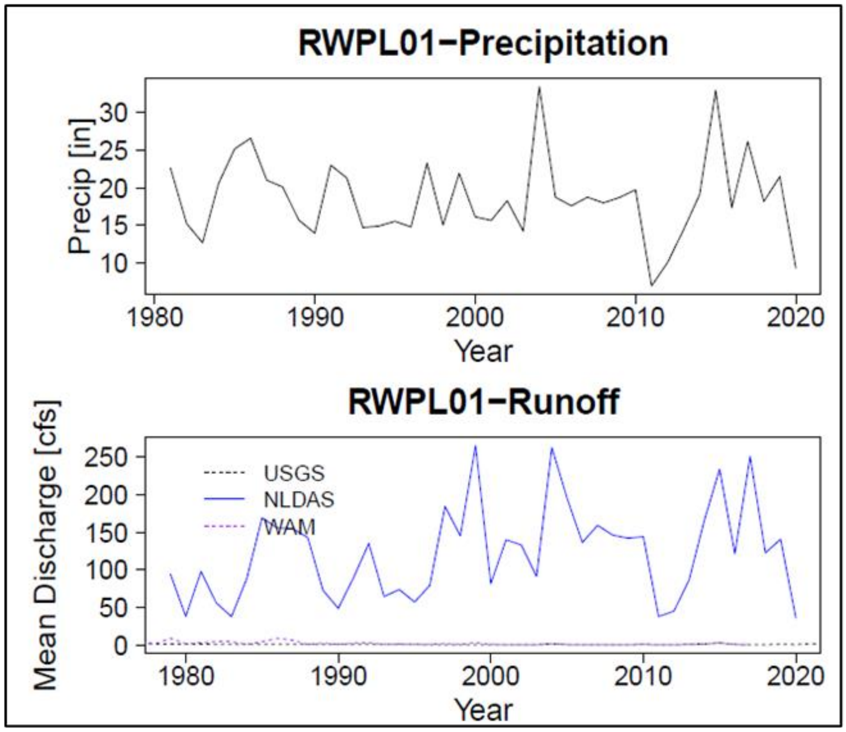


**Figure 4-14 Location of control point RWPL01 (left), and time series of annual precipitation and streamflow at RWPL01 (right). Shown in the bottom right panel are annual runoff series derived from a) NLDAS-2 analysis, b) USGS observations, and c) WAM naturalized flow.**

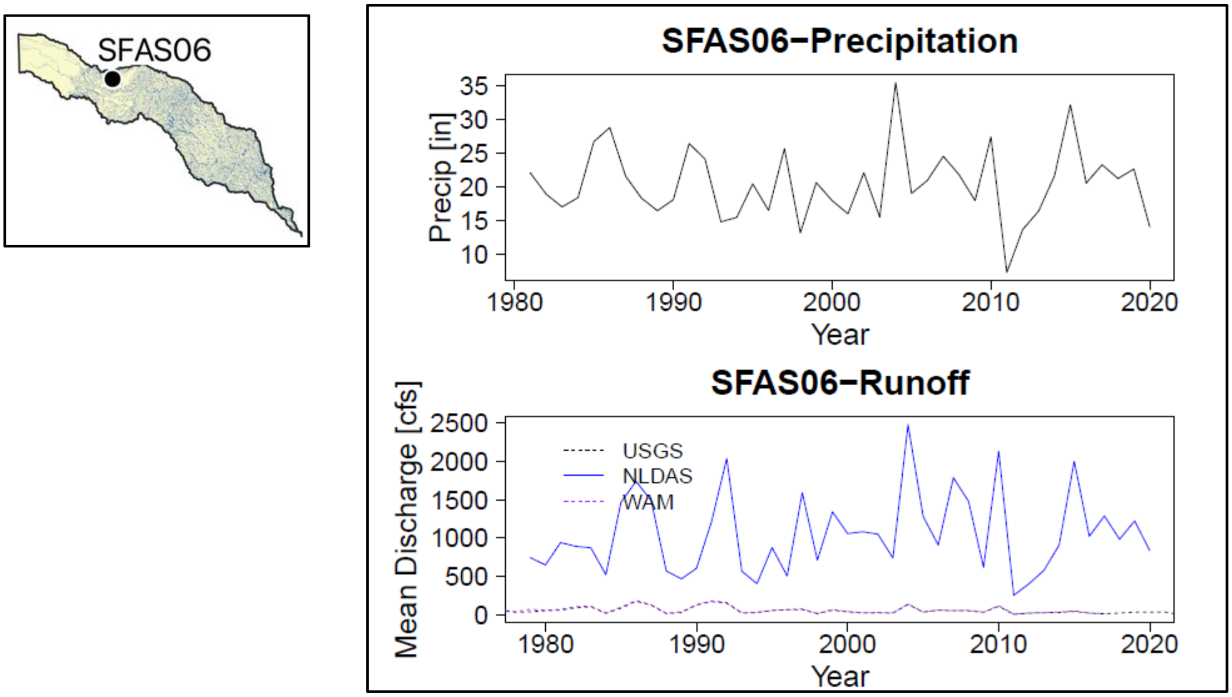


**Figure 4-15 Location of control point SFAS06 (left), and time series of annual precipitation and streamflow at SFAS06 (right). Shown in the bottom right panel are annual runoff series derived from a) NLDAS-2 reanalysis, b) USGS observations, and c) WAM naturalized flow.**

# 5. Analysis of Land Cover Changes

To determine factors other than changes in precipitation/temperature that may undergird the trends at the study site, we perform a longitudinal analysis of land cover for areas draining to each site from 2001 to 2019. The land cover data for 2001 and 2019 are retrieved from the Multi-resolution Land Characteristics (MRLC; Wickham et al., 2014). The MRLC classification scheme extends the Anderson Classification System (Anderson 1976) to incorporate 21 classes under eight broad categories. To simplify trend analysis, we re-map the MRLC classes into the Anderson level-1 categories as illustrated in Table 5-1.

**Table 5-1 Mapping of MRLC land classes to Anderson classes.**

| MRLC | | Anderson | |
|---|---|---|---|
| **Code** | **Description** | **Code** | **Description** |
| 11 | Open Water | 1 | Open Water |
| 12 | Ice/snow | 8 | Ice/snow |
| 21-23 | Urban | 2 | Urban |
| 31-33 | Barren | 3 | Barren |
| 41-43 | Forest | 4 | Forest |
| 51,52 | Shrubland | 5 | Shrub |
| 71-74 | Agriculture | 6 | Agriculture |
| 81-82 | Agriculture | 6 | Agriculture |
| 90,95 | Wetland | 7 | Wetland |

We focus on five sites with statistically significant trends in observed flow, i.e., AQAQ34, BRES11, CFRO13, DMSA09, SFAS06. For each site, we identify the land cover classes that have experienced the largest changes and describe the key observations below.

**AQAQ34**

As shown in Figure 5-1, the drainage to AQAQ34 is composed primarily of shrub and agricultural fields. Upstream of the control point is a small reservoir (Aquila Lake), and a small urban area (Hilsboro) is situated to its northeast. Between 2001 and 2019, the most salient changes in land cover include a reduction in agricultural land (-0.7%), and an increase in urban area (0.3%) and shrub (0.2%). The increase in urban land coverage corresponds to the expansion of the city of Hilsboro in the past two decades.  Note that the percentage changes are relatively small as the time window spans only 18 years.

Note that the expansion of urban land typically leads to increased imperviousness and elevated runoff response, and therefore it may be a potential factor that contributes to the positive trend in streamflow over the past four decades. However,  as the MRLC data set only goes back to 2001, it is not clear if similar expansions occurred in earlier decades.

**BRSE11**

As shown in Figure 5-2, the drainage of BRSE11 is made up of mostly agricultural land, with cultivated crops and grasslands being the predominant classes. The primary changes in land cover from 2001 to 2019 include an expansion in agricultural land (0.8%), a reduction in shrubland (1%), and a small increase in urban land (0.2%).

**CFRO13**

As shown in Figure 5-3, the land cover for the drainage of CFRO13 is similar to that for BRSE11, with cultivated crops and grasslands being the predominant classes. Relatively large changes are seen in agricultural land (1.7%) and shrubland (-1.9%). Urban and barren lands experience slight expansions (0.1%).

**DMAS09**

As shown in Figure 5-4, the land cover for the drainage of DMAS09 is similar to that for BRSE11, with cultivated crops and grasslands being the predominant classes .   Relatively large changes are seen in agricultural land (0.9%) and shrubland (-1.4%). Urban and barren lands experience slight expansions (0.3%).

**SFAS06**

As shown in Figure 5-5, the land cover for the drainage of CFRO is similar to that for BRSE11, with cultivated crops and grasslands being the predominant classes.   The largest change is the reduction of shrubland (-0.4%). Urban, agricultural, open water, and wetland all experience small expansions (0.1%).

To summarize, while all the study drainages underwent varying degrees of urbanization between 2001 and 2019, the changes in percentage of urban land cover are rather small (0.1-0.3%).  All four sites in the upper basin experienced expansions in agricultural land.  As the land cover data only goes back to 2001, it remains unknown if these trends are present in the earlier decades. If these trends are persistent over time, then there is a possibility that the declining streamflow over the upper basin is tied to expanding agricultural activities, and possibly to changing agricultural land management practice. Conversely, the expansion of urban land upstream of AQAQ34 and a reduction in agricultural land may have both contributed to the increase in streamflow at the site.

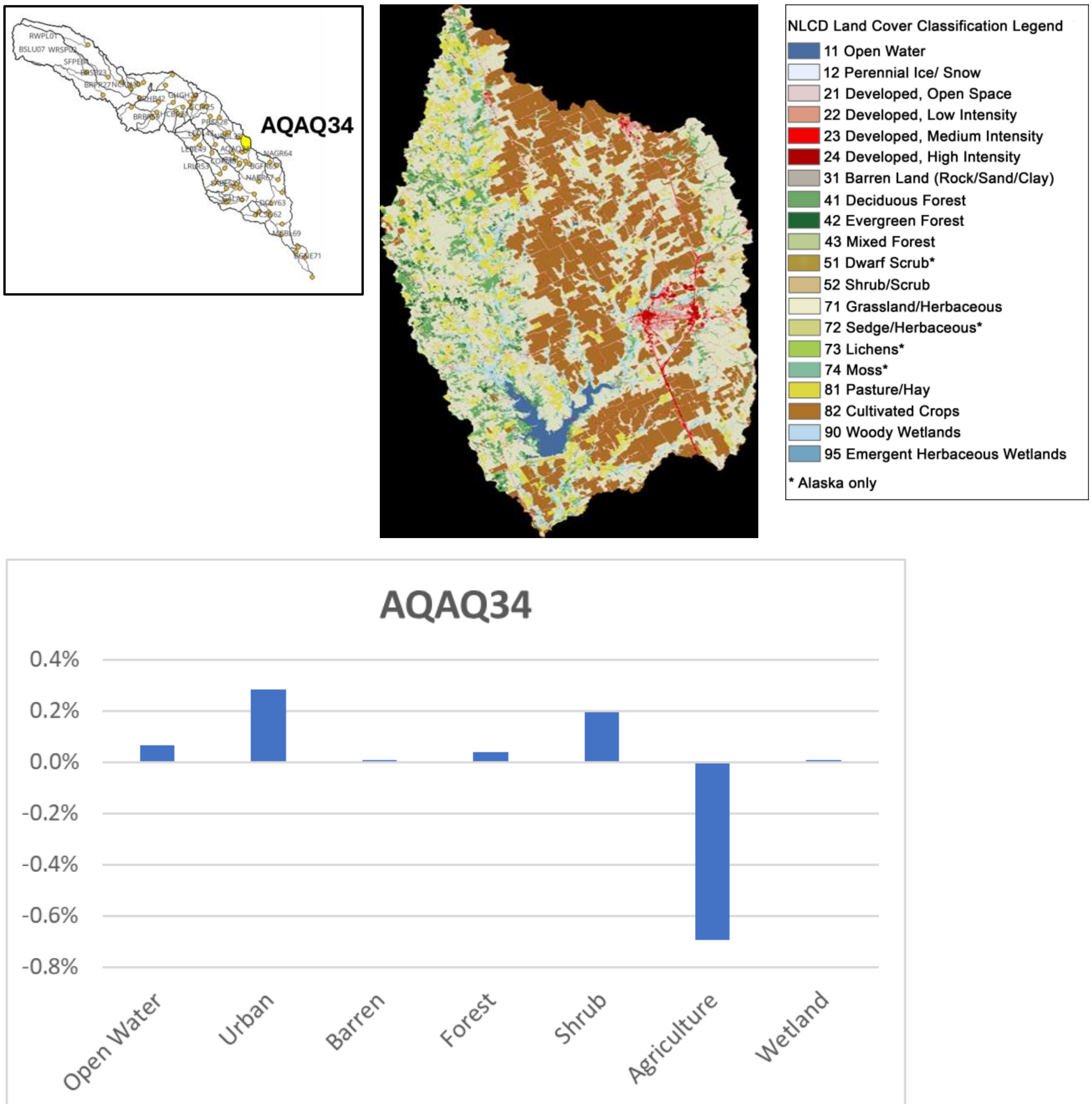


**Figure 5-1 Drainage of AQAQ34, and land cover classes for within the drainage per MRLC 2019 (top), and changes in percentage coverage for each land cover class from 2001 to 2019 (bottom).**

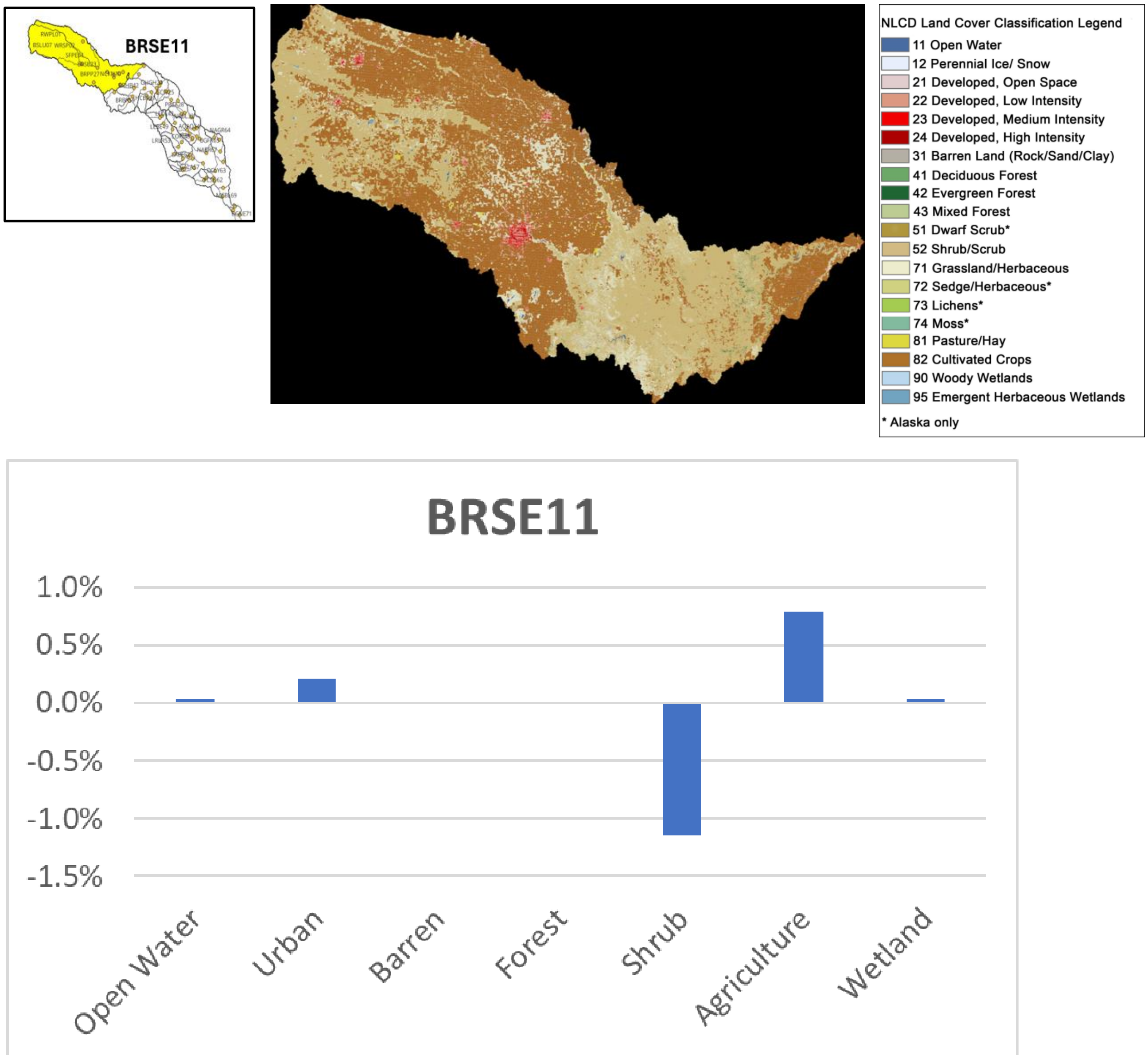


**Figure 5-2 Drainage of BRASE11, and land cover classes for within the drainage per MRLC 2019 (top), and changes in percentage coverage for each land cover class from 2001 to 2019 (bottom).**

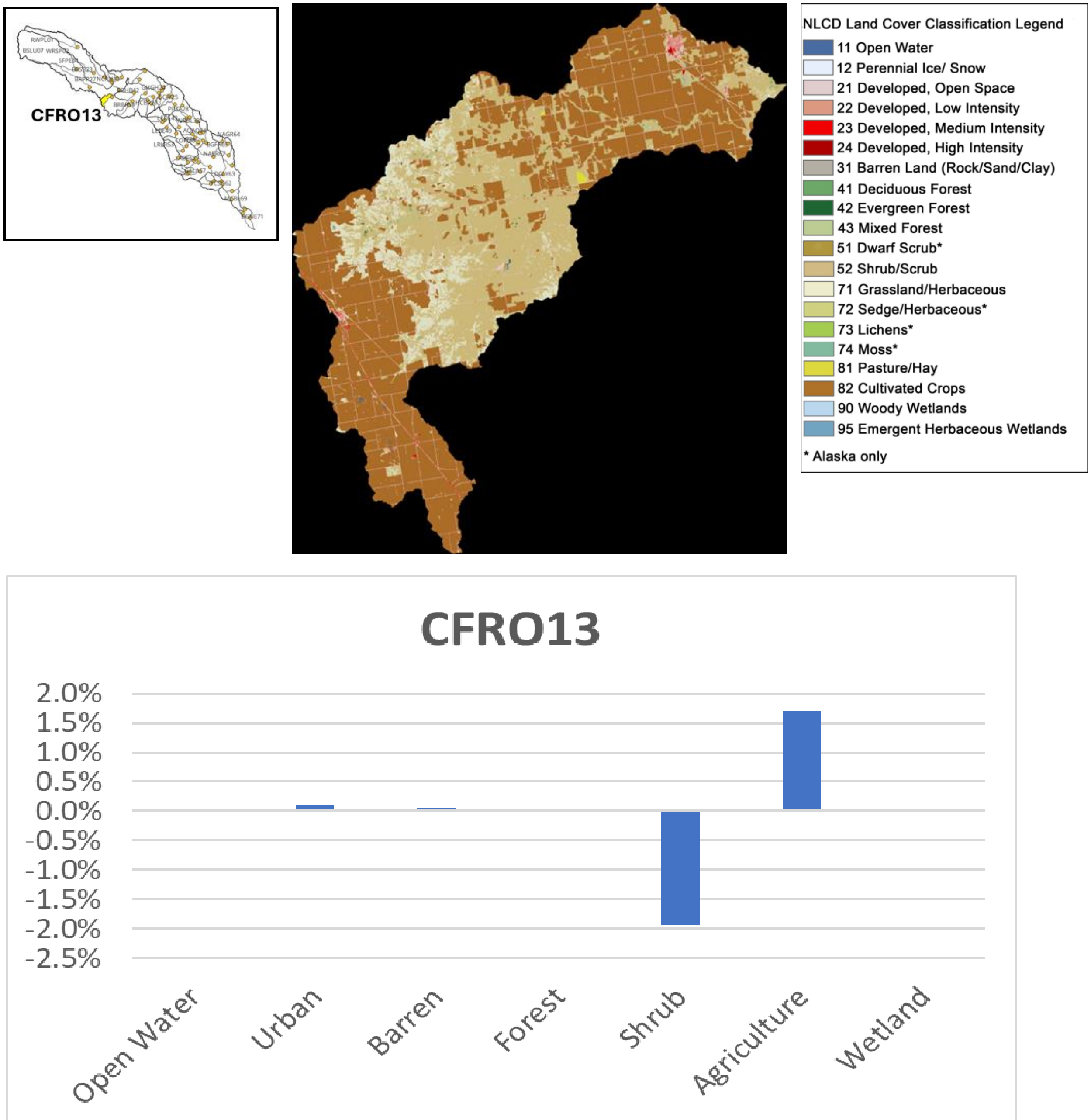


**Figure 5-3 Drainage of CFRO13, and land cover classes for within the drainage per MRLC 2019 (top), and changes in percentage coverage for each land cover class from 2001 to 2019 (bottom).**

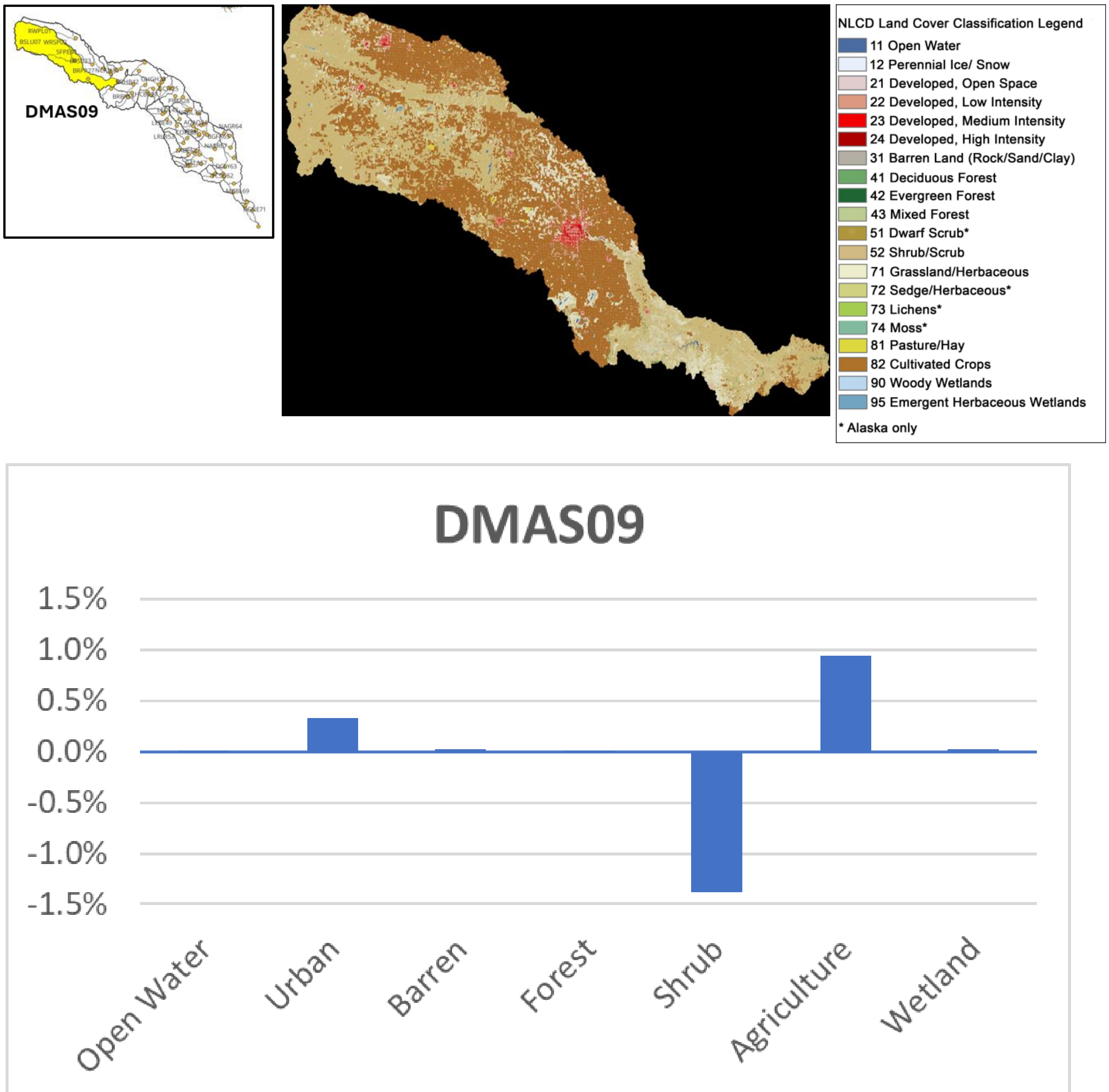


**Figure 5-4 Drainage of DMAS09, and land cover classes for within the drainage per MRLC 2019 (top), and changes in percentage coverage for each land cover class from 2001 to 2019 (bottom).**

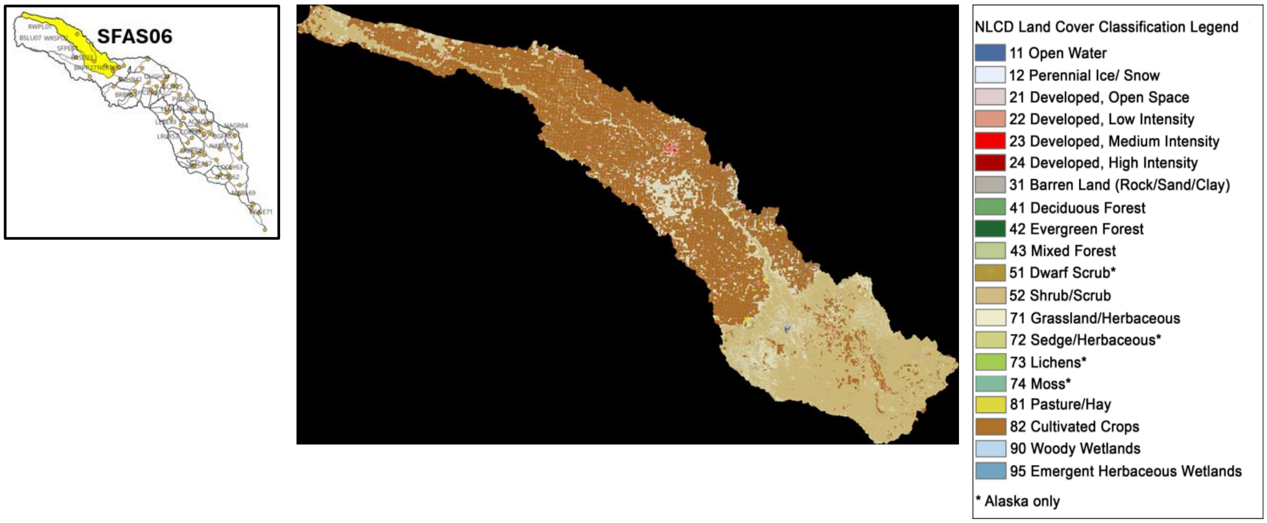


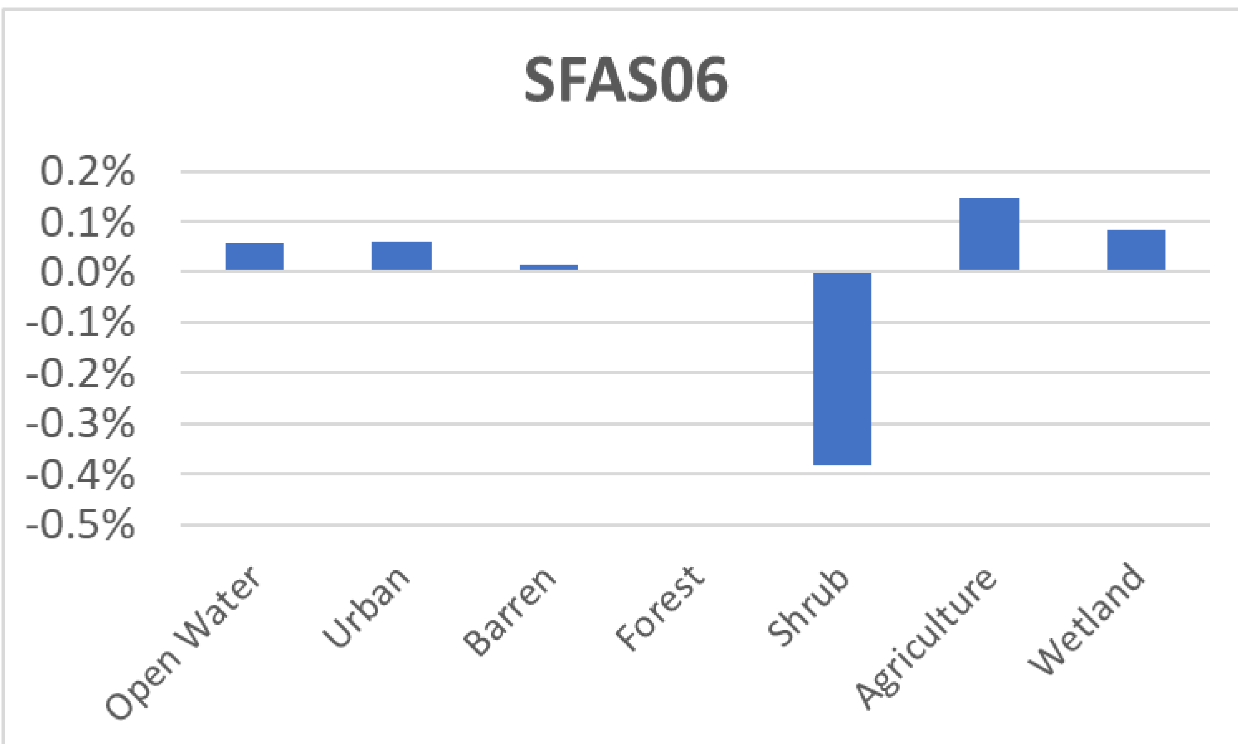


**Figure 5-5** Drainage of SFAS06, and land cover classes for within the drainage per MRLC 2019 (top), and changes in percentage coverage for each land cover class from 2001 to 2019 (bottom).

# 6. Conclusions and Recommendations

This study was undertaken to identify and assess potential drivers of streamflow trends in the Brazos River Basin. These drivers include changes in precipitation and temperature patterns, and land cover changes. While earlier works (Harwell et al., 2020; Freese and Nichols, 2021) have explored the trends through statistical analysis, this study focuses on attribution of these trends by adopting a model-based approach. This approach allows for an examination of the specific and integrated impacts of changes in precipitation and temperature. As rising temperature has been identified in many parts of the state, a particular focus was placed on assessing the impacts of this sustained warming on streamflow production. Recognizing the possibility that factors other than changes in meteorological patterns might be at play, the study also incorporated a characterization of land cover changes from 2001 to 2019 with the intent of underscoring the potential role of changes to land features in shaping the observed trends.

Unlike the earlier studies, the present work focuses on a subset of seven locations (WAM control points) within the Brazos River Basin, each corresponding to a USGS station with a sufficiently long archive of flow records (less than 10% missing data in 40 years). We chose not to include all WAM control points because some are not collocated with USGS stations; the WAM naturalized flow for these points was constructed through regression from records at adjacent USGS stations. By selecting sites with actual observed flows, we minimize the uncertainties associated with the reconstruction.

Of the seven sites selected for this study, five feature statistically significant trends in streamflow between 1979 and 2020 (i.e., AQAQ34, BRSE11, CFRO13, DMAS09, and SFAS06). Among these, AQAQ34 is located in the middle portion of the basin and is the only location with an upward trend in streamflow, whereas the remaining four are located in the upper basin and feature declining trends. Two additional sites without clear trends in streamflow are selected for their geographic locations: DMJU09 is located upstream of DMAS09, and RWPL01 is upstream of SFAS06.

The model-based analyses encompassed two elements, namely 1) determining the ability of models to reproduce the trends in streamflow at the study sites; and 2) conducting sensitivity experiments to assess the potential contributions of rising temperature to the declining streamflow at the sites in the upper basin. To reduce impacts from spurious model errors, we examined three process-based models, namely the HL-RDHM, NWM, and NLDAS-2. All three models incorporate temperature in calculating evapotranspiration. Notably, we implemented a version of HL-RDHM with SAC-HTET water balance model that features Noah-like soil moisture distribution and ET schemes.

The outcomes from the analysis suggest that the models are broadly unable to reproduce the declining trends in streamflow, though some models (NLDAS-2, NWM) are able to resolve, to varying extents, the upward trend in streamflow at AQAQ34. At most of the upper basin sites, model simulations exhibit upward trends, diverging from the trends of observed flows. Among the models, HL-RDHM underwent calibration by the project team and its simulations feature the lowest overall biases; NLDAS-2 runoff simulations are often severely biased to the positive side; and flows from NWM reanalysis are also biased though not as severely as NLDAS-2. It is worth noting that NWM also underwent calibration for selected USGS stations to match streamflow observations, and apparently the efficacy of the calibration strategy is mixed.

Closer examinations of annual flow time series from NWM 2.1 reanalysis and observations reveal the following features:

- Variability in precipitation widens in recent years, marked by large precipitation amounts in the wetter years (e.g., 2004, 2015), and near-zero precipitation during the drought of 2011.
- For the four sites with significant declines in streamflow (e.g., BRSE11, CFRO13, DMAS09, SFAS06), streamflow was higher during the wet years in the 1980s and 1990s despite the relatively lower annual precipitation amounts. At SFAS06, the watershed's response to annual precipitation is increasingly muted after the late 1990s: it produced much less streamflow during 2015 than say 2010 in spite of a higher precipitation amount in the former year.
- For the larger watersheds, the trends in NWM reanalysis generally mirror those in precipitation. NWM tends to exhibit more severe, positive biases during wet years of the recent two decades (e.g., 2004, 2015) than in the 1980s and early 1990s.

The sensitivity experiments entailed running HL-RDHM with original (baseline) and detrended temperature (perturbed) as forcing. To establish a firm baseline, we retrieved the AORC precipitation and temperature products but performed bias-adjustment to the former per experience from past works (Zhang et al., 2011, 2017). The bias-correction has substantially enhanced the correlation between simulated and observed flow prior to model calibration, suggesting improvements to the quality of precipitation products. We then calibrated the model at each site using a combination of automated searching and manual adjustment. The calibration has rendered the simulations nearly bias-neutral for all sites except RWPL01, where the model was unable to capture the anomalously low runoff production.

The temperature series from AORC underwent detrending, and the resulting, detrended temperature serves as input to the HL-RDHM along with the bias-corrected precipitation product. The resulting, perturbed simulations show broader higher streamflow across all sites, and the difference between the baseline and perturbed simulations tends to widen over time at each site. These observations confirm the ability of rising temperature in suppressing runoff generation by enhancing ET. However, as the baseline simulations are unable to reproduce the downward trends at the upper basin sites, it is evident that a) the overall trends in precipitation across the region are conducive to increased runoff and streamflow; b) rising temperature alone was insufficient to produce the observed declines in streamflow and there are other factors at play; and b) the latter factors are not fully accounted for in HL-RDHM, or the other two models (NWM and NLDAS-2).

It so far remains unclear what the alternative drivers are, or how they induce/contribute to the observed trends, in particular the downward trends in streamflow. But we surmise that there must have been fundamental changes to the runoff generation mechanisms that reshaped the water balance in the upper basin. In particular, it appears that the efficiency and magnitude of abstraction have increased over time. Possible explanations include expanded storage capacity at surface, enhanced permeability, and depletion of soil water. For the upper portion of Brazos, our analysis of land cover suggested that there has been an expansion of agricultural land even in the past two decades.  Though earlier data are scarce, there are good reasons to believe that the expansion took place in the 1980s and 1990s, if not over earlier eras.  This expansion may have brought several changes that have latent impacts, which include an expansion in small impoundments in the region, increased soil water retention capacity, and increased irrigation demand that suppressed shallow groundwater table.

Expansion of impoundments is a known phenomenon for northern and central Texas.  A contracted report by Furnans et al. (2019) found similar declines in runoff yield in central Texas within the drainage of Upper Colorado River, and attributed the declines to the expansion of agriculture ponds. However, we found this explanation unsatisfactory due to the following reasons. First, the percentage increases in agricultural land are small (< 1.5%), implying that the collective storage of added impoundments associated with the expansion would be limited. Second, while clear downward trends are observed at sites situated at the mid or downstream of major tributaries (DMAS09, SFAS06), these trends become less pronounced at sites upstream (DMJU08 and RWPL01).  If the impoundments had played a key role, these would have manifested in sharper downward trends in smaller drainages rather than the opposite. There is a possibility that the impoundments are concentrated in the lower portion of the tributaries and therefore disproportionately impact the flow downstream. Unfortunately, owing to the lack of consistent monitoring data, it is difficult to gauge the magnitude of expansion in impoundments or to ascertain its hydrologic effects.

Increased water detention can be achieved through the adoption of agricultural management practices (Libohova et al., 2018; Vlček et al., 2028), which has become more common in recent years (US Department of Agriculture, 2017).   A number of studies (Zhou et al., 2022, Wooliver and Jagadamma, 2023) reported that the adoption of cover crops led to increased soil organic matters which positively impact the water holding capacity of soils. However, thus far there is insufficient evidence to confirm the linkage between declining runoff yield and agricultural management practices.

Increasing irrigation demand due to intensifying agricultural production is a plausible thesis given the expansion in agricultural land.  Cotton and corn are important crops over the region (Almas and Colette, 2024), and about half of the cotton fields are irrigated, and groundwater is a key source of irrigation water.  Note that if water is pumped from shallow, unconfined aquifers, then the declining water table may enhance downward moisture flux and reduce soil water near the surface. This will result in an increase in abstraction. Unfortunately, there is a paucity of data on irrigation and groundwater in the region to confirm this thesis.

Apart from the forgoing hypotheses, there are other regional processes that warrant attention. In particular, the upper reach of Brazos River and tributaries intersect with the High Plains Aquifer, which has been experiencing continuous decline over the past few decades (Haacker et al., 2016; Rhodes et al., 2023).  Whether and how this decline contributes to the declining runoff in the upper basin remains unclear.  It is worth noting that the upstream sites (DMJU08 and RWPL01) have their drainages overlapping with the aquifer, but streamflow for neither site exhibits strong trends. Moreover, there remain uncertainties about the accuracy of PRISM and bias-corrected AORC products in the 1980s and early 1990s.  PRISM daily product since 2002 benefits from the infusion of radar data, and therefore a shift in bias behavior around that time frame cannot be ruled out.

On the basis of the findings, we recommend that the following actions be taken to narrow down and ascertain the mechanistic origins of the declines.

**Recommendation I:**
Gather historical data on additional variables that may have contributed to the trends in runoff, such as expansion of agricultural impoundments, change in agricultural management practice, and depletion in groundwater. Specifically, as declining groundwater level has been reported in the region, it is necessary to perform a detailed investigation of how this decline may have contributed to the declining runoff yield. To this end, one may first assess groundwater pumping and irrigation in the region on groundwater level, and then estimate the impacts of resulting groundwater depletion on discharge to streams. Observations from groundwater monitoring wells maintained by TWDB, and possibly remotely sensed soil moisture and evapotranspiration data can be used for these purposes.

**Recommendation II:**
Assess, and potentially improve the precipitation product for the period prior to 2002 when the AORC hourly and PRISM daily products are both based primarily on gauge reports. One strategy is to compare the adjusted AORC against the PRISM monthly product, which to date does not incorporate radar data. If the former exhibits positive bias in the later period (after 2002) but not in the earlier one, then there is reason to suspect that nonstationarity in bias at least in part contributes to the inability of models to reproduce the downward trend in streamflow.

**Recommendation III:**
Perform additional, in-depth analysis of streamflow dynamics at the two sites, namely DMAS09 and SFAS06, for selected events in the past two decades. Both sites feature sharp contrasts in runoff yield between two recent wet spells (i.e., 2004-2010; 2015-2019). As satellite observations of soil moisture have become widely available from late-2000s , it will be useful to leverage these observations to diagnose the intransigent, negative bias over events after the flood of 2015. This will help provide clues on whether exogenous mechanisms are in play that led to more rapid depletion of soil moisture than what models are able to resolve.

**Recommendation V:**
Improve monitoring of the watersheds to better discern impacts of impoundments, soil moisture, and shallow groundwater on streamflow during dry and wet conditions. In particular, monitoring storage in small ponds prior to major rainfall events will provide a basis for assessing their collective roles in subduing streamflow response. Similarly, more comprehensive root-zone soil moisture and groundwater data sets will determine if percolation has become more efficient over time that undercuts the runoff generation.

# Acknowledgement

The project team benefited from discussions with Diana Bailey and Jerry Cotter from the USACE Fort Worth, Glenn Harwell and Monica Yesildirek at USGS, Aaron Abel, August

Dreyer, Peyton Lisenby and Chris Higgins at Brazos River Authority, and John Zhu and Nelun Fernando at the Texas Water Development Board. Zhengtao Cui helped resolve errors in the HL-RDHM and contributed to model calibration. Amanda Burke was the project manager and her effort to connect the project team with stakeholders is duly acknowledged here.

# References

Ahmadalipour, A., Moradkhani, H. and Demirel, M.C., 2017. A comparative assessment of projected meteorological and hydrological droughts: elucidating the role of temperature. Journal of Hydrology, 553, pp.785-797.

Almas, L.K. and Colette, W.A., 2007. Irrigation Management Strategies for Cotton Production in the Texas Panhandle. In World Environmental and Water Resources Congress 2007: Restoring Our Natural Habitat (pp. 1-10).

Anderson, J.R., 1976. A land use and land cover classification system for use with remote sensor data (Vol. 964). US Government Printing Office.

Brunner, M.I., Swain, D.L., Gilleland, E. and Wood, A-W., 2021. Increasing importance of temperature as a contributor to the spatial extent of streamflow drought. Environmental Research Letters, 16(2), p.024038.

Cosgrove, B-, Gochis, D., Clark, E.P., Cui, Z., Dugger, A-L., Feng, X., Karsten, L.R., Khan, S., Kitzmiller, D., Lee, H.S. and Liu, Y., 2016, December. An overview of the National Weather Service national water model. In AGU Fall Meeting Abstracts (Vol. 2016, pp. H42B-05).

Daly, C., Neilson, R.P. and Phillips, D.L., 1994. A statistical-topographic model for mapping climatological precipitation over mountainous terrain. Journal of Applied Meteorology and Climatology, 33(2), pp.140-158.

Emerson, D.G., Vecchia, A.V. and Dahl, A.L., 2005. *Evaluation of drainage-area ratio method used to estimate streamflow for the Red River of the North Basin, North Dakota and Minnesota* (No. 2005-5017). US Geological Survey.

Freese and Nichols 2021. Assessment of How Trends in the Brazos River Basin May Affect Surface Water Availability and Attainment of Environmental Flow Standards. Texas Water Development Board Contract Number 2100012466. Retrieved July 8, 2024 from https://www.twdb.texas.gov/publications/reports/contracted_reports/doc/2100012466.pdf

Furnans, J., Keester, M., Kennedy K., (2019). Evaluation of Rainfall-Runoff Trends in the Upper Colorado River Basin. Contracted report, Texas Water Development Board.

Gochis, D.J., Barlage, M., Dugger, A-, FitzGerald, K., Karsten, L., McAllister, M., McCreight, J., Mills, J., RafieeiNasab, A-, Read, L. and Sampson, K., 2018. The WRF-Hydro modeling system technical description,(Version 5.0). NCAR Technical Note, 107.

Harwell, G. R., McDowell, J., Gunn-Rosas, C., & Garrett, B. 2020. Precipitation, temperature, groundwater-level elevation, streamflow, and potential flood storage trends within the Brazos, Colorado, Big Cypress, Guadalupe, Neches, Sulphur, and Trinity River basins in Texas through 2017. In Scientific Investigations Report (2019–5137). U.S. Geological Survey. https://doi.org/10.3133/sir20195137

Haacker, E.M., Kendall, A.D. and Hyndman, D.W., 2016. Water level declines in the High Plains Aquifer: Predevelopment to resource senescence. *Groundwater*, *54*(2), pp.231-242.

Koren, V., Reed, S., Smith, M., Zhang, Z. and Seo, D.J., 2004. Hydrology laboratory research modeling system (HL-RMS) of the US national weather service. Journal of Hydrology, 291(3-4), pp.297-318.

Koren, V.I., Smith, M.B., Cui, Z., Cosgrove, B-A., Werner, K.V. and Zamora, R., 2010. Modification of Sacramento soil moisture accounting heat transfer component (SAC-HT) for enhanced evapotranspiration.

Kuzmin, V., Seo, D.J. and Koren, V., 2008. Fast and efficient optimization of hydrologic model parameters using a priori estimates and stepwise line search. Journal of Hydrology, 353(1-2), pp.109-128.

Libohova, Z., Seybold, C., Wysocki, D., Wills, S., Schoeneberger, P., Williams, C., … Owens, P. R. (2018). Reevaluating the effects of soil organic matter and other properties on available water-holding capacity using the National Cooperative Soil Survey Characterization Database. Journal of Soil and Water Conservation, 73(4), 411–421.

Linacre, E. T. (1977). A simple formula for estimating evaporation rates in various climates, using temperature data alone. Agricultural Meteorology, 18(6), pp. 409–424. https://doi.org/10.1016/0002-1571(77)90007-3

MannKendall function—RDocumentation. (n.d.). Retrieved July 3, 2024, from https://www.rdocumentation.org/packages/Kendall/versions/2.2.1/topics/MannKendall

Rhodes, E.C., Perotto-Baldivieso, H.L., Tanner, E.P., Angerer, J.P. and Fox, W.E., 2023. The declining Ogallala aquifer and the future role of rangeland science on the North American High Plains. *Rangeland Ecology & Management*, *87*, pp.83-96.

Samaniego, L., Thober, S., Kumar, R., Wanders, N., Rakovec, O., Pan, M., Zink, M., Sheffield, J., Wood, E.F. and Marx, A-, 2018. Anthropogenic warming exacerbates European soil moisture droughts. Nature Climate Change, 8(5), pp.421-426.

Smith, M., Koren, V., Zhang, Z., Moreda, F., Cui, Z., Cosgrove, B-, Mizukami, N., Kitzmiller, D., Ding, F., Reed, S. and Anderson, E., 2013. The distributed model intercomparison project–Phase 2: Experiment design and summary results of the western basin experiments. Journal of Hydrology, 507, pp.300-329.

U.S. Department of Agriculture. 2017. "United States 2017 Census of Agriculture." Washington, DC: U.S. Department of Agriculture, National Agriculture Statistics Service, Form 17-A100. Available online:
https://www.nass.usda.gov/AgCensus/Report_Form_and_Instructions/2017_Report_Form/17a100_121316_general_final.pdf.

USGS Current Conditions for Texas_ Streamflow. (n.d.). United States Geological Survey. Retrieved July 23, 2024, from https://waterdata.usgs.gov/tx/nwis/current/?type=flow

Vicente-Serrano, S.M., Lopez-Moreno, J.I., Beguería, S., Lorenzo-Lacruz, J., Sanchez-Lorenzo, A-, García-Ruiz, J.M., Azorin-Molina, C., Morán-Tejeda, E., Revuelto, J., Trigo, R. and Coelho, F., 2014. Evidence of increasing drought severity caused by temperature rise in southern Europe. Environmental Research Letters, 9(4), p.044001.

Vlček, L., Šípek, V., Zelíková, N., Čáp, P., Kincl, D. and Vopravil, J., 2022. Water retention and infiltration affected by conventional and conservational tillage on a maize plot; rainfall simulator and infiltrometer comparison study. Agricultural Water Management, 271, p.107800.

Water Availability Models. (n.d.). Texas Commission on Environmental Quality. Retrieved July 8, 2024, from https://www.tceq.texas.gov/permitting/water_rights/wr_technical-resources/wam.html

Water Rights Analysis Package (WRAP) Modeling System. (2022). Texas A&M University Engineering. Retrieved July 8, 2024, from https://wrap.engr.tamu.edu/

Wickham, J., Homer, C., Vogelmann, J., McKerrow, A-, Mueller, R., Herold, N. and Coulston, J., 2014. The multi-resolution land characteristics (MRLC) consortium—20 years of development and integration of USA national land cover data. Remote Sensing, 6(8), pp.7424-7441.

Wolaver, B.D., Reynolds, L.V., Caldwell, T.G., Bongiovanni, T., Pierre, J.P., Breton, C. and Mayes, K.B., 2024. Hydrologic changes in the Brazos River Basin and implications for Great Plains fishes. *Journal of Hydrology*, *629*, p.130351.

Wooliver, R., & Jagadamma, S. 2023. Response of soil organic carbon fractions to cover cropping: A meta-analysis of agroecosystems. Agriculture, Ecosystems & Environment, 351, 108497.

Wurbs, R. A. 2005. Texas Water Availability Modeling System. Journal of Water Resources Planning and Management, 131(4), pp. 270–279. https://doi.org/10.1061/(ASCE)0733-9496(2005)131:4(270)

Wurbs, R. A. 2019. Daily Water Availability Model for the Brazos River Basin and Brazos-San Jacinto Coastal Basin. Texas Water Resources Institute TR-513. Retrieved July 8, 2024 from https://twri.tamu.edu/media/4215/tr-513.pdf

Wurbs, R.A., 2020. Institutional framework for modeling water availability and allocation. *Water*, *12*(10), p.2767.

Xia, Y., Mitchell, K., Ek, M., Sheffield, J., Cosgrove, B-, Wood, E., Luo, L., Alonge, C., Wei, H., Meng, J. and Livneh, B-, 2012. Continental-scale water and energy flux analysis and validation for the North American Land Data Assimilation System project phase two (NLDAS-

2): 1. Intercomparison and application of model products. Journal of Geophysical Research: Atmospheres, 117(D3).

Xiao, M., Udall, B- and Lettenmaier, D.P., 2018. On the causes of declining Colorado River streamflow. Water Resources Research, 54(9), pp.6739-6756.

Yang, Q., & Scanlon, B- R. (2019). How much water can be captured from flood flows to store in depleted aquifers for mitigating floods and droughts? A case study from Texas, US. Environmental Research Letters, 14(5), 054011. https://doi.org/10.1088/1748-9326/ab148e

Zhang, Y. and Wurbs, R., 2018. Long-term changes in river system hydrology in Texas. *Proceedings of the International Association of Hydrological Sciences*, *379,* pp.255-261.

Zhang, Y., Reed, S. and Kitzmiller, D., 2011. Effects of retrospective gauge-based readjustment of multisensor precipitation estimates on hydrologic simulations. Journal of Hydrometeorology, 12(3), pp.429-443.

Zhang, Y., and Coauthors, 2020. Developing a Multi-model  Simulation System for Estimation and Prediction of Freshwater Inflow to Matagorda Bay. Contracted report to TWDB.

Zhou, Q., Guan, K., Wang, S., Jiang, C., Huang, Y., Peng, B-, … Schaefer, D. (2022). Recent rapid increase of cover crop adoption across the US Midwest detected by fusingmulti-source satellite data. Geophysical Research Letters, 49(22), e2022GL100249

# Appendix A: Data and Figures for Temperature De-trending

**Table A-1:** **Summary statistics for linear regression of monthly temperature averages and Mann-Kendall trend tests as calculated for grid cells corresponding to each study point over 1979-2022. Highlighted rows have statistically significant (p-value ≤ 0.05) Mann-Kendall trends.**

| January | | | | | |
|---|---|---|---|---|---|
| **Point** | $R^2$ | **Slope** | **Intercept** | **MK Tau** | **MK p-value** |
| **AQAQ34** | 0.05 | 0.07 | -86.44 | 0.12 | 0.28 |
| **BRSE11** | 0.10 | 0.08 | -119.96 | 0.20 | 0.07 |
| **CFRO13** | 0.13 | 0.10 | -151.38 | 0.26 | 0.02 |
| **DMAS09** | 0.11 | 0.09 | -132.17 | 0.24 | 0.03 |
| **DMJU08** | 0.20 | 0.12 | -194.74 | 0.30 | 0.01 |
| **RWPL01** | 0.08 | 0.07 | -98.75 | 0.21 | 0.05 |
| **SFAS06** | 0.11 | 0.08 | -121.57 | 0.23 | 0.04 |

| February | | | | | |
|---|---|---|---|---|---|
| **Point** | $R^2$ | **Slope** | **Intercept** | **MK Tau** | **MK p-value** |
| **AQAQ34** | 0.02 | 0.04 | -34.16 | 0.08 | 0.49 |
| **BRSE11** | 0.02 | 0.04 | -36.61 | 0.06 | 0.60 |
| **CFRO13** | 0.02 | 0.05 | -50.64 | 0.09 | 0.41 |
| **DMAS09** | 0.02 | 0.04 | -33.94 | 0.04 | 0.69 |
| **DMJU08** | 0.05 | 0.07 | -99.18 | 0.15 | 0.18 |
| **RWPL01** | 0.01 | 0.03 | -25.86 | 0.08 | 0.47 |
| **SFAS06** | 0.01 | 0.03 | -10.75 | 0.02 | 0.85 |

| March | | | | | |
|---|---|---|---|---|---|
| **Point** | $R^2$ | **Slope** | **Intercept** | **MK Tau** | **MK p-value** |
| **AQAQ34** | 0.05 | 0.06 | -67.77 | 0.15 | 0.17 |
| **BRSE11** | 0.11 | 0.09 | -126.44 | 0.20 | 0.07 |
| **CFRO13** | 0.14 | 0.11 | -158.56 | 0.24 | 0.03 |
| **DMAS09** | 0.10 | 0.09 | -130.98 | 0.19 | 0.09 |
| **DMJU08** | 0.22 | 0.13 | -215.01 | 0.31 | < 0.01 |
| **RWPL01** | 0.16 | 0.10 | -157.94 | 0.25 | 0.02 |
| **SFAS06** | 0.10 | 0.09 | -120.24 | 0.19 | 0.09 |

| April | | | | | |
|---|---|---|---|---|---|
| **Point** | $R^2$ | **Slope** | **Intercept** | **MK Tau** | **MK p-value** |
| **AQAQ34** | 0.00 | 0.01 | 48.83 | 0.05 | 0.63 |
| **BRSE11** | 0.03 | 0.03 | -6.91 | 0.10 | 0.36 |
| **CFRO13** | 0.08 | 0.07 | -69.76 | 0.20 | 0.07 |
| **DMAS09** | 0.04 | 0.05 | -35.38 | 0.14 | 0.21 |
| **DMJU08** | 0.13 | 0.09 | -112.78 | 0.29 | 0.01 |
| **RWPL01** | 0.02 | 0.04 | -15.35 | 0.13 | 0.23 |
| **SFAS06** | 0.02 | 0.03 | -0.52 | 0.09 | 0.40 |

| May | | | | | |
|---|---|---|---|---|---|
| **Point** | $R^2$ | **Slope** | **Intercept** | **MK Tau** | **MK p-value** |
| **AQAQ34** | 0.01 | 0.02 | 42.81 | 0.04 | 0.69 |
| **BRSE11** | 0.06 | 0.06 | -39.88 | 0.16 | 0.15 |
| **CFRO13** | 0.04 | 0.06 | -39.22 | 0.10 | 0.36 |
| **DMAS09** | 0.03 | 0.05 | -20.89 | 0.08 | 0.47 |
| **DMJU08** | 0.07 | 0.08 | -82.50 | 0.19 | 0.08 |
| **RWPL01** | 0.03 | 0.04 | -17.51 | 0.10 | 0.37 |
| **SFAS06** | 0.02 | 0.04 | -1.99 | 0.04 | 0.71 |

| June | | | | | |
|---|---|---|---|---|---|
| **Point** | $R^2$ | **Slope** | **Intercept** | **MK Tau** | **MK p-value** |
| **AQAQ34** | 0.07 | 0.05 | -17.59 | 0.16 | 0.15 |
| **BRSE11** | 0.09 | 0.08 | -84.18 | 0.19 | 0.08 |
| **CFRO13** | 0.11 | 0.09 | -107.86 | 0.23 | 0.04 |
| **DMAS09** | 0.07 | 0.07 | -61.82 | 0.16 | 0.15 |
| **DMJU08** | 0.13 | 0.10 | -122.62 | 0.24 | 0.03 |
| **RWPL01** | 0.09 | 0.07 | -72.22 | 0.21 | 0.05 |
| **SFAS06** | 0.04 | 0.06 | -32.14 | 0.12 | 0.28 |

| July | | | | | |
|---|---|---|---|---|---|
| Point | $R^2$ | Slope | Intercept | MK Tau | MK p-value |
| AQAQ34 | 0.00 | 0.01 | 61.77 | 0.05 | 0.63 |
| BRSE11 | 0.00 | 0.01 | 71.48 | 0.05 | 0.66 |
| CFRO13 | 0.02 | 0.04 | 9.29 | 0.14 | 0.21 |
| DMAS09 | 0.01 | 0.02 | 51.41 | 0.06 | 0.60 |
| DMJU08 | 0.05 | 0.05 | -22.26 | 0.17 | 0.11 |
| RWPL01 | 0.00 | 0.00 | 70.83 | 0.01 | 0.94 |
| SFAS06 | 0.00 | -0.01 | 97.58 | -0.02 | 0.85 |

| August | | | | | |
|---|---|---|---|---|---|
| Point | $R^2$ | Slope | Intercept | MK Tau | MK p-value |
| AQAQ34 | 0.03 | 0.04 | 10.39 | 0.10 | 0.39 |
| BRSE11 | 0.00 | 0.02 | 51.75 | 0.02 | 0.83 |
| CFRO13 | 0.06 | 0.06 | -31.70 | 0.15 | 0.16 |
| DMAS09 | 0.02 | 0.03 | 15.60 | 0.10 | 0.34 |
| DMJU08 | 0.10 | 0.07 | -66.40 | 0.17 | 0.11 |
| RWPL01 | 0.02 | 0.03 | 15.66 | 0.12 | 0.26 |
| SFAS06 | 0.01 | 0.02 | 46.75 | 0.05 | 0.66 |

| September | | | | | |
|---|---|---|---|---|---|
| Point | $R^2$ | Slope | Intercept | MK Tau | MK p-value |
| AQAQ34 | 0.04 | 0.04 | -8.00 | 0.11 | 0.30 |
| BRSE11 | 0.02 | 0.03 | 13.61 | 0.05 | 0.68 |
| CFRO13 | 0.02 | 0.04 | 4.07 | 0.09 | 0.40 |
| DMAS09 | 0.03 | 0.04 | -7.01 | 0.09 | 0.43 |
| DMJU08 | 0.09 | 0.07 | -60.03 | 0.19 | 0.09 |
| RWPL01 | 0.02 | 0.03 | 10.57 | 0.09 | 0.44 |
| SFAS06 | 0.02 | 0.03 | 19.73 | 0.04 | 0.73 |

| October | | | | | |
|---|---|---|---|---|---|
| Point | $R^2$ | Slope | Intercept | MK Tau | MK p-value |
| AQAQ34 | 0.02 | 0.02 | 23.58 | 0.03 | 0.78 |
| BRSE11 | 0.03 | 0.03 | -0.39 | 0.10 | 0.39 |
| CFRO13 | 0.03 | 0.03 | -5.49 | 0.09 | 0.40 |
| DMAS09 | 0.02 | 0.03 | 11.90 | 0.05 | 0.68 |
| DMJU08 | 0.10 | 0.06 | -52.59 | 0.19 | 0.08 |
| RWPL01 | 0.01 | 0.02 | 23.09 | 0.06 | 0.57 |
| SFAS06 | 0.00 | 0.01 | 39.63 | 0.01 | 0.92 |

| November | | | | | |
|---|---|---|---|---|---|
| Point | $R^2$ | Slope | Intercept | MK Tau | MK p-value |
| AQAQ34 | 0.01 | 0.03 | -4.75 | 0.08 | 0.47 |
| BRSE11 | 0.06 | 0.06 | -76.00 | 0.18 | 0.09 |
| CFRO13 | 0.07 | 0.07 | -91.69 | 0.17 | 0.12 |
| DMAS09 | 0.07 | 0.07 | -88.32 | 0.14 | 0.20 |
| DMJU08 | 0.12 | 0.09 | -138.01 | 0.19 | 0.08 |
| RWPL01 | 0.05 | 0.06 | -69.41 | 0.10 | 0.36 |
| SFAS06 | 0.06 | 0.07 | -81.92 | 0.14 | 0.20 |

| December | | | | | |
|---|---|---|---|---|---|
| Point | $R^2$ | Slope | Intercept | MK Tau | MK p-value |
| AQAQ34 | 0.05 | 0.06 | -78.90 | 0.16 | 0.14 |
| BRSE11 | 0.08 | 0.09 | -129.96 | 0.19 | 0.09 |
| CFRO13 | 0.11 | 0.10 | -157.66 | 0.22 | 0.04 |
| DMAS09 | 0.12 | 0.10 | -149.56 | 0.24 | 0.03 |
| DMJU08 | 0.15 | 0.11 | -169.00 | 0.27 | 0.01 |
| RWPL01 | 0.05 | 0.06 | -78.00 | 0.14 | 0.20 |
| SFAS06 | 0.09 | 0.09 | -129.57 | 0.21 | 0.06 |

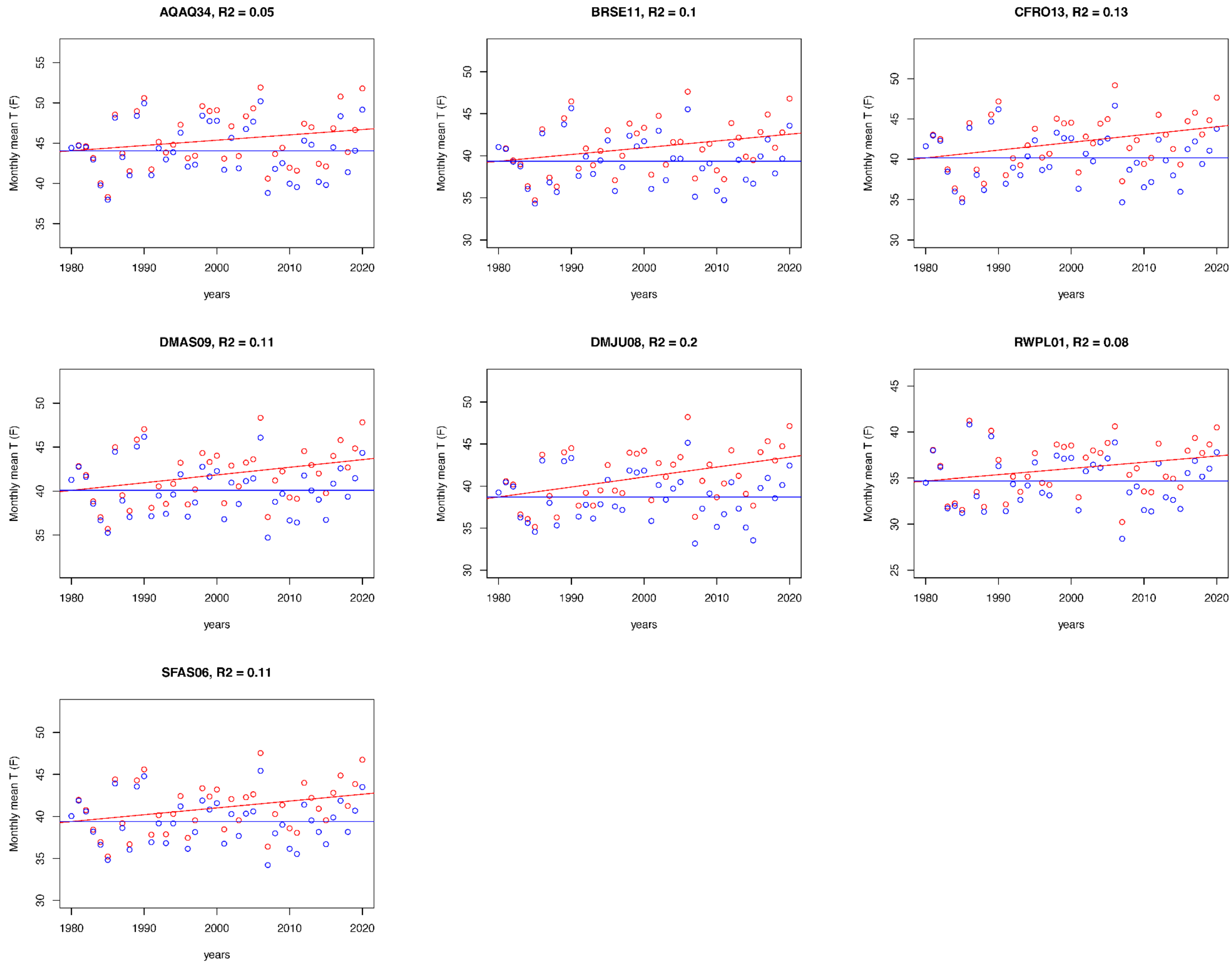


**Figure A-1:** **January monthly mean temperatures from 1980 – 2020 (red) and corresponding detrended data (blue) with linear fits.**

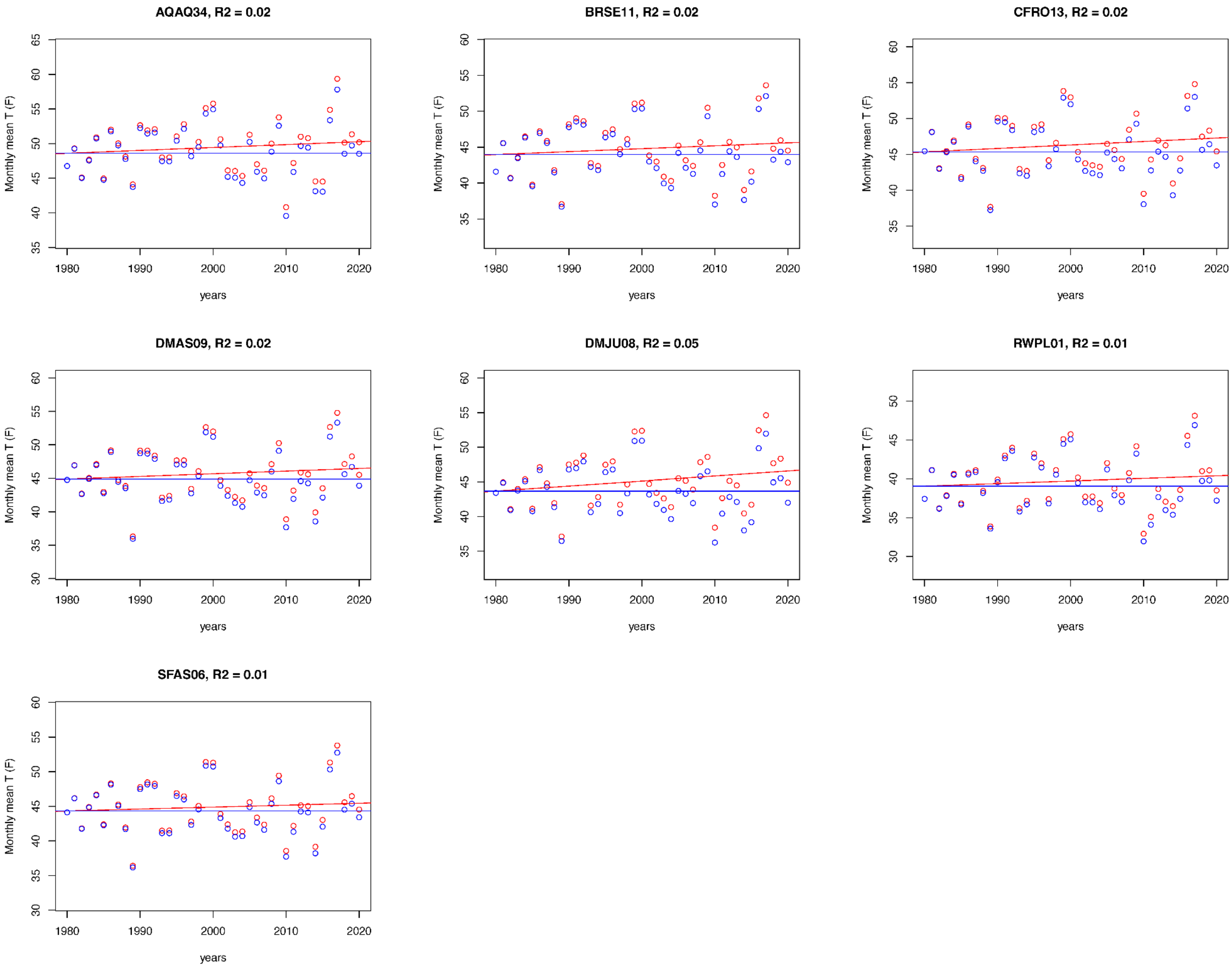


**Figure A-2:** **February monthly mean temperatures from 1980 – 2020 (red) and corresponding detrended data (blue) with linear fits.**

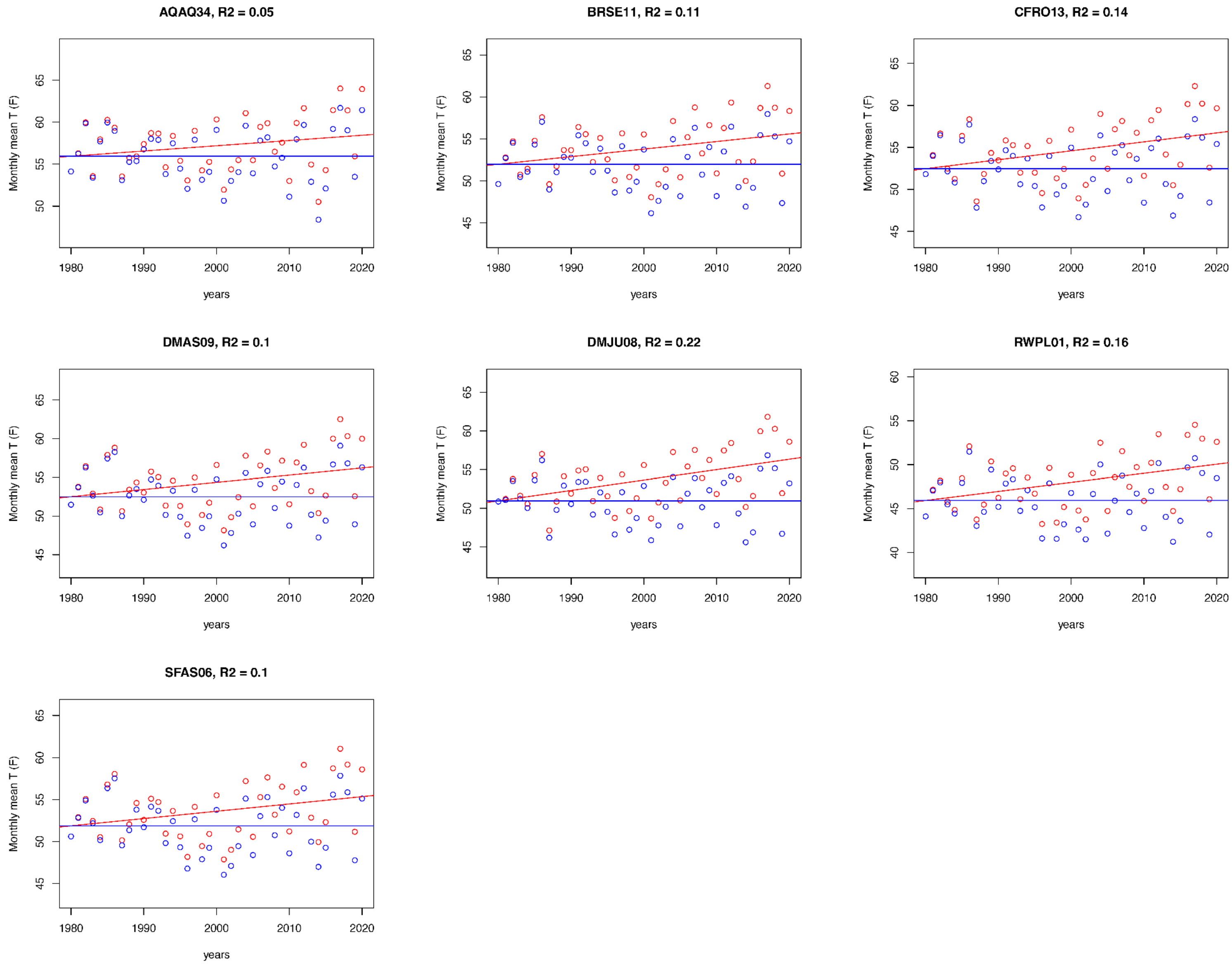


**Figure A-3:** **March monthly mean temperatures from 1980 – 2020 (red) and corresponding detrended data (blue) with linear fits.**

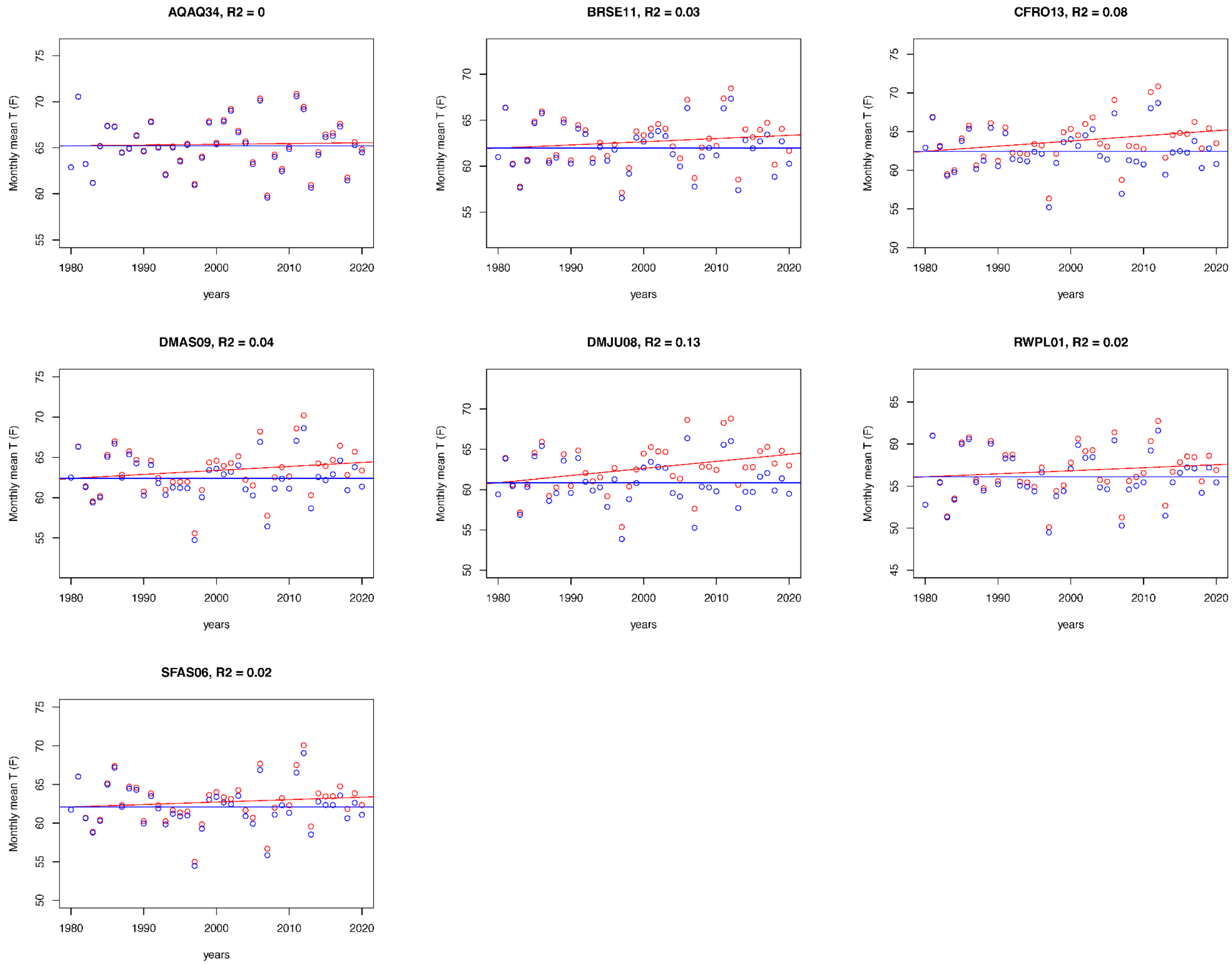


**Figure A-4:** **April monthly mean temperatures from 1980 – 2020 (red) and corresponding detrended data (blue) with linear fits.**

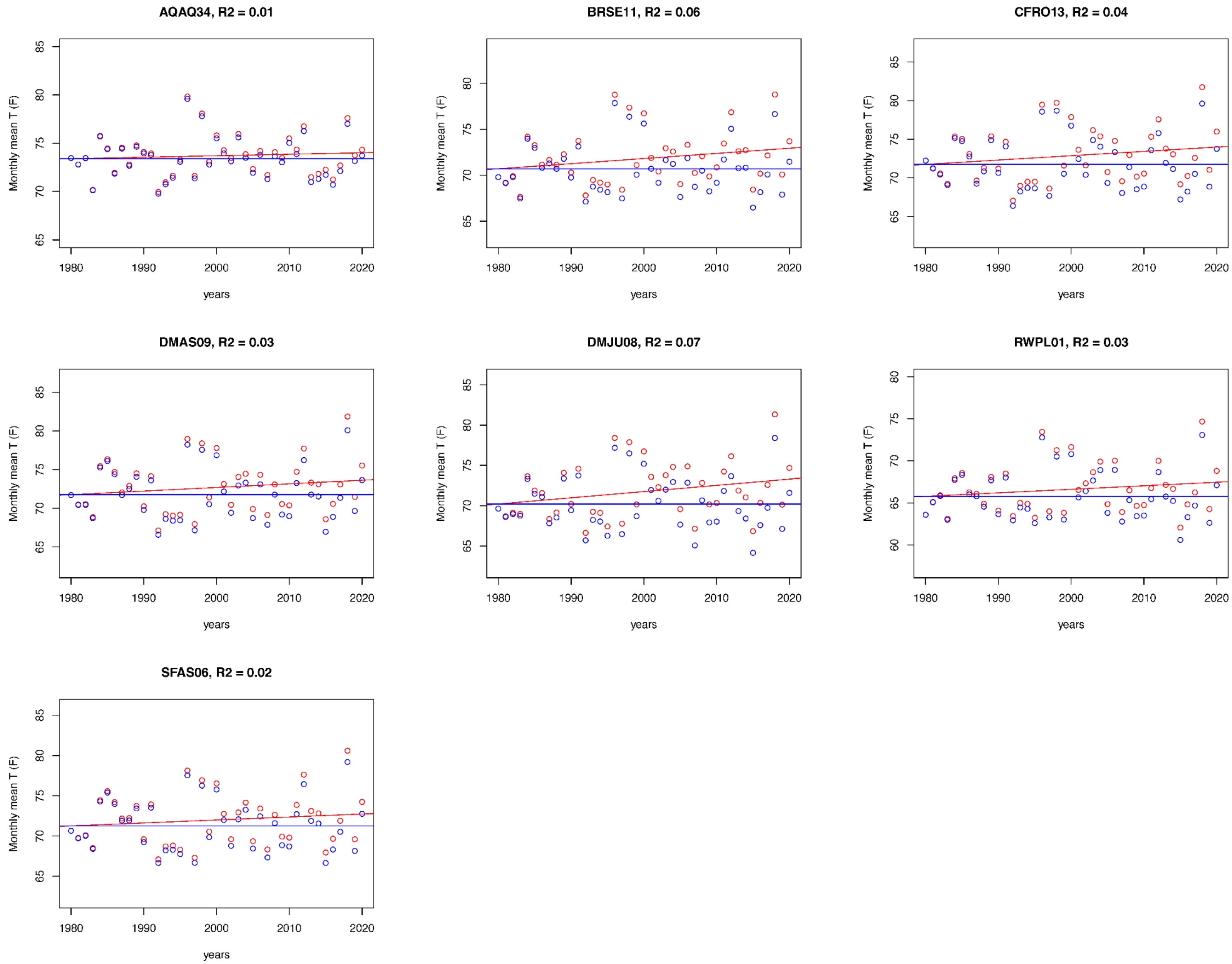


**Figure A-5: May monthly mean temperatures from 1980 – 2020 (red) and corresponding detrended data (blue) with linear fits.**

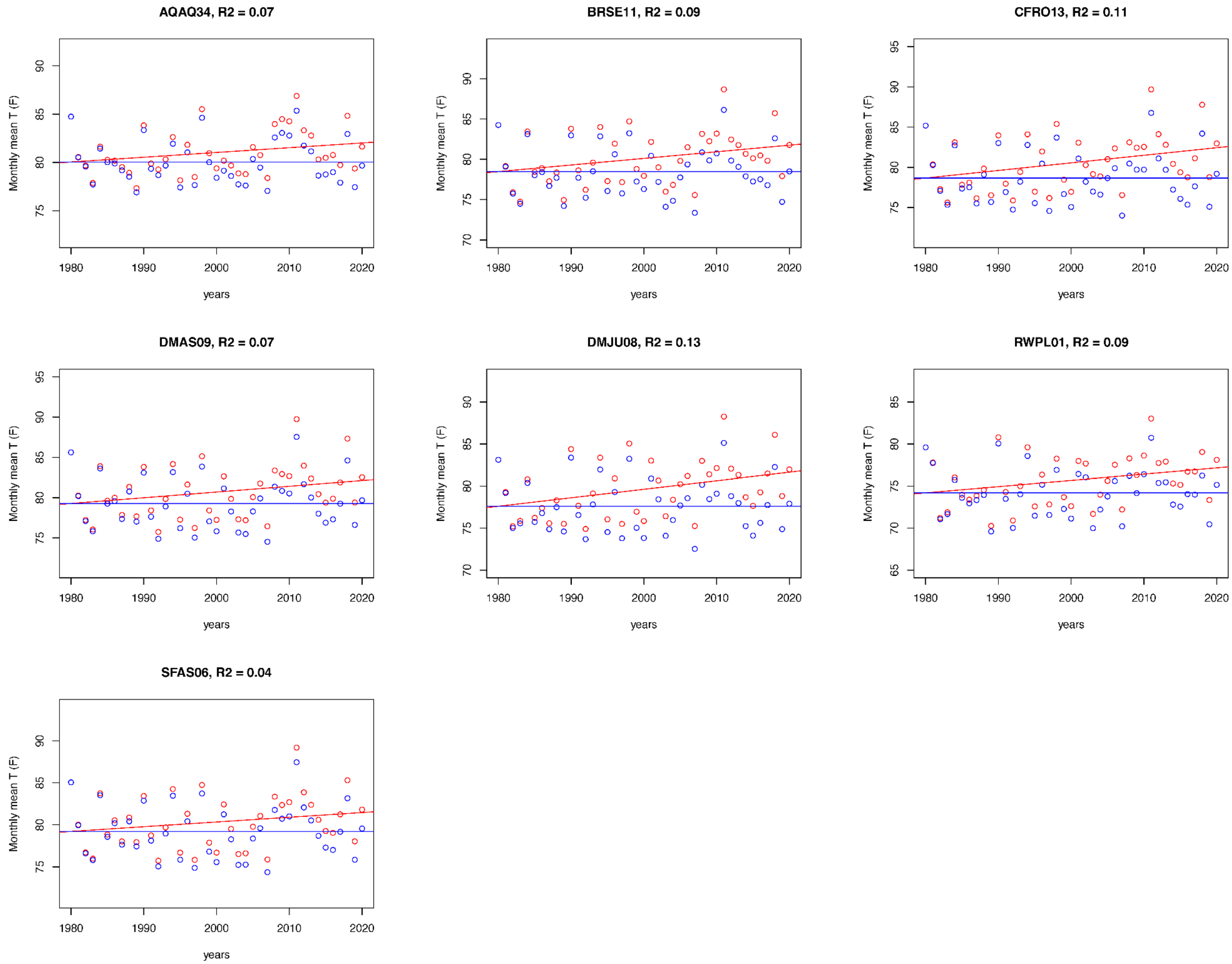


**Figure A-6: June monthly mean temperatures from 1980 – 2020 (red) and corresponding detrended data (blue) with linear fits.**

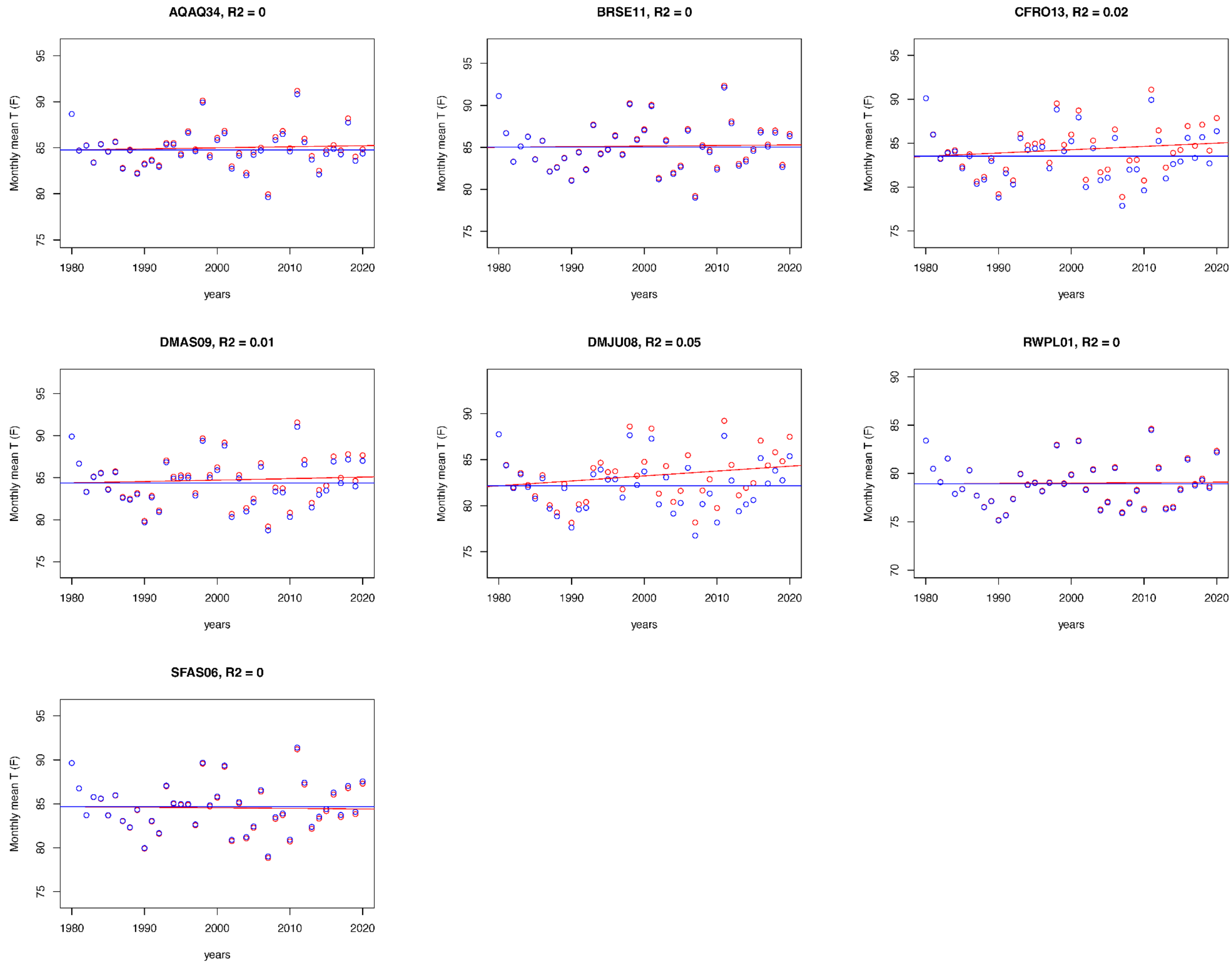


**Figure A-7:** **July monthly mean temperatures from 1980 – 2020 (red) and corresponding detrended data (blue) with linear fits.**

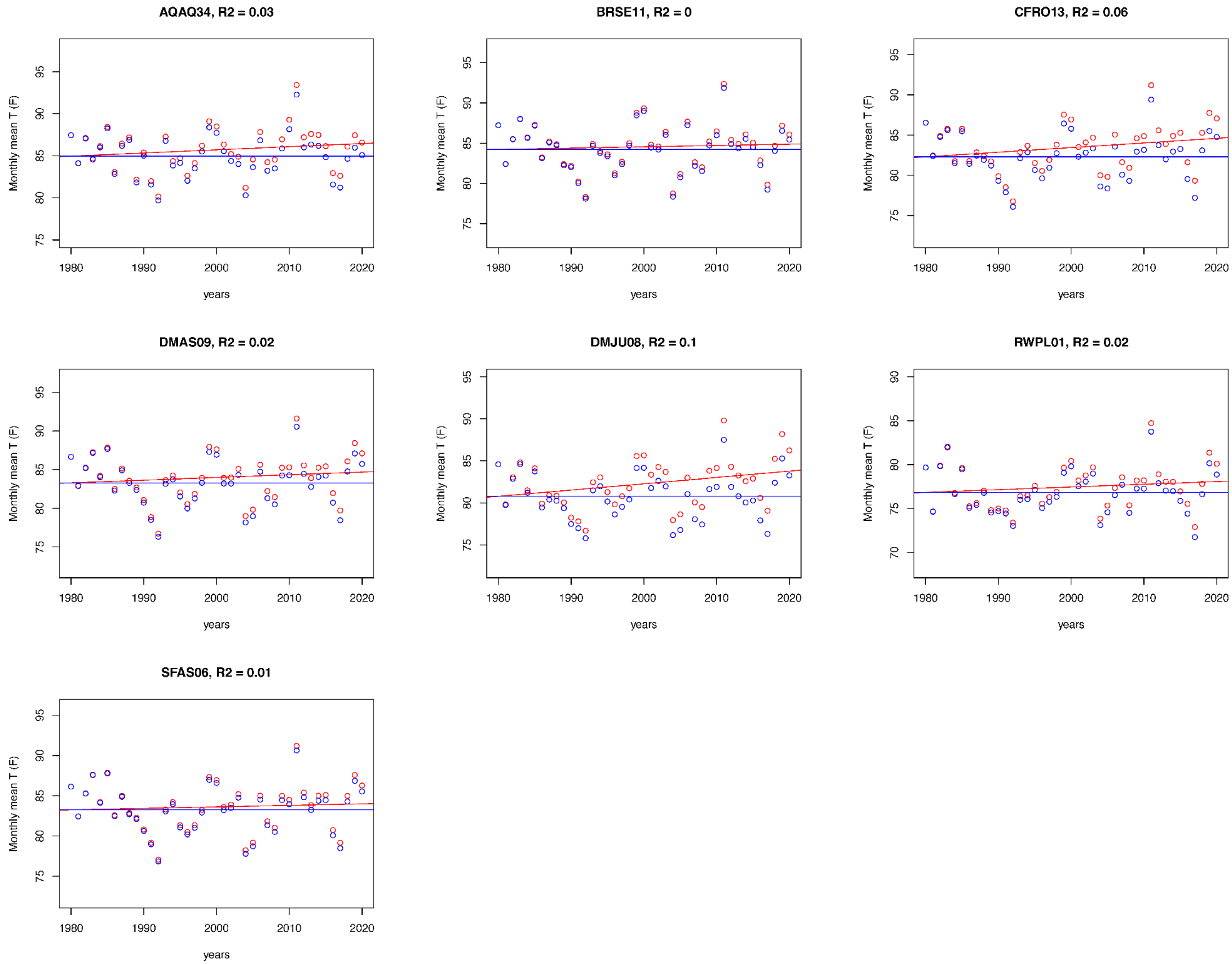


**Figure A-8:** **August monthly mean temperatures from 1980 – 2020 (red) and corresponding detrended data (blue) with linear fits.**

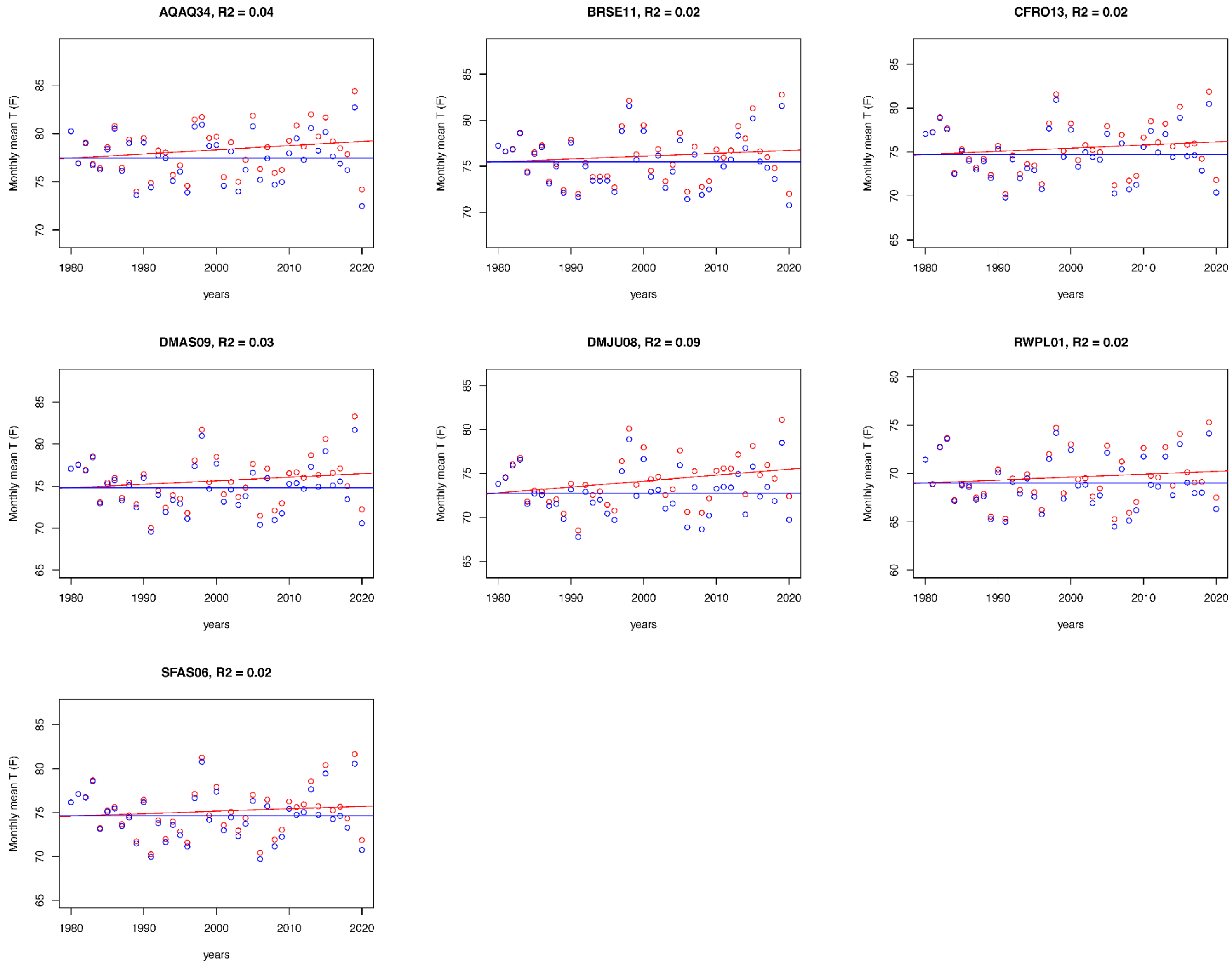


**Figure A-9:** **September monthly mean temperatures from 1980 – 2020 (red) and corresponding detrended data (blue) with linear fits.**

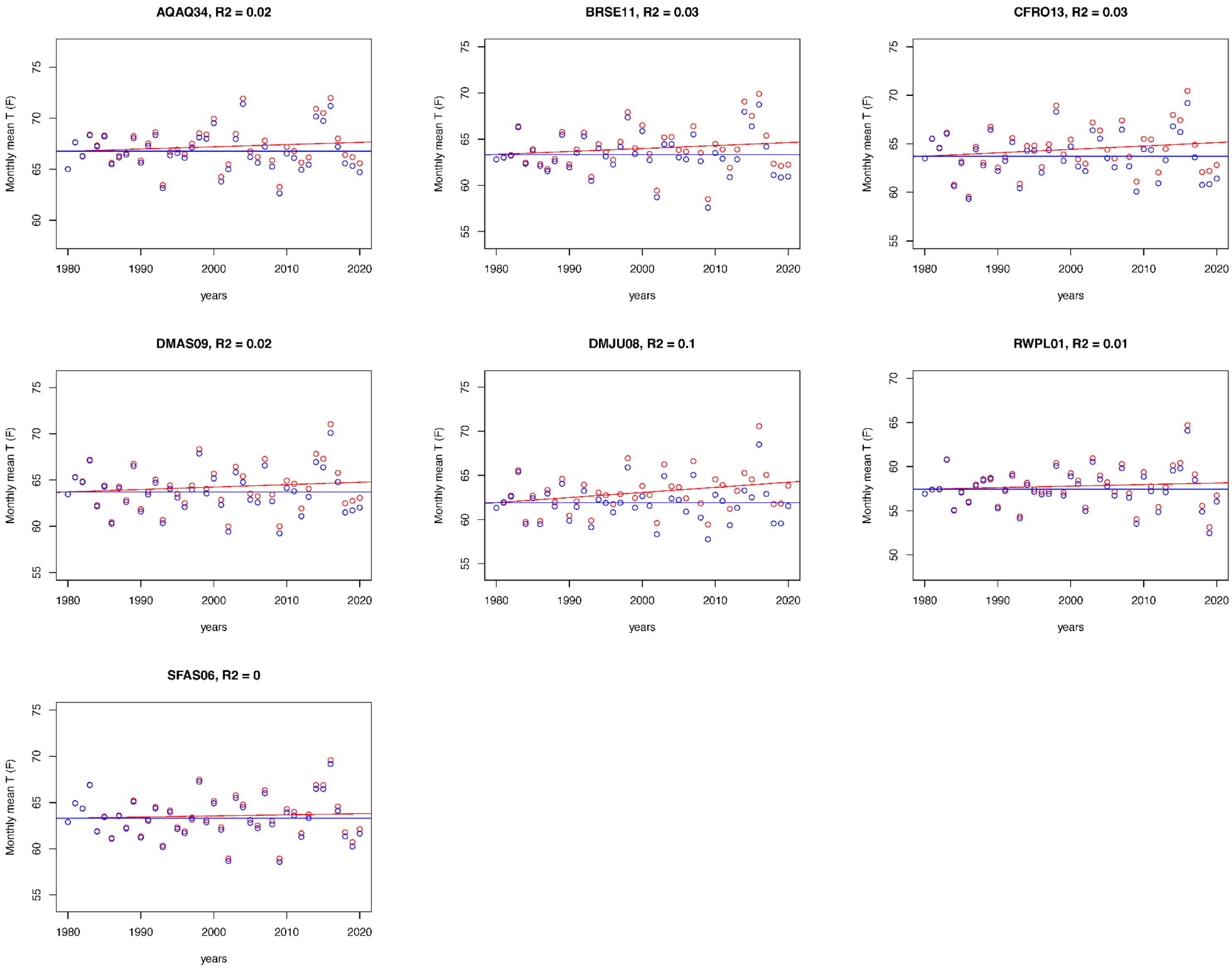


**Figure A-10:** **October monthly mean temperatures from 1980 – 2020 (red) and corresponding detrended data (blue) with linear fits.**

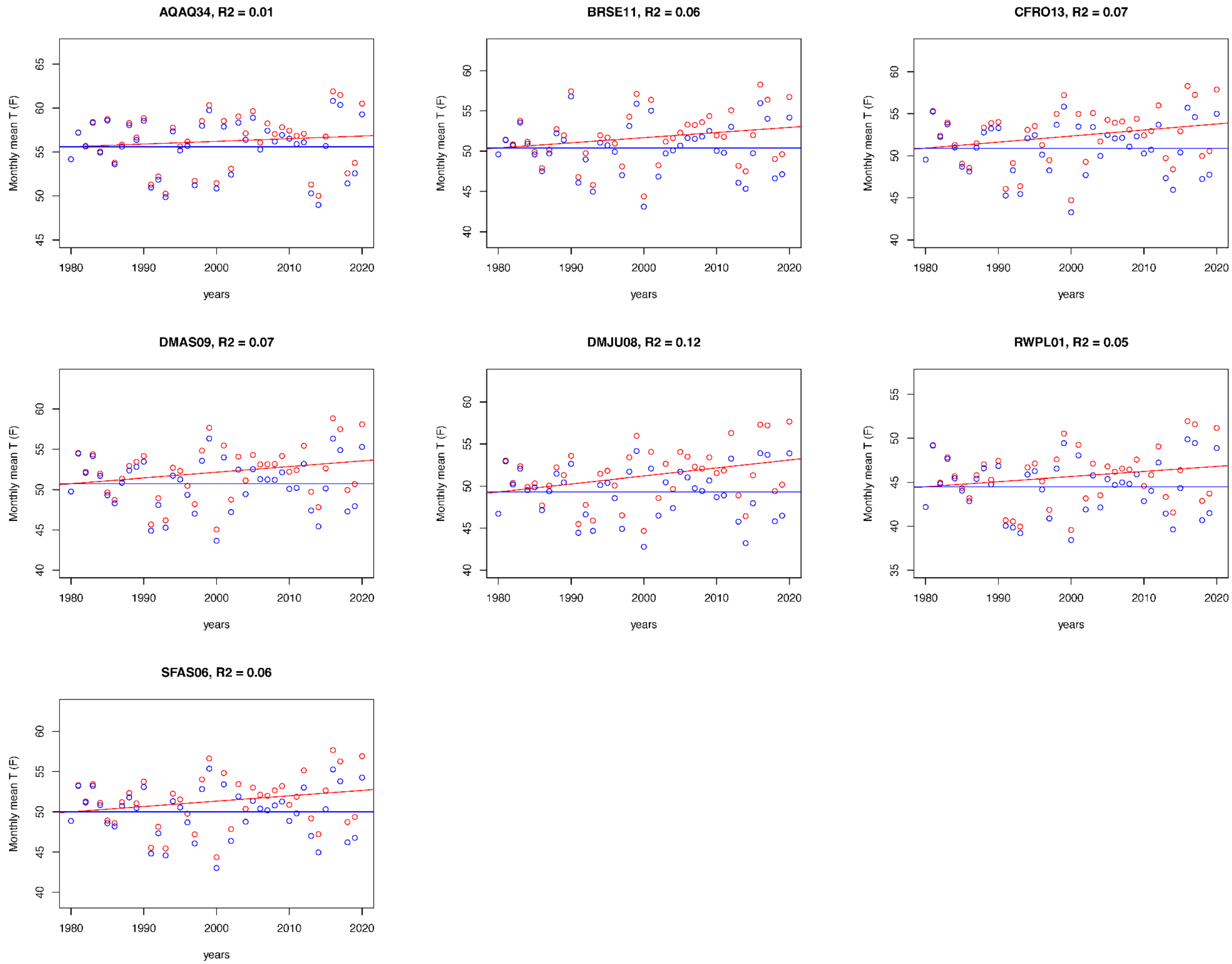


**Figure A-11: November monthly mean temperatures from 1980 – 2020 (red) and corresponding detrended data (blue) with linear fits.**

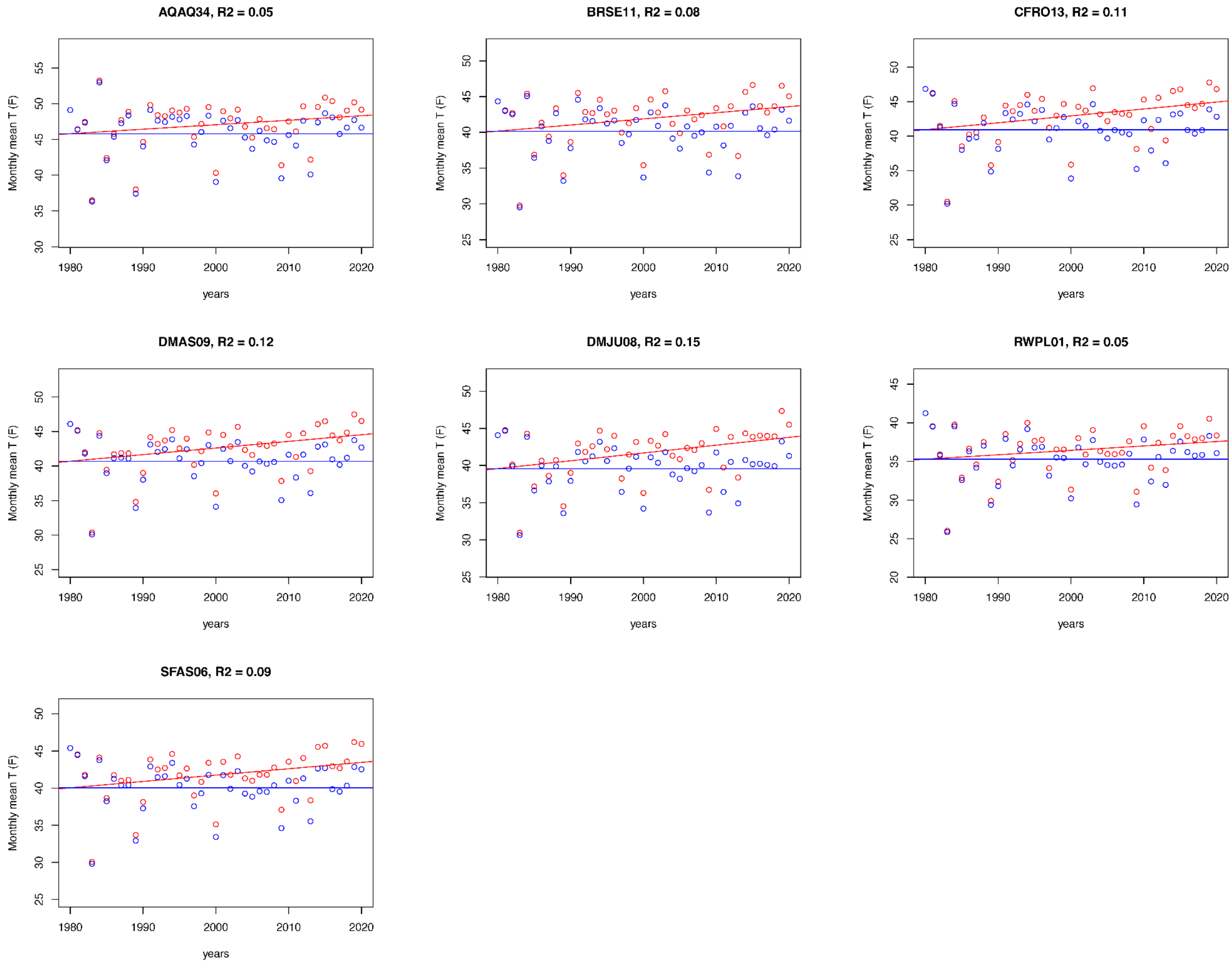


**Figure A-12: December monthly mean temperatures from 1980 – 2020 (red) and corresponding detrended data (blue) with linear fits.**

# Appendix B: Temperature Perturbation Experiments

**Table B-1: Average naturalized flow by season (AF/day), 1982-2017.**

| | Winter | | | Spring | | | Summer | | |
|---|---|---|---|---|---|---|---|---|---|
| **Control Point** | WAM | RDHM Control | RDHM Detrended | WAM | RDHM Control | RDHM Detrended | WAM | RDHM Control | RDHM Detrended |
| AQAQ34 | 279.42 | 276.76 | 281.72 | 385.55 | 303.07 | 307.52 | 108.23 | 119.64 | 120.53 |
| BRSE11 | 226.66 | 242.25 | 243.72 | 779.92 | 367.27 | 377.17 | 542.47 | 364.88 | 371.02 |
| CFRO13 | 3.79 | 4.73 | 5.02 | 19.05 | 7.75 | 8.23 | 9.59 | 6.54 | 6.81 |
| DMAS09 | 90.73 | 143.24 | 142.14 | 314.93 | 168.11 | 171.33 | 245.32 | 155.91 | 159.00 |
| DMJU08 | 17.93 | 51.66 | 53.55 | 68.98 | 61.38 | 64.13 | 88.18 | 71.96 | 73.47 |
| RWPL01 | 0.88 | 2.23 | 2.24 | 4.64 | 6.98 | 7.11 | 3.55 | 6.36 | 6.42 |
| SFAS06 | 49.37 | 57.45 | 59.31 | 175.43 | 79.10 | 82.20 | 140.50 | 88.81 | 90.51 |

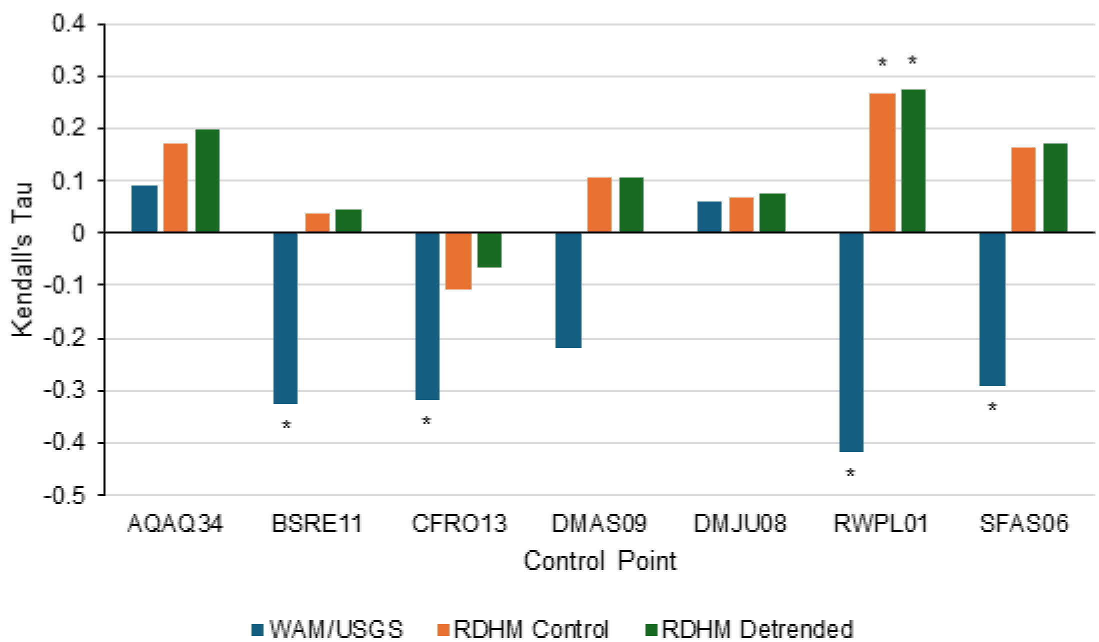


**Figure B-1: Mann-Kendall test results for WAM, HL-RDHM control, and HL-RDHM detrended annual regulated streamflow, 1982-2017. Statistically significant results (p<0.05) are reflected by " * " data labels.**

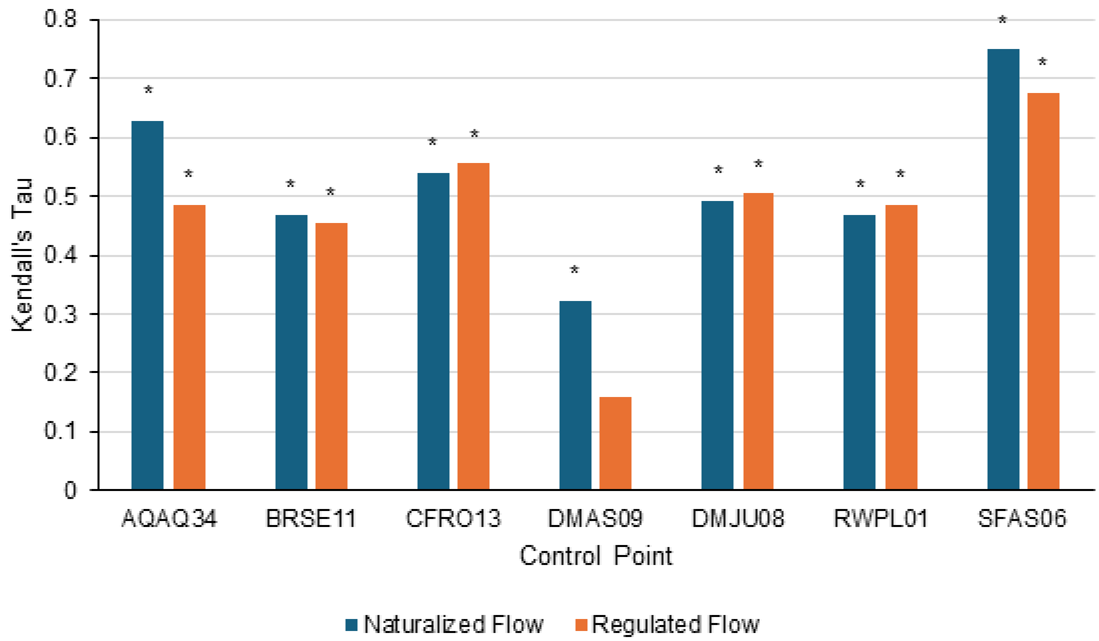


**Figure B-2:** **Mann-Kendall test results for percent difference between HL-RDHM detrended and control annual streamflow, 1982-2017. Statistically significant results (p<0.05) are reflected by " * " data labels.**

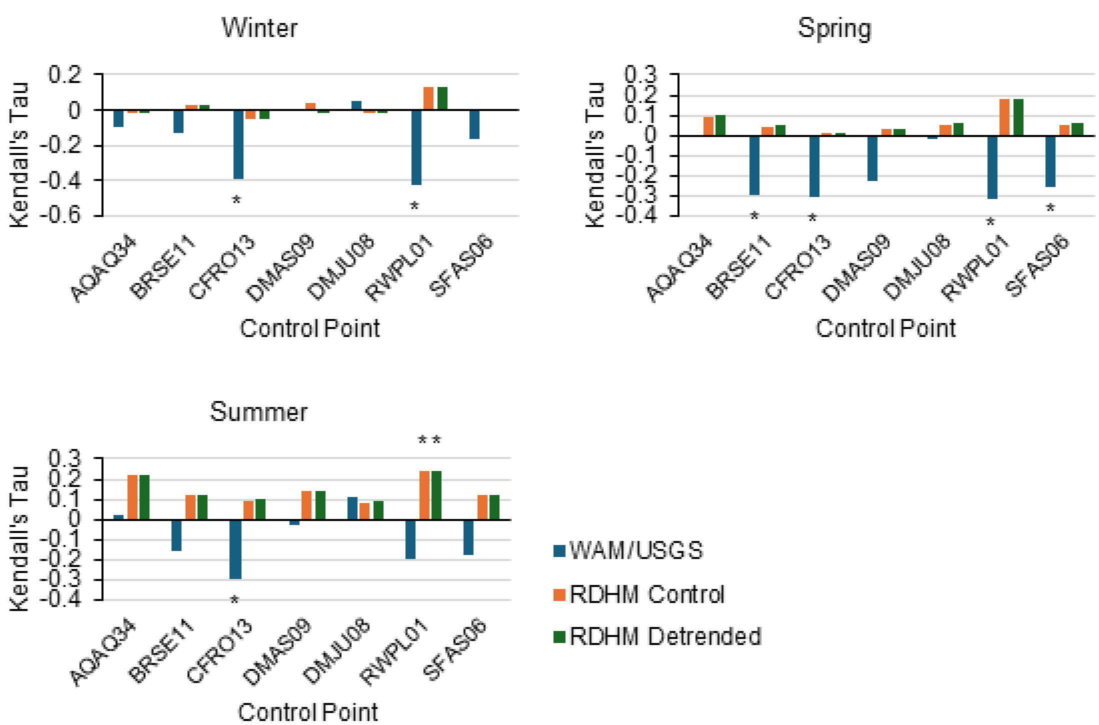


**Figure B-3:** **Mann-Kendall test results for WAM, HL-RDHM control, and HL-RDHM detrended seasonal (winter, spring, summer) naturalized streamflow, 1982-2017. Statistically significant results (p<0.05) are reflected by " * " data labels.**

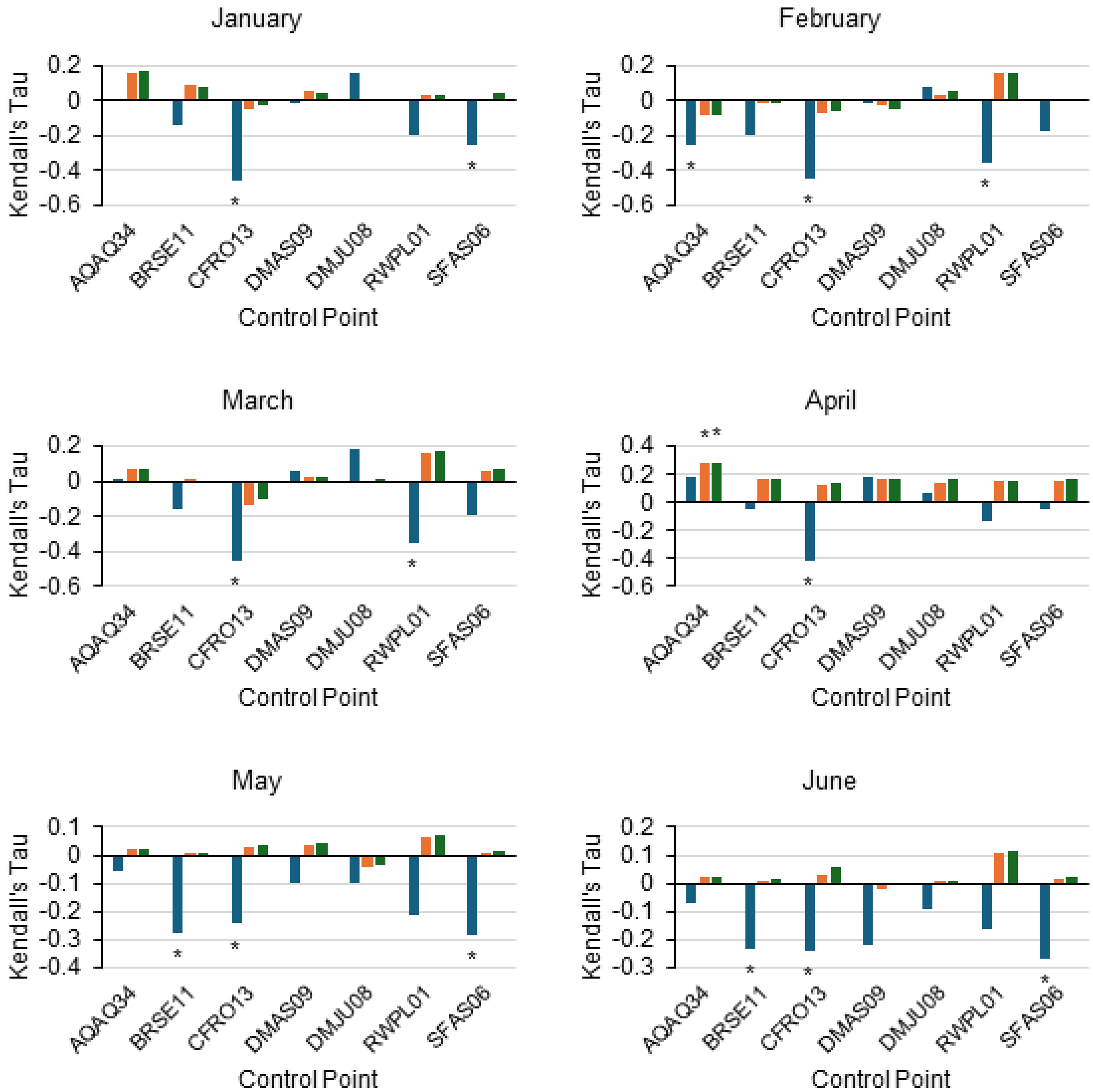
January
February
March
April
May
June
Kendall's Tau
Control Point
AQAQ34
BRSE11
CFRO13
DMAS09
DMJU08
RWPL01
SFAS06
0.4
0.2
0.1
0
-0.1
-0.2
-0.3
-0.4
-0.6
*
**

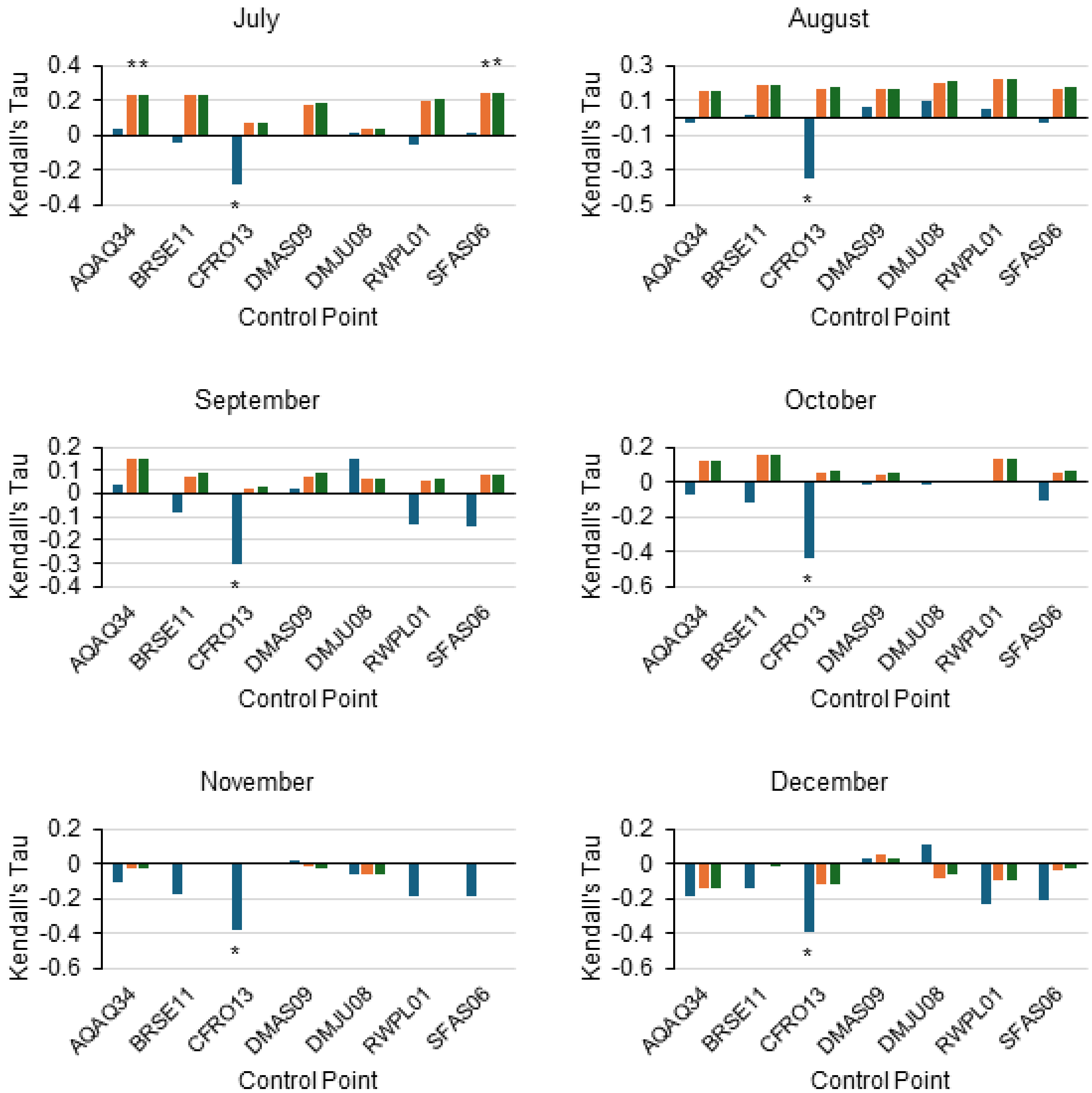


**Figure B-4:** **Mann-Kendall test results for WAM, HL-RDHM control, and HL-RDHM detrended naturalized streamflow by month, 1982-2017. Statistically significant results (p<0.05) are reflected by “ * ” data labels.**

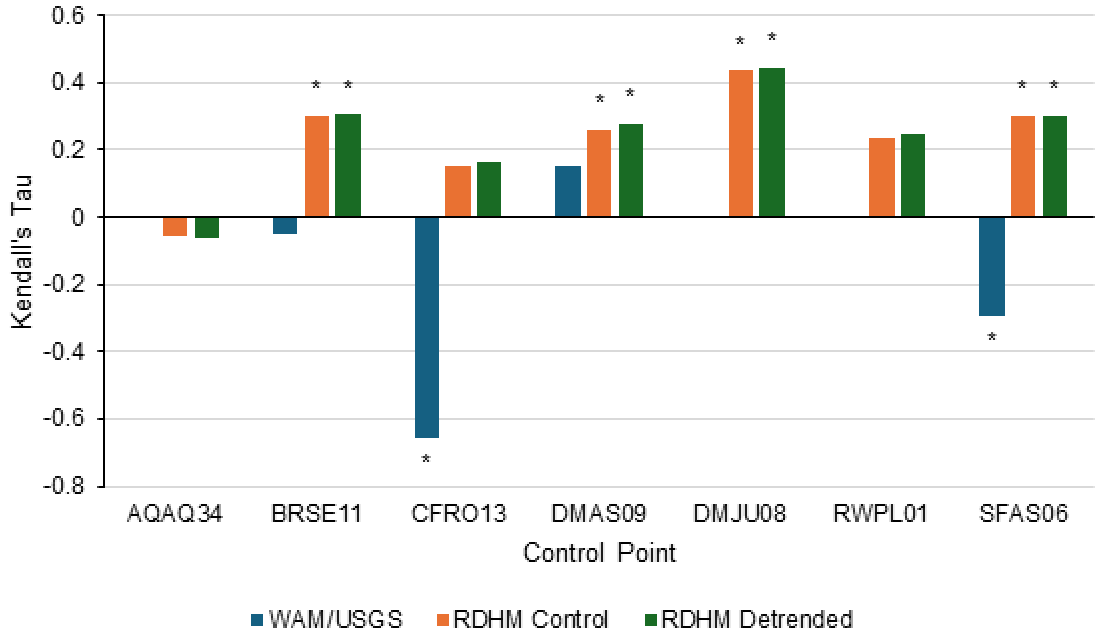


**Figure B-5:** **Mann-Kendall Test Results for WAM, HL-RDHM Control, and HL-RDHM Detrended Annual Peak Naturalized Streamflow, 1982-2017. Statistically significant results ($p<0.05$) are reflected by “ * ” data labels.**

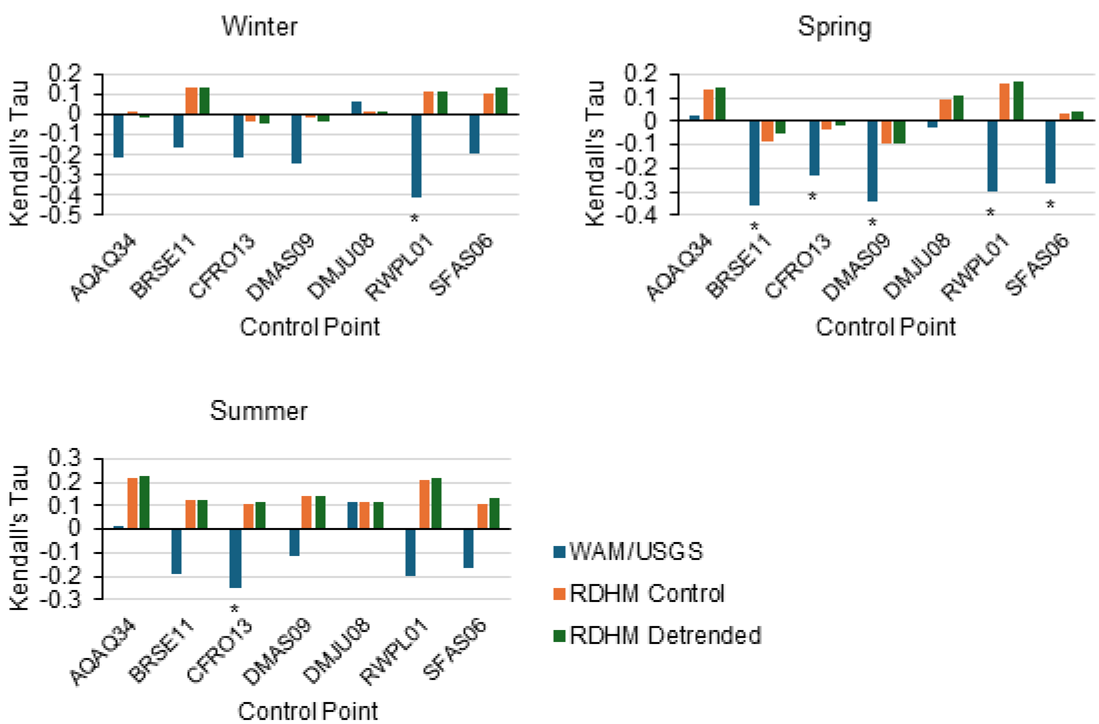


**Figure B-6:** **Mann-Kendall test results for WAM, HL-RDHM control, and HL-RDHM detrended seasonal (winter, spring, summer) HMF total naturalized volume, 1982-2017. Statistically significant results ($p<0.05$) are reflected by “ * ” data labels.**

**Table B-2: Percent difference in naturalized streamflow by year, 1982-2017.**

| Year | AQAQ34 | BRSE11 | CFRO13 | DMAS09 | DMJU08 | RWPL01 | SFAS06 |
|---|---|---|---|---|---|---|---|
| **Overall** | 1.47 | 1.80 | 5.30 | 1.13 | 3.31 | 1.22 | 2.95 |
| **1982** | 0.43 | 0.33 | 0.53 | 0.35 | 0.52 | 0.28 | 0.55 |
| **1983** | 0.77 | 0.32 | 0.95 | 0.27 | 0.51 | 0.55 | 0.59 |
| **1984** | 0.46 | 0.50 | 1.43 | 0.29 | 1.37 | 0.54 | 1.35 |
| **1985** | 0.52 | 0.80 | 1.90 | 0.48 | 0.97 | 0.49 | 0.85 |
| **1986** | 0.71 | 0.63 | 1.41 | 0.55 | 0.95 | 0.33 | 0.85 |
| **1987** | 0.80 | 0.99 | 3.10 | 0.48 | 1.26 | 0.34 | 1.05 |
| **1988** | 1.39 | 0.38 | 1.51 | 0.19 | 2.30 | 0.74 | 1.57 |
| **1989** | 0.71 | 0.69 | 1.96 | 0.25 | 2.31 | 0.43 | 1.85 |
| **1990** | 0.78 | 1.14 | 1.95 | 0.73 | 3.40 | 0.60 | 1.95 |
| **1991** | 0.78 | 1.12 | 3.08 | 0.85 | 1.50 | 0.75 | 1.49 |
| **1992** | 0.99 | 1.86 | 5.93 | 0.75 | 1.75 | 1.17 | 2.43 |
| **1993** | 1.15 | 0.92 | 6.62 | -0.05 | 2.71 | 0.62 | 2.78 |
| **1994** | 1.36 | 0.86 | 3.73 | 0.43 | 4.97 | 0.53 | 2.64 |
| **1995** | 1.01 | 1.05 | 3.38 | 1.10 | 2.96 | 0.72 | 1.74 |
| **1996** | 1.59 | 0.79 | 2.94 | 0.18 | 1.43 | 0.91 | 2.77 |
| **1997** | 1.20 | 2.06 | 5.21 | 1.19 | 4.42 | 0.71 | 2.74 |
| **1998** | 1.08 | 0.31 | 10.00 | -0.83 | 4.34 | 0.60 | 3.69 |
| **1999** | 3.12 | 1.70 | 3.67 | 1.37 | 4.35 | 1.15 | 3.15 |
| **2000** | 1.19 | 1.62 | 3.87 | 1.41 | 5.79 | 0.87 | 2.65 |
| **2001** | 1.96 | 2.56 | 6.48 | -0.45 | 4.36 | 3.61 | 3.80 |
| **2002** | 2.74 | 2.23 | 5.69 | 1.62 | 4.90 | 0.78 | 3.72 |
| **2003** | 2.53 | 2.33 | 6.04 | 1.22 | 5.74 | 1.18 | 3.92 |
| **2004** | 1.50 | 2.02 | 7.23 | 1.97 | 3.29 | 1.10 | 3.27 |
| **2005** | 3.52 | 2.36 | 8.61 | 1.38 | 4.04 | 0.57 | 4.83 |
| **2006** | 2.79 | 1.94 | 10.40 | 1.63 | 3.54 | 0.84 | 3.30 |
| **2007** | 0.95 | 2.52 | 8.39 | 1.46 | 5.39 | 0.94 | 4.55 |
| **2008** | 2.84 | 2.30 | 9.43 | 2.02 | 3.20 | 0.88 | 3.28 |
| **2009** | 1.26 | 1.27 | 3.05 | 0.05 | 4.16 | 1.33 | 5.12 |
| **2010** | 2.43 | 2.81 | 8.24 | 1.64 | 2.48 | 1.54 | 2.84 |
| **2011** | 4.23 | -1.07 | 3.87 | -3.08 | 3.85 | 0.26 | 7.65 |
| **2012** | 2.39 | 0.11 | 4.17 | -0.13 | 2.50 | 1.50 | 5.10 |
| **2013** | 2.90 | 0.88 | 2.60 | 0.25 | 2.25 | 0.95 | 3.79 |
| **2014** | 3.51 | 2.60 | 5.49 | 2.22 | 4.61 | 1.28 | 5.32 |
| **2015** | 1.23 | 2.82 | 4.05 | 1.79 | 6.70 | 3.62 | 4.19 |
| **2016** | 2.32 | 2.08 | 10.43 | 2.11 | 9.56 | 1.34 | 3.65 |
| **2017** | 3.93 | 3.27 | 13.19 | 1.18 | 5.69 | 0.46 | 6.20 |
| **1982-1990** | 0.70 | 0.69 | 1.35 | 0.44 | 1.19 | 0.47 | 1.00 |
| **1991-1999** | 0.78 | 1.13 | 2.77 | 0.80 | 1.96 | 0.70 | 1.59 |
| **2000-2008** | 1.12 | 1.41 | 4.61 | 0.74 | 2.68 | 0.82 | 2.25 |
| **2009-2017** | 1.40 | 1.65 | 3.80 | 1.40 | 5.11 | 1.05 | 2.84 |

**Table B-3: Percent difference in regulated streamflow by year, 1982-2017.**

| Year | AQAQ34 | BRSE11 | CFRO13 | DMAS09 | DMJU08 | RWPL01 | SFAS06 |
|---|---|---|---|---|---|---|---|
| **Overall** | 1.76 | 1.83 | 5.43 | 0.69 | 3.35 | 1.31 | 3.27 |
| **1982** | 0.10 | 0.36 | 0.54 | 0.42 | 0.52 | 0.18 | 0.90 |
| **1983** | 0.58 | 0.33 | 1.06 | 0.22 | 0.52 | 0.08 | 1.00 |
| **1984** | 0.18 | 0.51 | 1.51 | 0.29 | 1.39 | 0.53 | 1.34 |
| **1985** | 1.16 | 0.91 | 2.12 | 0.27 | 0.99 | 0.54 | 1.33 |
| **1986** | 0.84 | 0.63 | 1.38 | 0.12 | 0.96 | 0.56 | 0.96 |
| **1987** | 1.06 | 1.05 | 3.11 | -0.07 | 1.28 | 0.40 | 1.22 |
| **1988** | 1.02 | 0.43 | 1.58 | 0.38 | 2.29 | 0.74 | 1.57 |
| **1989** | 1.10 | 0.84 | 1.84 | 0.04 | 2.44 | 0.46 | 2.12 |
| **1990** | 1.19 | 1.10 | 1.88 | 0.24 | 3.38 | 0.67 | 2.53 |
| **1991** | 1.01 | 1.20 | 3.12 | 0.84 | 1.61 | 0.16 | 1.70 |
| **1992** | 1.15 | 2.03 | 5.93 | -0.80 | 1.76 | 1.27 | 2.74 |
| **1993** | 1.18 | 0.87 | 6.76 | -1.14 | 2.87 | 0.55 | 3.18 |
| **1994** | 2.45 | 0.70 | 3.93 | -0.34 | 4.88 | 0.55 | 4.08 |
| **1995** | 1.10 | 1.02 | 3.33 | 0.61 | 3.08 | 0.67 | 1.95 |
| **1996** | 0.39 | 0.82 | 3.07 | 0.14 | 1.39 | 0.94 | 2.94 |
| **1997** | 1.89 | 2.06 | 5.24 | -0.03 | 4.53 | 0.82 | 3.34 |
| **1998** | 1.22 | 0.27 | 11.68 | -1.08 | 4.19 | -0.96 | 3.71 |
| **1999** | 0.81 | 0.96 | 3.93 | 0.94 | 4.34 | 1.16 | 1.33 |
| **2000** | 1.24 | 1.64 | 4.00 | 1.25 | 5.81 | 0.42 | 2.91 |
| **2001** | 3.40 | 2.68 | 6.77 | -0.73 | 4.40 | 3.68 | 4.00 |
| **2002** | 2.24 | 2.26 | 5.76 | 1.32 | 4.91 | 0.71 | 3.95 |
| **2003** | 3.29 | 2.44 | 6.42 | 1.17 | 5.80 | 1.12 | 4.39 |
| **2004** | 1.98 | 1.84 | 7.26 | 0.16 | 3.30 | 0.76 | 3.50 |
| **2005** | 3.90 | 2.45 | 8.74 | 0.71 | 4.12 | 0.14 | 4.98 |
| **2006** | 2.11 | 2.01 | 10.97 | 1.43 | 3.61 | 1.15 | 3.51 |
| **2007** | 1.22 | 2.52 | 8.54 | 0.39 | 5.47 | 1.65 | 4.72 |
| **2008** | 2.42 | 2.41 | 10.34 | 2.10 | 3.22 | 0.75 | 3.45 |
| **2009** | 1.89 | 1.63 | 3.64 | 0.63 | 4.41 | 1.35 | 5.85 |
| **2010** | 2.39 | 3.03 | 8.44 | 1.91 | 2.53 | 1.55 | 3.07 |
| **2011** | 1.01 | -1.07 | 5.08 | -3.24 | 3.94 | 0.19 | 8.17 |
| **2012** | 4.96 | 0.05 | 4.53 | -0.34 | 2.53 | 1.60 | 5.36 |
| **2013** | 2.25 | 1.29 | 3.14 | 1.46 | 2.29 | 3.25 | 4.09 |
| **2014** | 65.74 | 2.75 | 5.93 | 2.48 | 4.62 | 1.37 | 5.31 |
| **2015** | -3.48 | 2.83 | 4.10 | 1.38 | 6.84 | 3.30 | 4.30 |
| **2016** | 2.35 | 1.75 | 10.56 | -0.35 | 9.77 | 2.00 | 3.79 |
| **2017** | 4.47 | 3.19 | 13.74 | -0.93 | 5.74 | 0.98 | 6.43 |
| **1982-1990** | 0.95 | 0.72 | 1.37 | 0.22 | 1.21 | 0.53 | 1.27 |
| **1991-1999** | 1.08 | 1.16 | 2.78 | 0.56 | 2.04 | 0.32 | 1.85 |
| **2000-2008** | 1.29 | 1.40 | 4.69 | 0.06 | 2.73 | 0.65 | 2.48 |
| **2009-2017** | 1.13 | 1.35 | 3.97 | 1.10 | 5.11 | 0.89 | 2.27 |

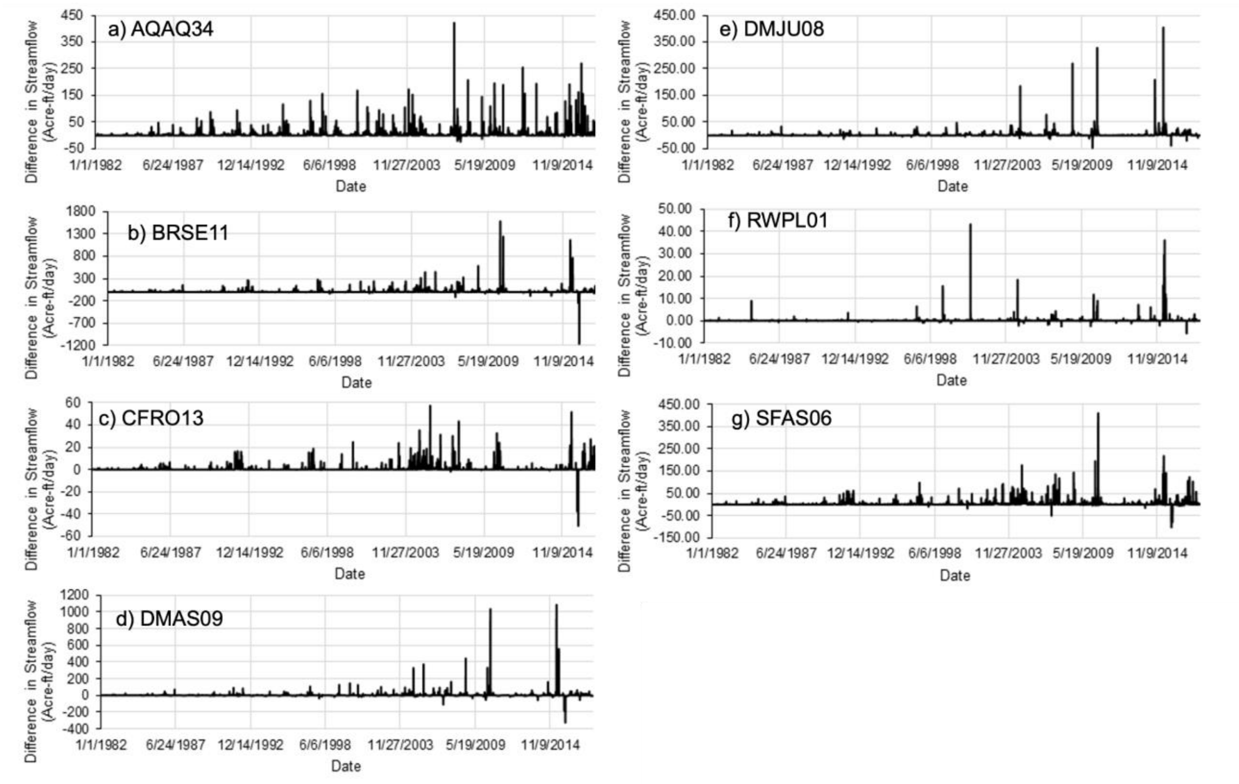


**Figure B-7:** **Time series of difference in daily naturalized streamflow between HL-RDHM detrended and control (AF/day). 1982-2017.**

# Appendix C: Modification of Input Files for the WRAP Modeling System

To account for the impact of temperature detrending within the WRAP modeling system, two different input files were modified to reflect impacts to naturalized flow and net evaporation-precipitation. A summary of EV, DF, and IN records discussed herein is shown in Table C-1. The temperature-detrended naturalized flow results from the RDHM model were integrated into the WAM by averaging on a per day (SIMD) or per month (SIM) basis. Then, these values were replaced in the "DF" (daily) and/or "IN" (monthly) naturalized flow records for the selected control points in the input files. All these records in the Daily Brazos WAM extend from January 1940 to December 2017. Implementing net evaporation-precipitation ("EV") records is more difficult since RDHM model does not directly output this parameter. Therefore, we needed to estimate temperature-detrended evaporation records ("EV").

**Table C-1. Summary of EV, DF, IN records.**

| Record | Parameter | Units | Resolution | Number of Control Points |
|---|---|---|---|---|
| EV | Net Evaporation-Precipitation | ft/month | Monthly | 67 |
| DF | Naturalized Flow | acre-ft/day | Daily | 58 |
| IN | Naturalized Flow | acre-ft/month | Monthly | 77 |

**Construction of Net Evaporation-Precipitation Records from RDHM Output**

The net evaporation-precipitation records must be adjusted for locations corresponding to the 7 control points based on the RDHM results. While adjustment of evaporation records across the entire Brazos River Basin would better capture upstream effects on downstream locations, we limited the scope of this study to 7 control points of interest.

Using air temperature, minimum daily temperature, maximum daily temperature, it is possible to estimate the evaporation rates. For this report, the Penman model was used. It has been reported in the literature to have good alignment within measured values, approximately 0.5 mm day$^{-1}$ (Linacre, 1977). The model equation is as follows:

$$Evaporation\left(\frac{mm}{d}\right) = \frac{\frac{700(T + 0.006h)}{100 - Latitude} + 15(T - T_d)}{(80 - T)}$$

$$T - T_d = 0.0023h + 0.53R + 0.35R_{annual} - 10.9℃$$

$$R(℃) = T_{max} - T_{min}$$

where $T$ is the air temperature in °C, $T_{max}$ is the maximum daily temperature, $T_{min}$ is the minimum daily temperature, $h$ is the altitude of the control point in meters, the $Latitude$ of the control point is in degrees, and $R_{annual} = 12℃$ is the difference between summer and winter temperatures. Elevations and latitudes corresponding to control point locations are shown in Table C-2.

| **Control Point** | **Location** | **Drainage Area ($km^2$)** | **Elevation (m)** | **Latitude** |
|---|---|---|---|---|
| AQAQ34 | Aquilla Creek near Aquilla | 795.1 | 159 | 31.85 |
| BRSE11 | Brazos River at Seymour | 4,147 | 393 | 33.59 |
| CFRO13 | Clear Fork Brazos River near Roby | 688.9 | 598 | 32.74 |
| DMAS09 | Double Mountain Fork Brazos River near Aspermont | 4,211 | 543 | 33.13 |
| DMJU08 | Double Mountain Fork Brazos River at Justiceburg | 686.3 | 687 | 33.04 |
| RWPL01 | Running Water Draw at Plainview | 764.0 | 1,026 | 34.18 |
| SFAS06 | Salt Fork Brazos River near Aspermont | 5,721 | 542.85 | 33.13 |

The daily estimates were aggrgated on a monthly interval and converted to units of ft/mon for consistency with the Daily Brazos WAM input files. The Daily Brazo WAM DSS input file requires ‘EV records’ of monthly reservoir evaporation in feet minus precipitation. The original ‘EV records’ are monthly values based on TWDB daily precipitation and evaporation data as described in Wurbs (2019). For consistency with the required EV file structure, daily estimates where aggregated to monthly values. The precipitation rates were subtracted from the evaporation rates to create the modified net evaporation-precipitation records.

$$Evaporation\left(\frac{ft}{mon}\right) = \sum_{i=1}^{Days\ in\ Month} \left(\frac{0.00328084\ ft}{mm}\right) * \left(Evaporation\left(\frac{mm}{d}\right) - \frac{24\ hr}{d} * Precipitation\left(\frac{mm}{hr}\right)\right)$$

**Comparison of Control EV records with Brazos WAM EV records**

To assess the validity of using this approach, the Penman equation was used to reconstruct the historic evaporation records (i.e., non-detrended temperature) in the WAM input files. Herein, these historic Penman estimates are referred to as ‘control EV records.’ The coefficient of determination was used to evaluate agreement between reconstructed control EV records using the Penman equation and the EV records used in the Daily Brazos WAM.

The 7 control points listed in **Error! Reference source not found.** do not correspond to the location IDs of the EV records of the Brazos WAM. However, the TWDB quadrangles do correspond to the control points of these records (FNI, 2017). These quadrangles can in turn be related to the 7 control points that are located within the same quadrangle as summarized in Table .

**Table C-3. Corresponding EV record control point for each point in RDHM analysis**

| Control Point | Location | TWDB Quadrangle | WAM EV Record Control Point |
|---|---|---|---|
| AQAQ34 | Aquilla Creek near Aquilla | 610 | 228731 |
| BRSE11 | Brazos River at Seymour | 408 | 341331 |
| CFRO13 | Clear Fork Brazos River near Roby | 507 | 372031 |
| DMAS09 | Double Mountain Fork Brazos River near Aspermont | 407 | 341131 |
| DMJU08 | Double Mountain Fork Brazos River at Justiceburg | 406 | 368931 |
| RWPL01 | Running Water Draw at Plainview | 306 | 368131 |
| SFAS06 | Salt Fork Brazos River near Aspermont | 407 | 341131 |

Note that DMAS09 and SFAS06 are located in quadrangles containing the same WAM EV record location. The EV records for the 6 WAM control points were taken from the 2021 Monthly Brazos WAM available on the TCEQ website at the time of this report (TCEQ, n.d.), and plotted against the RDHM control EV records constructed for the 7 RDHM control points. The time series for these two records are compared in Figure  for all points.

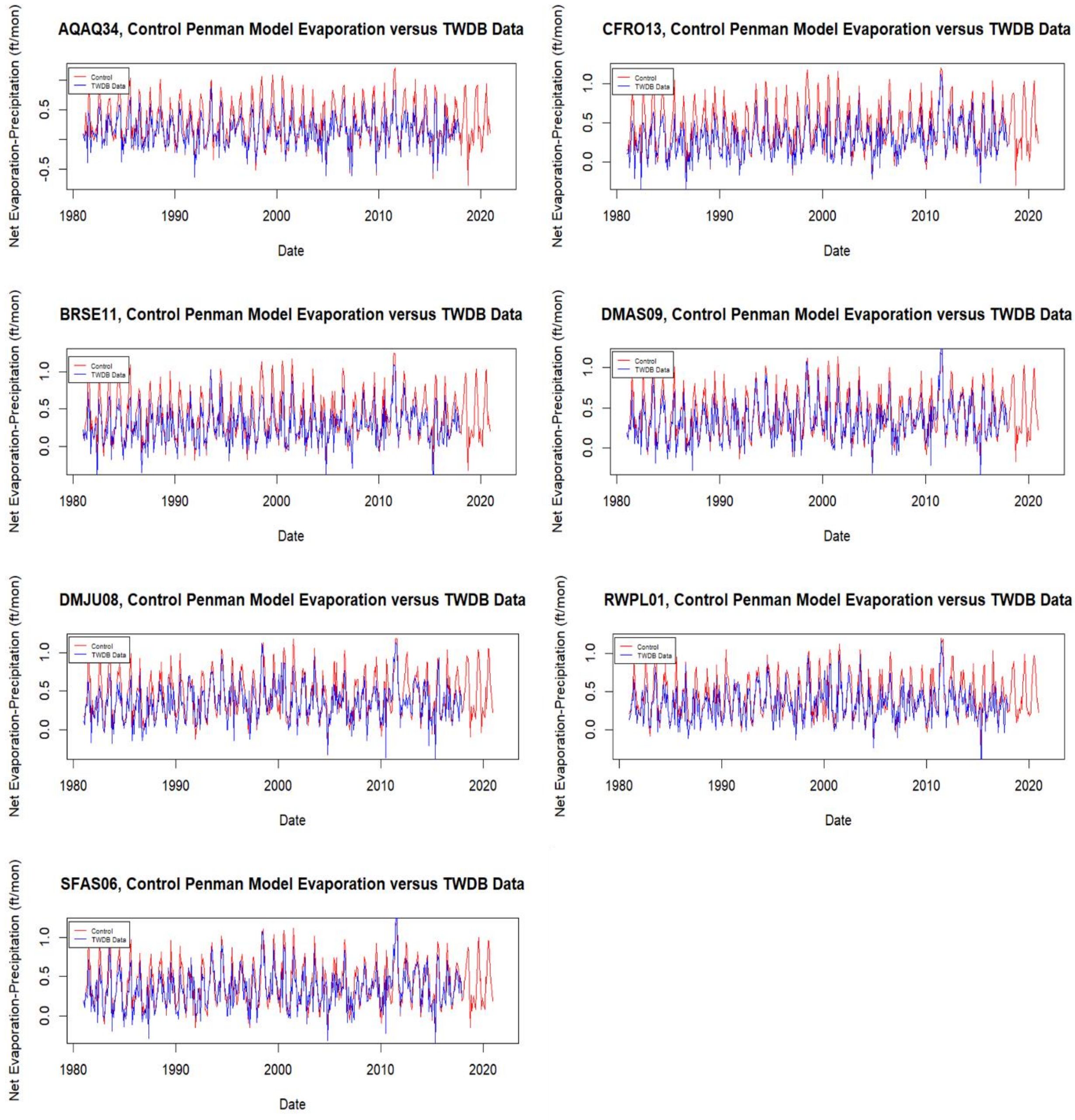


**Figure 23**.Control Point EV records.

**Figure C-1. Control EV record reconstructed using the Penman model (red) versus Brazos WAM EV records developed from TWDB quadrangle data (blue).**

The plots in Figure  suggest good alignment between the TWDB pan evaporation data and the EV records constructed based on RDHM results though the Penman estimates generally overestimate net evaporation-precipitation. The coefficient of determination between the control scenario and the Brazos WAM EV records was calculated to better quantify the correlation and is summarized in Table . The correlation between the control EV records and WAM records for Net-Evaporation have an average $R^2$ of 0.75.

**Table C-4. Coefficient of Determination between Control EV records and TWDB records in Brazos WAM.**

| Control Point | Location | $R^2$ between Control and TWDB Data |
|---|---|---|
| AQAQ34 | Aquilla Creek near Aquilla | 0.806 |
| BRSE11 | Brazos River at Seymour | 0.747 |
| CFRO13 | Clear Fork Brazos River near Roby | 0.754 |
| DMAS09 | Double Mountain Fork Brazos River near Aspermont | 0.761 |
| DMJU08 | Double Mountain Fork Brazos River at Justiceburg | 0.705 |
| RWPL01 | Running Water Draw at Plainview | 0.687 |
| SFAS06 | Salt Fork Brazos River near Aspermont | 0.776 |
| Average | - | 0.748 |

**Source:**


• E. T. Linacre, "A simple formula for estimating evaporation rates in various climates, using temperature data alone," Agricultural Meteorology, vol. 18, no. 6, pp. 409-424, 1977.

• FREESE AND NICHOLS, INC., "DROUGHT STUDY REPORT," August 2017. [Online]. Available: https://brazos.org/Portals/0/Documents/WMP/2018/DroughtStudyFinal.pdf.

• "Water Availability Models," Texas Comission on Environmental Quality (TCEQ), [Online]. Available: https://www.tceq.texas.gov/permitting/water_rights/wr_technical-resources/wam.html.

# A model-based Investigation of Streamflow Trends in Upper Brazos River Basin 2022-2024

## TWDB Contract #2200012624 Comments to Draft Final Report

## REQUIRED CHANGES

**General Draft Final Report Comments:**

- The authors are commended on their methodological approach to evaluating the mechanisms that may serve to explain observed changes in streamflow, specifically with regard to isolating the influence of coincident trends in temperature, precipitation, and land use change.

Response: Thank you.

- The authors do not present any reanalysis of the validity of the statistically significant trends found by the FNI study. The authors of the present study rely solely on the previous FNI work to define 'evident' or observed trends. A select subset (those in the Upper Basin and one near Aquilla Lake) of the trends noted in the FNI study are effectively taken at 'face value' in this work; however, no explanation is given as to why the authors did not include all of the statistically significant trends, noted by FNI, in the present study. The FNI work noted the presence of statistically significant and declining trends (p-value $< 0.05$) in streamflow across the basin but most prevalent in the central and upper reaches. The present study assesses only the upper basin declining trends: As this study functions as an expansion and continuation of the FNI work, the discontinuity between the two studies needs to be addressed so that the reader can sufficiently relate the significance of each study to the other. Also, the Scope of Work (SOW) objectives for the present study established the expectation that drivers for trends observed at all control points in the Brazos WAM (basin wide) would be assessed, and the SOW Tasks include work to "Check trends in temperature in the reanalysis data set against station observations for stations where trends were evident."

**Response: We did review the streamflow records at each USGS station over the period of 1980-2020, and re-computed the MK statistics for each station with sufficient data. We found only five stations with statistically significant trends. At the remaining stations, either there is excessive missing data, or the MK statistics show insignificant trends.**

**Note that trends computed from FN2022 using WAM flows can be skewed by the errors in such data (obtained by extrapolating records from nearby stations). In the revision, we have included a table (Table 2-1) to summarize the MK stats and data availability.**

**Due to the fact that only a few stations are showing statistically significant trends, and the time required to calibrate flow for a large number of stations, the PI had conferred with the project manager in 2023 to descope the project to focus on only the five stations and two additional, upstream WAM control points.**

**In the revised report, a comparison between the AORC temperature product and observations from Global Historical Climate Network (GHCN) stations is shown in Table 3-1.**

- The authors note that the FNI work utilized regression analysis to 'fill in' gaps in the hydrologic record at several control points that are not collocated with USGS gaging stations; however, it is unclear if this distinction was used to filter the control points assessed by FNI down to only those assessed by this study. Resultingly, the Background section of this study should be augmented to communicate to the reader why the present study is relying on the FNI work to define 'evident' or observed trends but not for all control points.

**This is being addressed in the response to the preceding comment. The five stations were the only ones with conspicuous trends.**

- Pg 3-5, Please check the formatting and alignment of the list of tables and list of figures for ease of readability and consistency.

We went over the captions for tables and figures and updated the lists.

- Pg 8, Executive Summary, first paragraph: Please spell out USGS.

Done

- Pg 11, and all other instances of use, Background: Please use FNI instead of F&N or FN to denote Freese and Nichols, Inc.

Done

- Pg 20, Section 3.2 and all other instances of use, Impacts of rising temperature on runoff yield: Please use superscript for the 2 in R2, so that it reads as "$R^2$".

Done

- Please spell out all numbers less than 10.

**Done**

**Specific Draft Final Report Comments:**

- Trends in precipitation are referenced multiple times in the Background and Project Overview sections and are compared with trends in temperature and streamflow. However, no data reference (figure or table) is presented to communicate the extent and distribution of those precipitation trends. Figure(s) and/or data tables need to be included in the Background section to better contextualize the comparisons made to precipitation trends on pages 14 and 16.

The trends in precipitation referenced in the first two sections were based on results from FNI2021. Per an earlier comment, we excluded figures/tables from the report by FNI2021, and kindly refer the readers to their findings. The temperature trends can be found in Appendix A.

- Please provide a complete citation for Zhang et al., 2020 mentioned on pages 17 and 20.

Added.

- Pg 8, Executive Summary, third paragraph, first bullet point: Please include the year of the Brazos Water Availability Model used, and the citation for the version used.

Done

- Pg 8, Executive Summary, last paragraph, last sentence (and in all other instances within the report): please use an "n-dash" to denote time period (i.e., 1980–2020 instead of 1980-2020).

Done

- Pg 9, Executive Summary, third bullet point: Please specify the type of land cover type that has expanded.

Done. Added "agricultural land".

- Pg 10, Background, first paragraph: add "source" before "across much of its drainage."

Done

- Pg 10, first sentence: change (Figure1) to Figure 1-1.

Done

- Pg 10, Background, second paragraph: Please elaborate briefly what changes the Brazos River Basin has undergone in the past century and add citations to back statements.

Done

- Pg 10, last paragraph, third sentence: change Figure2.2 to Figure 1-2

Corrected.

- Pg 12, the WAM does not produce naturalized flow. Naturalized flow is an input to the WAM at primary control points.

Corrected to "that serves as input to WAM model"

- Pg 13, Background: Please change "…appears to be a monotonic trend in the averaged temperature…." to "appears to be a monotonic trend in the average temperature…".

Done

- Pg 13-14, Background: The figures from FNI2021 can be referenced in the text. Please do not include more than a single figure from the previous report in this study report.

We removed all figures taken from previous reports in the report.

- Pg 14, last paragraph, change Figure3.1 to Figure 2-1, and Table 3-1 to Table 2-1

Done

- Pg 14, Project Overview: Please add wording to the report explaining that streamflow consists of two portions of flow. One part is directly linked to rainfall, commonly known as surface runoff. The other portion is baseflow received from groundwater discharge. Please specify that the current study is focused on surface runoff.

Added a sentence: "The analysis tacitly assumes that precipitation plays a predominant role in modulating streamflow volume whereas contribution of baseflow owing to deep groundwater discharge is minor.". Note that the precipitation indirectly impacts baseflow through regulating groundwater recharge. The SAC-SMA model does calculate baseflow by assigning a portion of percolated rainfall to a lower zone that represents groundwater reservoir.

- Pg 16, Project overview: The Daily WAM has not been introduced previously. Therefore, please include a brief description of what the Daily WAM is and provide the key citation for the Brazos Daily WAM. Also, include the period of record in the Daily WAM.

Done

- Pg 16, Table 2-1, Please provide additional description (preferably in the text but possibly in the table) regarding what is meant by "Drainage Area" in Table 2-1. "Drainage Area" in the table does not refer to the traditional meaning of drainage area (*e.g.* land area from which precipitation drains to a particular location on a creek, stream, river, lake, or reservoir). This is clear because the drainage area of control point BRSE11 is less than that of upstream control point SFAS06. With the traditional meaning of drainage area, downstream points would always have equal or greater areas than upstream points. Perhaps drainage area in Table 2-1 refers to incremental drainage area (e.g. drainage area at control point that is not accounted for in modeling of upstream control points)?

Added a footnote underneath the table to explain that the drainage area is the incremental one ( excluding the upstream area)

- Pg 17, Section 3.1, third paragraph, Impacts of rising temperature on runoff yield: Please define HRAP.

Done

- Pg 17, Explain how the hour shift for daylight time in obtained measurements was taken into consideration in time adjustments aligned with UTC.

Done. Added 'No adjustments were made for shift in daylight time as this was not expected to appreciable impact simulated runoff.'

- Pg 18, Impacts of rising temperature on runoff yield, Section 3.1, first paragraph: Please clarify whether "improves bias" means "reduces the bias". If so, please consider replacing "improves the bias" with "reduces the bias."

Done

- Pg 18, There are many types of flows in the daily WAM: naturalized, regulated, unappropriated. Explain how the flows from the WAM are an adequate comparison to other streamflow simulations.

Done. Added 'Naturalized flows from the daily WAM were selected for use as calibration data because HL-RDHM simulated naturalized flows. Therefore, these WAM data are the most relevant compared to regulated flow. Daily WAM naturalized flows were used rather than monthly to provide finer temporal resolution calibration data.'

- Pg 20, paragraph one, second sentence states that there were "30 data points for each monthly regression." Figures A-1 through A-12 clearly show 41 data points. Please provide the correct number of data points in the text.

Done – thanks for catching that. Text now says '…resulting in 41 years with average monthly temperature for year (i.e., 41 data points for each monthly regression)..

- Pg 20, Section 3.2, first paragraph, Impacts of rising temperature on runoff yield: Please add "Brazos" before WAM for "monthly WAM" and "daily WAM".

Done

- Pg 21, Impacts of rising temperature on runoff yield, Section 3.2, last paragraph: Please add "(see Table 3-1 for definitions)" after "...LZFWM".

Done

- Pg 21, paragraph two states that the “The first 23 months of HL-RDHM simulated flows are used to ‘spin up’ the model.” In the same paragraph, the model run is described as February 1979 – 2017 and model output data from 1982 – 2017 as being used in the analysis. That would seem to indicate a “spin up” period of 35 months of model output (11 months in 1979 and 12 each in 1980 and 1981). Please double check this paragraph and make any necessary corrections.

Done. Thank you for catching that. Corrected to say 35 months.

- Pg 22, remove automatically generated table description and weblink on top of Table 3-1.

Done

- Pg 22 and all other instances in the report, Impacts of rising temperature on runoff yield, Section 3.2: Please add “coefficient of determination” before R2.

Done

- Pg 23 and all other instances in the report, Impacts of rising temperature on runoff yield, Section 3.2: Please change “coefficient of correlation” to “coefficient of determination”.

Done

- Pg 25, Impacts of rising temperature on runoff yield, Section 3.3: Please clarify whether the evaporation dataset (i.e., the .eva file) in the Brazos WAM was detrended as well.

Yes, a temperature-detrended evaporation file was also produced at the relevant locations. We have updated the main text to clarify: “To simulate the impact of detrended temperature within the WRAP modeling system, input files were modified to include temperature-detrended naturalized flows and estimates of temperature-detrended evaporation. Evaporation was estimated using the Penman equation and the temperature detrended data as described in Appendix C.” And we have added Appendix C with more information on methodology.

- Page 27, change *resolution* to timestep.

Done

- Pg 27, Impacts of rising temperature on runoff yield, Section 3.3: In this exercise, please clarify whether the net evaporation (.eva) files in the daily WAM were also detrended for use in conjunction with the temperature-detrended naturalized flow, simulated by the HL-RDHM, in WRAP. If not, please include a discussion on the implications of not doing so on the results of the study. Note, there is a brief discussion on page 35 about this subject, but it needs to be fleshed out more and included with the material discussed on page 27.

Done – see response to previous comment.

- Pg 27, the Brazos WAM period of record is 1940 through 2018.

For the 2019 WAM, the period of record is through 2017

Done

- Page 27-28, Current words: *These files are used as input to the WRAP software, which allows users to simulate how much water would be available at each control point after water rights appropriations have taken place, referred to as regulated flow*. Please change "regulated flow" to "unappropriated flow". The understanding of regulated flows as calculated in the WAM is not consistent with the use of regulated flows for the purpose of this analysis. Regulated flows in the WAM while allowing for regulation through reservoirs and water supply diversions, also include flows passed for downstream senior water rights. In the absence of an official senior or priority call on flows, junior diversions and impoundments are not curtailed by TCEQ. The modeled regulated streamflow is not in reality passed but captured and diverted by the upstream junior water right holders. Also, existing subordination agreements between upstream junior and downstream senior allow the priority system to be circumvented. Regulated flows in the WAM do not represent any historical streamflow for comparison, but merely flows available for determining reliability and availability for appropriation.

Done – thank you for the clarification

- Pg 35, Impacts of rising temperature on runoff yield, Section 3.3, first paragraph: Ideally, the detrending should be applied to all the control points prior to running the WAM. The .eva files are usually input to WRAP and adjustments are made before input to WRAP. Therefore, please explain how the adjustment was made "in the WRAP software."

Done – see earlier comments. These were modifications to the input files.

- Pg 39, last paragraph, pg 40, last paragraph before section 4., and throughout the report, please be consistent with the capitalization of all forms of the Brazos River Basin, Upper Brazos…, etc.

Done

- Pg 40, Impacts of rising temperature on runoff yield, Section 3.3, fourth paragraph: Please change "deviations" to "diversions", and omit "pumpage", in the examples of flow regulation represented in the WAM.

Done

- Pg 40, Impacts of rising temperature on runoff yield, Section 3.3, fourth paragraph, last sentence: Please change "impaired" to "unappropriated".

Done

- Pg 41, Trends in streamflow/runoff by alternative operational models, Section 4.1, first paragraph: Please spell out WRF on first use.

Done

- Pg 41, Trends in streamflow/runoff by alternative operational models, Section 4.1, first paragraph: Please spell out Noah-MP on first use.

Done. Note that Noah-MP is known as it is and it does not have a full-name. “MP” stands for multi-physics.

- Pg 41, last paragraph, write out Mann Kendall for MK- not listed in the List of Acronyms and not referenced this way anywhere else in the report.

Expanded the acronym

- Pg 41, last paragraph, Table 5-1 should be Table 4-1.

Corrected

- Page 41, When it is first time use “WRF-Hydro” please use full words, Weather Research and Forecasting, and also better to put in Acronyms.

Added to the list of acronyms.

- Pg 42-44, Changes in available flows in one portion of the basin can impact how water is allocated in water right priority in another area, possibly explaining inconsistencies at some gages and especially the Aquilla Creek gage. Unless specifically looking for the illogical consequences of the water right analysis, results can be difficult to interpret.

That’s a possibility.

- Pg 51, last paragraph references Figs. 5.9-5.16, this should be Figures 4-9 thru 4-15.

Corrected.

- Pg 51, last paragraph (Figure5.9), should be (Figure 4-9).

Corrected.

- Pg 59, last paragraph, first sentence “Figure6.1” should be Figure 5-1.

Corrected.

- Pg 59, last paragraph, first sentence, Shrub does not need to be capitalized.

Corrected.

- Pg 59, BRA found increased sedimentation rates at Aquilla and worked with NRCS to promote land use practices to reduce sedimentation rate at the reservoir. Not only changes in land use types but also agricultural practices caused changes in the watershed.

Thanks for bringing this to our attention. We revised the sentence to "If these trends are persistent over time, then there is a possibility that the declining streamflow over the upper basin is tied to expanding agricultural activities, **and possibly to changing agricultural land management practice**".

- Pg 60, First sentence under **BRSE11,** (Figure6-2), should be (Figure 5-2).

Corrected.

- Pg 59-60, Add references to the Figure numbers within the paragraphs for AQAQ34 (Figure 5-1), CFRO13 (Figure 5-3), DMAS09 (Figure 5-4), and SFAS13 (Figure 5-5).

Added.

- Pg 60, next to last paragraph heading references control point SFAS13, but Figure 5-5 (Pg 65) is for SFAS06, please make necessary changes to have consistency.

Corrected to SFAS06

- Page 66, original words: *the WAM naturalized flow for these points was constructed through regression from records at adjacent USGS stations*. Please consider using wording that conveys that the records were developed using the flow-watershed-area-ratio method.

Thanks for the clarification. The method has been corrected with a reference to Emerson et al. (2005).

- Page 67, last paragraph, next to last sentence and page 68, fourth paragraph, next to last sentence: Change "*abstraction*" to infiltration.

We would like to retain "abstraction" as infiltrated water can turn into runoff through interflow, whereas abstraction is about rainfall loss that does not translate into runoff.

- Pg 68, Conclusions and recommendations, second paragraph: Please provide citations to back the statement: "Expansion of impoundments is a well-known phenomenon in the Panhandle."

The report by Furnans (2019) has already been cited here.

- Pg 68, Conclusions and recommendations, second paragraph, second sentence: Please change "northern Texas" to "central Texas".

Changed.

- Pg 68, Conclusions and recommendations, second paragraph, third sentence: Please reword statement to clarify that the explanation was found to be unsatisfactory when applied to the Brazos River Basin.

Changed to “However, thus far there is insufficient evidence to confirm the linkage between declining runoff yield and agricultural management practices in the upper Brazos Basin.”

- Pg 68, Conclusions and recommendations, third paragraph: Please add year to the U.S. Department of Agriculture citation.

Added.

- Pg 68, Conclusions and recommendations, fourth paragraph, last sentence: Note, the TWDB does have groundwater well data for the Upper Brazos Basin. Therefore, please reword this statement to convey that a detailed investigation of groundwater pumping and irrigation records should be considered using all available ground-based and remotely sensed (e.g., OpenET) data.

Added to recommendation 1 on the need for a further investigation of irrigation-related groundwater withdrawal and impacts on runoff.

- Pg 68, Conclusions and recommendations, fifth paragraph, second sentence: Please clarify whether “Highland Aquifer” is a reference to the “High Plains Aquifer”. If so, please change the term to “High Plains Aquifer.” Also, please include a few key citations to back the statement that the High Plains Aquifer has been experiencing continuous decline over the past few decades.

Added two references.

- Pg 69, first sentence, change PRIM to PRISM.

Corrected.

- Pg 71, 2nd entry, add a line between 1st and 2nd reference (Kuzmin).

Added

- Pg 71, next to last entry, remove the indentation before Vincente-Serrano.

Corrected.

- Pg 73, add to the caption the applicable year range associated with Table A-1.

Added.

- Pg 91, bottom of the page, move Table B-2 caption to the top of Pg 92 with Table B-2.

Changed.

**Figures and Tables Comments:**

- Please adopt a consistent format for referring to figures in the text of the report and correct any discrepancies between how the figures are titled and how they are referred to in the text. The figures are formatted as follows in their titles: Figure <Chapter No.>-<Figure No.> (*e.g.* Figure 1-4). Please use this same format when referring to figures in the text as well.

We have reviewed the references and made corrections throughout the text to ensure consistency.

- Pg 10, Figure 1-1: Please move the source within parentheses.

Done

- Pg 12, Figure 1-3: Please delete.

Done

- Pg 12, WAM control point may better to have as WAM primary control point.

We are not sure about the necessity of including WAM primary control point.

- Pg 13, Figure 1-4: Please delete.

Done

- Pg 13, Table 1-1: Please delete.

Done

- Pg 14, Figure 1-5: Please delete.

Done

- Pg 16, Table 2-1 note says: **Daily WAM naturalized flows are used for naturalized flows for all points except CFRO13 which was not included as a primary control point in the daily WAM. Therefore, USGS streamflow observations are used to approximate naturalized flow at this point*. Please note that the daily WAM can be run to generate the naturalized flow for CFR013. Therefore, please consider rewording this sentence to reflect the fact that the Daily WAM could have been used to generate naturalized flow for CFR013, but a different method was adopted. Please explain why a different method was adopted.

Done. This approach was chosen because the 2019 daily WAM uses USGS gage records for 1998-2017 to disaggregate the monthly naturalized flows.

- Pg 30-31, Figure 3-5: Please develop a multi-panel figure so that all plots can fit on one page.
- adopted.

Done

- Pg 62, Change Figure 5-2 caption to reflect Drainage of BRSE11.

Corrected.

- Pg 63, Change Figure 5-3 caption to reflect Drainage of CFRO13.

Corrected

- Pg 64, Change Figure 5-4 caption to reflect Drainage of DMAS09.

Corrected

- Pg 94-95, Appendix, Figure B-7: Please develop a multi-panel figure so that all plots can fit on one page.

Done

# SUGGESTED CHANGES

**Specific Draft Final Report Comments:**

- Pg 11, Background: Suggested rewording: "….and moreover they examined the changes in temperature and net evaporation within overlapping climate divisions".

Changed to ", and reviewed the changes in temperature and net evaporation within climate divisions that overlap with the Brazos River Basin. "

- Pg 20, Section 3.2, and all other instances within the report, Impacts of rising temperature on runoff yield: Please change "streamflows" to "streamflow".

**Changed.**

- Pg 24, Section 3.2, Impacts of rising temperature on runoff yield: Suggest moving: *"The percent biases in the validation period are much higher than calibration, with 3 exceeding 50% (BRSE11, CFRO13, SFAS06). The negative percent biases of all the control points except DMJU08 also reflect the average HL-RDHM control streamflow results being higher than the WAM records during this period"* from first paragraph to second paragraph.

Changed

- Pg 41, Section 4.1 and all instances in the report: Trends in streamflow/runoff by alternative operational models, please spell out LSM as "land surface model" without using the acronym.

Changed

- Pg 69, Recommendation I could be strengthened by discussing more about decreasing trends in the regional groundwater level. To support a potential future study on this subject, we have **attached** groundwater level well records for Hale County. The record indicates that the water level or water table has been declining during past decades. With decreased groundwater levels, the aquifer would lose its ability to discharge groundwater to streams. Therefore, a previously perennial stream may become a seasonal stream.

Thanks for the information. We have expanded recommendation 1 to include the need for an investigation of groundwater level and impact on discharge to streams. In the executive summary, a sentence is added “ In particular, as declining groundwater level has been reported in the upper basin, it is key to investigate the impacts of this decline on the discharge to surface water and its potential contribution to the declining runoff yield”.

**Figures and Tables Comments:**

- Please consider using a consistent set of units within the document (metric or customary). For example, in Table 2-1, drainage areas are provided in units of square kilometers (metric) but mean naturalized flow is provided in acre-feet per day (customary). Recommend presenting both values (drainage area and mean naturalized flow) in customary units (square miles and acre-feet per day) to allow easy comparison to previous studies.

Changed.

- Page 21, paragraph four, first sentence states that “WAM records of daily naturalized flows … are nearly identical to USGS observations.” Please consider providing a figure from a select location and time-period to explicitly demonstrate how these data sets are related. Consider providing a graphic (or graphics) similar to the following for daily naturalized flows at WAM control point SFAS06 and observed average daily flows from USGS gage 08082000 during calendar year 2011. Note, in the figures below, gaged flows were obtained from the USGS. Naturalized flows were created for WAM control point SFAS06 by distributing WAM monthly naturalized flow volumes to daily flows following the pattern of the gaged data in a manner believed to be consistent with WAM documentation (Wurbs, 2019). These graphs are provided only to demonstrate the types of figures the authors may consider.

ATTACHMENT 1

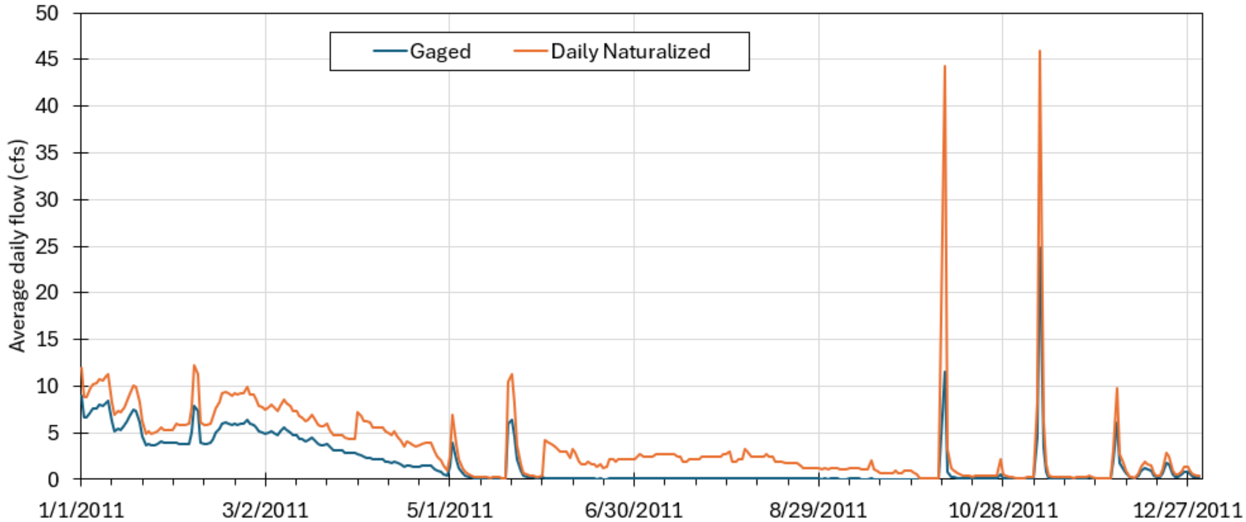


- Same data on a logarithmic vertical scale:

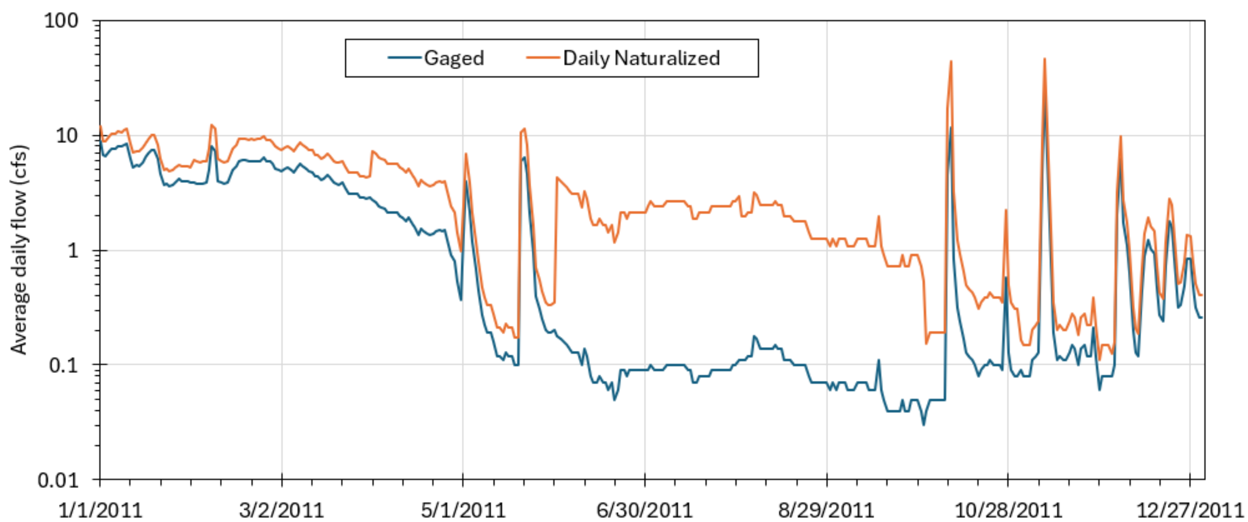


- Pg 21, paragraph four, last sentence, states that "A visual comparison of monthly USGS streamflows and monthly WAM records for CFRO13 showed minimal differences in monthly flows." Please consider providing a figure (or table) of monthly data from this location for a select time-period to explicitly demonstrate how these data sets are related. For example, a graphic similar to the following of monthly naturalized flows at WAM control point CFRO13 and monthly average gaged flows for USGS gage 08080700 during calendar year 2011 could be provided.

ATTACHMENT 1

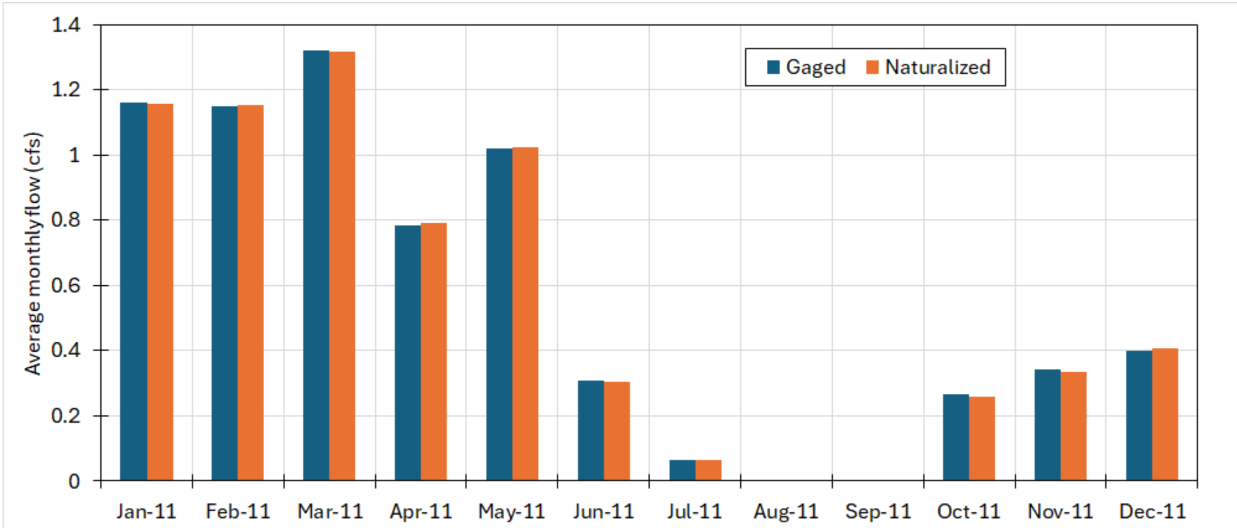


- Pg 44-50, Figures 4.2-4.8, it is difficult to see the difference between the dashed lines for the USGS and the WAM. Colors that are more distinguishable between each other may make it easier.
- 

Time series for USGS and WAM are already plotted with different colors (black and purple).